AD-A132 953 THE APPLICATION OF FRACTURE MECHANICS TO THE GROWTH OF CREEP CRACKS(U) ADVISORY GROUP FOR AEROSPACE RESEARCH AND DEVELOPMENT NEUILLY-SUR-SEINE (FRANCE) H P LEEUWEN 1/1

UNCLASSIFIED JUN 83 AGARD-R-705 F/G 20/11 NL

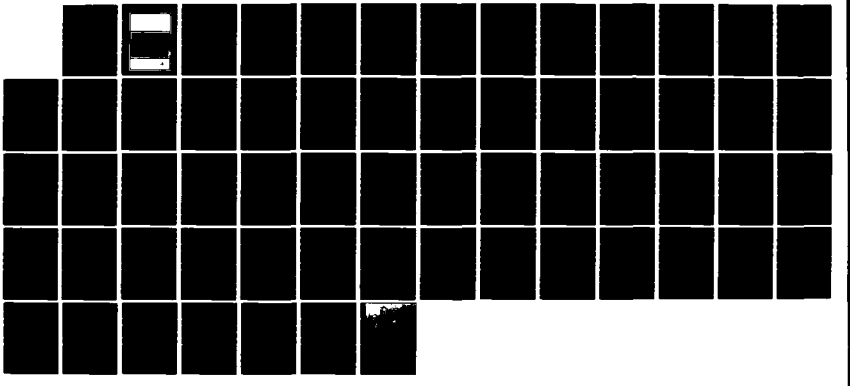

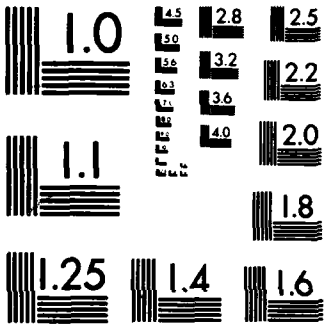

AGARD-R-705

AGARD

ADVISORY GROUP FOR AEROSPACE RESEARCH & DEVELOPMENT

7 RUE ANCELLE 92200 NEUILLY SUR SEINE FRANCE

AGARD REPORT No. 705

The Application of Fracture Mechanics to the Growth of Creep Cracks

NORTH ATLANTIC TREATY ORGANIZATION

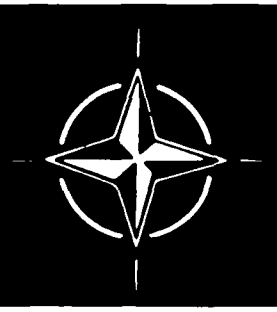

NORTH ATLANTIC TREATY ORGANIZATION

ADVISORY GROUP FOR AEROSPACE RESEARCH AND DEVELOPMENT

(ORGANISATION DU TRAITE DE L'ATLANTIQUE NORD)

AGARD Report No. 705

THE APPLICATION OF FRACTURE MECHANICS TO THE GROWTH OF CREEP CRACKS

by

H.P. van Leeuwen
National Aerospace Laboratory NLR
P.O. Box 90502
1006 BM Amsterdam
The Netherlands

This Report was presented at the 56th Meeting of the Structures and Materials Panel
in London, UK, April 1983.

THE MISSION OF AGARD

The mission of AGARD is to bring together the leading personalities of the NATO nations in the fields of science and technology relating to aerospace for the following purposes:

- Exchanging of scientific and technical information;
- Continuously stimulating advances in the aerospace sciences relevant to strengthening the common defence posture;
- Improving the co-operation among member nations in aerospace research and development;
- Providing scientific and technical advice and assistance to the North Atlantic Military Committee in the field of aerospace research and development;
- Rendering scientific and technical assistance, as requested, to other NATO bodies and to member nations in connection with research and development problems in the aerospace field;
- Providing assistance to member nations for the purpose of increasing their scientific and technical potential;
- Recommending effective ways for the member nations to use their research and development capabilities for the common benefit of the NATO community.

The highest authority within AGARD is the National Delegates Board consisting of officially appointed senior representatives from each member nation. The mission of AGARD is carried out through the Panels which are composed of experts appointed by the National Delegates, the Consultant and Exchange Programme and the Aerospace Applications Studies Programme. The results of AGARD work are reported to the member nations and the NATO Authorities through the AGARD series of publications of which this is one.

Participation in AGARD activities is by invitation only and is normally limited to citizens of the NATO nations.

Published June 1983

ISBN 92-835-1453-X

Printed by Specialised Printing Services Limited
40 Chigwell Lane, Loughton, Essex IG10 3TZ

PREFACE

The Structures and Materials Panel of AGARD has sponsored a number of activities concerned with the behaviour of materials at elevated temperatures in gas turbines. These have covered a number of aspects from laboratory investigations to the practical difficulties of service maintenance of gas turbine engine parts. This is demonstrated in the Specialists' Meetings held by the SMP, namely:–

"Characterisation of Low Cycle High Temperature Fatigue by the Strain Range Partitioning Method" (Aalborg 1978, AGARD CP-243)

"Ceramics for Gas Turbine Applications" (Porz-Wahn 1979, AGARD CP-276)

"Maintenance in Service of High Temperature Parts" (Noordwijkerhout 1981, AGARD CP-317).

In the final discussion of the last Specialists' Meeting there was a clear indication that more materials performance data under engine conditions was needed by the user. There was also a requirement for some basis of damage prediction upon which to build an approach of damage tolerance design and use of engine components. In response to this the SMP approved a follow-on activity entitled "Damage Tolerance Concepts for Critical Engine Components".

One of the early activities of the group involved was to receive a presentation from Dr-Ir. H.P. van Leeuwen of NLR on "The Application of Fracture Mechanics to the Growth of Creep Cracks" in London, Spring 1983. I am pleased to see this significant review published as an AGARD Report.

D.A.FANNER
Chairman – Sub-Committee on
Damage Tolerance Concepts for Critical
Engine Components

A

CONTENTS

THE APPLICATION OF FRACTURE MECHANICS TO THE GROWTH OF CREEP CRACKS

by
Dr.Ir. H.P. van Leeuwen
National Aerospace Laboratory NLR
P.O. Box 90502, 1006 BM AMSTERDAM
The Netherlands

SUMMARY

The literature concerning the application of fracture mechanics to the growth of creep cracks is discussed.

As an introduction it is shown that linear elastic fracture mechanics have been applied successfully to the residual strength of brittle materials, crack growth due to stress corrosion and crack growth due to fatigue.

Next the methods are discussed to account for plasticity.

Then a survey is made of the attempts to correlate the crack growth rate under creep conditions with the stress intensity factor, the net section stress, the reference stress, the crack opening displacement rate, the contour integral J and the contour integral J*.

A few sections are devoted to alternative methods to calculate J and J*.

A survey is made also of theoretical predictions of the crack growth rate as a function of parameters that are considered to be determining.

The report ends with a discussion and a few conclusions.

LIST OF ABBREVIATIONS

ASTM	American Society for Testing and Materials
CCP	Centre Cracked Plate
CCT	Centre Cracked Tension
CDCB	Contoured Double Cantilever Beam
CN	Centre Notch
CNC	Centre Notch Cylindrical
CNP	Centre Notched Plate
CNRS	Circumferentially Notched Round Specimen
CNT	Centre Notch Tension
COD	Crack Opening Displacement
CT	Compact Tension
CTOA	Crack Tip Opening Angle
CTOD	Crack Tip Opening Displacement
DEN	Double Edge Notch
DENT	Double Edge Notch Tension
FEM	Finite Element Method
LEFM	Linear Elastic Fracture Mechanics
NCH	Notched Central Hole
RNB	Round Notched Bar
SCC	Stress Corrosion Cracking
SEN	Single Edge Notch
SENB	Single Edge Notch Bending
SENT	Single Edge Notch Tension
TDCB	Tapered Double Cantilever Beam
WOL	Wedge Opening Loading

1. INTRODUCTION

The last two decades have seen the development of an aircraft design philosophy based on the principle of damage tolerance. This means that the fact is accepted that the occurrence of cracks or other forms of damage in the aircraft structure cannot always be prevented.
It is then required that the cracked component can sustain a certain fraction of its design load without collapse due to unstable crack growth. It is required also that in service the crack will grow so slowly that it can be detected by periodic inspections before it reaches a catastrophic size. If a crack is expected in a location which is inaccessible for inspection it will have to grow so slowly that it will not become catastrophic during the entire design life of the structure. An alternative design measure is to provide a neighbouring component that will take the load from a failing component without failing itself. This design philosophy requires calculations leading to prediction of crack growth rates and residual strength. Fracture mechanics provide the tools for such calculations.

Fracture mechanics have been applied successfully to airframe structures where crack growth is mainly by fatigue at moderate or normal temperatures.

In recent years the desire has grown to apply principles similar to damage tolerance to aircraft jet engines. This has raised the question whether fracture mechanics can be applied to crack growth by creep and fatigue in engine components operating at high temperatures.

A similar problem has arisen with regard to stationary high temperature installations such as furnaces, chemical reactors and boilers, especially those in electric power plants. Such installations have been designed typically for a finite life and on the basis of creep rupture strength. Many of such installations have now reached their design life time. For economic reasons their owners wish to keep these installations in service. The question is how long this can be done and how safety can be guaranteed. An important aspect is that in some of these installations cracks have been found and that present requirements do not allow cracks.
This has spurred many investigations regarding the applicability of fracture mechanics to crack growth under creep conditions.
Here the problem is that conventional fracture mechanics are based on linear-elastic stress-strain relations. Because the used structural materials show a certain measure of plasticity before failure one was forced to account for plasticity effects.
Many equations in linear elastic fracture mechanics (LEFM), can if necessary by some adaptation, be applied provided, however, the region where plasticity occurs remains small relative to the length of the crack and the dimensions of the specimen or the component. Plastic fracture mechanics, for cases where this condition is not fulfilled, are still under development.
In the creep case one is dealing with an important amount of time-dependent plastic deformation which renders the applicability of conventional fracture mechanics highly doubtful.
In the past 15 years or so several empirical and theoretical studies have been made into the possibility of applying fracture mechanics to the growth of creep cracks.
Reviews of such studies have been published earlier by Haigh (1), Van Leeuwen (2, 3), Ohji (4), Ellison and Harper (5), Ashby and Tomkins (6), Pilkington (7), Fu (8), Radhakrishnan and McEvily (9) and by Sadananda and Shahinian (10).
The present review tries to be more complete and will treat some more recent literature.
As an introduction the application will be treated of LEFM to the residual strength of brittle materials, crack growth by stress corrosion and crack growth by fatigue. Next a review will be given of methods to account for plasticity, largely taken from an article by Eftis and Liebowitz (11). Then a review is presented of attempts to correlate creep crack growth rate with the stress intensity factor K, the net section stress σ_{net}, the reference stress σ_{ref}, the crack (tip) opening displacement rate $\dot{v}$ (or $\dot{\delta}$), the contour integral J and the contour integral J*. The report ends with conclusions and recommendations.

2. LINEAR ELASTIC FRACTURE MECHANICS

LEFM has found a successful application in the description and the prediction of several types of crack growth. A condition is that the extent of plastic deformation will remain small. This implies that the plastic zone at the crack tip will remain small and will remain embedded in the field where deformation is elastic only. In this way the plastic deformation will have a negligible effect on the stresses in the elastic field and on the quantities calculated with them.

2.1 Residual Strength

If LEFM is applied to a residual strength test on a cracked specimen it is assumed that unstable crack growth will occur if the stress intensity factor reaches a critical value K_c. It is then found that K_c is not really a material constant independent of specimen shape and size but K_c will depend heavily on specimen thickness. See for instance figure 1 taken from Sullivan and Freed (12).

2.2 Stress Corrosion Cracking

In the application of LEFM to SCC it is found that the crack growth rate depends on K in a very typical way (Fig. 2, Speidel, 13) and shows a region I where $\frac{da}{dt}$ depends strongly on K, a region II where $\frac{da}{dt}$ is constant (velocity plateau) and a region III where $\frac{da}{dt}$ again rises rapidly with K. In practice the relationship between da/dt and K appears to be influenced extensively by such conditions as material susceptibility, relative humidity, halide concentration, pH-value, electrode potential, temperature, viscosity of the corrodent, nature of the corrodent (e.g. liquid metal v.s. water).

2.3 Fatigue

The application of LEFM to SCC is possible because there stresses usually remain small. This is usually also the case with fatigue. In this case the crack growth rate da/dN is determined by the variation

ΔK of K. The relationship is influenced rather heavily, however, by frequency and environment (Fig. 3, Speidel, 14).

2.4 Conclusion

Although certain relationships have been established between fracture mechanics parameters and various types of cracking, these relationships are influenced strongly by a number of additonal conditions or parameters. If, therefore, a correlation can be found in the case of creep cracking one must be prepared to accept that also in this case a number of additional parameters can influence the correlation to a large extent.

3. PLASTICITY EFFECTS

In many technical materials appreciable plastic deformation can occur before the crack becomes unstable. If the plastic zone at the crack tip remains small and remains embedded in the elastic field certain corrections can be applied to the equations used to calculate the stress intensity factor K. When plastic deformation becomes more extensive, the K factor may lose its validity and one tries to apply other parameters that can be expected to give a better description of crack tip conditions. Such parameters are for instance
- the crack (tip) opening displacement, C(T)OD
- the J integral
- the net section stress

These parameters will now be reviewed because they provide suggestions for the treatment of creep cracking by fracture mechanics methods.

3.1 Effective Crack Length

The value of the K-factor depends essentially on the square root of the crack length a. In the case of plasticity it can be assumed that the plastic zone at the crack tip is a circle with radius r_Y where r_Y can be calculated as

$$r_Y = \beta \frac{K^2}{\sigma_Y} \tag{3.1}$$

where $\beta = 1/2\pi$ for the plane stress case and $\beta = 1/6\pi$ for the plane strain case.
Plasticity is then acccounted for by introduction of an effective crack length

$$a_e = a + r_Y \tag{3.2}$$

In this way the effect plastic deformation has on the elastic stress field is accounted for in a approximative manner.

3.2 Energy Dissipation

The K-value is a scaling factor for the elastic stress field at the crack tip that can be represented as

$$\sigma_{jk} = \frac{K}{\sqrt{2\pi r}} \cdot f_{jk}^{1}(\theta) \tag{3.3}$$

In reality this is the first term of a series expansion with increasing powers of the quantity

$$(r/a)^{\frac{n}{2} - 1} \quad \text{with } n = 1, 2, 3, \ldots$$

Higher values of $(\frac{n}{2} - 1)$ can be neglected if r remains sufficiently small relative to a, e.g. for $r < 0.05a$.
The original fracture mechanics are based on energy considerations however.
A characteristic quantity is the strain energy release rate

$$G = - \frac{dU}{da} \tag{3.4}$$

where U is the potential energy.
For the elastic case G can be calculated as

$$G = \frac{P^2}{2B} \cdot \frac{dC}{da} \tag{3.5}$$

Here B is the specimen thickness, C the compliance v/P wherein v is the load line displacement and P the load.
It can be shown that for the elastic case G is proportional to K^2.
If the extent of plasticity is so great that the K-factor loses its significance, G may still be a useful parameter to describe the material's resistance to cracking.
In thin sheet, where the plastic zone may be larger than the sheet thickness, stable crack growth will occur when the gross section stress σ is raised monotonically. The resistance to stable crack growth can be depicted by the R-curve (Fig. 4).
If on a specimen with a precrack of length a_0 the stress σ is raised, G will rise in proportion with σ^2 and a. Every stress increase $\Delta\sigma$ will result in a crack length increase Δa. The locus of the points on the G-lines corresponding to a certain stress σ_i and the resulting crack length a_i forms the R-curve.
Fracture instability will occur when the G-line is tangent to the R-curve because this implies that at constant stress σ more energy is released than is needed for crack growth since

$$\frac{dG}{da} \geq \frac{dR}{da} \tag{3.6}$$

Related to this approach is the one by Eftis and Liebowitz (11) who calculate the energy release when the load-displacement or P-v diagram is non-linear due to crack growth and plasticity (Fig. 5).
They represent the non-linear curve by the equation

$$v = \frac{P}{M} + k\left(\frac{P}{M}\right)^n \tag{3.7}$$

where M is the initial rigidity.
Through application of

$$\tilde{G} = -\frac{dU}{da} \tag{3.8}$$

they arrive at the effective energy release rate $\tilde{G}$ as

$$\tilde{G} = G\left\{1 + \frac{2nk}{n+1}\left(\frac{P}{M}\right)^{n-1}\right\} \tag{3.9}$$

Unstable crack growth will occur for a critical energy release rate $\tilde{G}_c$.

3.3 J-integral

Related to the approach based on G is the one based on the contour integral J, proposed by (Jim) Rice (Fig. 6)

$$J = \oint_\Gamma \left\{W_{dy} - T_j \frac{\partial u_j}{\partial x} ds\right\} \tag{3.10}$$

W is the strain energy density

$$W = \int_0^{\varepsilon_{mn}} \sigma_{jk} d\varepsilon_{jk} \tag{3.11}$$

T_j is $\sigma_{jk} n_k$, the traction normal to the contour Γ and u_j is the displacement vector.
J can be determined for the elastic/plastic case through a numerical finite element calculation or analytically e.g. using a polar coordinate system around the crack tip.
It has been show that H is path iundependent provided the contour stays away from the crack tip sufficiently.
Proof has been given however, using the so called deformation theory of plasticity which is valid only for monotonically rising stresses.
It has been shown that J is also a measure of the energy release rate

$$J = -\frac{dU}{da} \tag{3.12}$$

For the elastic case one finds J = G.

J can be determined empirically from a non-linear diagram of load P versus load line displacement v, see figure 7, (Landes and Begley, 15). It is postulated that further crack growth will occur for a critical J value J_c.

3.4 Crack (Tip) Opening Displacement

A seemingly different approach is the one based on crack (tip) opening displacement.
The COD can be measured in the load line, or at other distances from the crack tip, using e.g. clip gauges.
By calculation and/or calibration the CTOD can be derived.
It can be calculated using the plastic crack tip model of Dugdale

$$\delta = \frac{8\sigma_Y a}{\pi E} \ln \sec\left(\frac{\pi}{2}\frac{\sigma}{\sigma_Y}\right) \tag{3.13}$$

From a quasi-elastic calculation, using a circular plastic zone around the tip of the effective crack $(a + r_y)$, δ is found as the displacement at the real crack tip.
The result is

$$\delta = \alpha G/\sigma_Y \tag{3.14}$$

where $\alpha = 4/\pi\sqrt{3}$ for plane strain and $\alpha = 4/\pi$ for plane stress.
This shows the relation to the energy dissipation approach since

$$G = \frac{1}{\alpha}\left(\sigma_Y \cdot \delta\right) \tag{3.15}$$

3.5 Stable Versus Unstable Crack Growth

When plasticity plays a role appreciable stable crack growth can occur prior to failure.
To investigate what parameters would govern or describe this process finite element calculations have been made in which the behaviour of v, the load line displacement, was forced to vary with a in the manner as had been determined experimentally.
De Koning (16) found that re-initiation of the crack occurred at critical values J_c or δ_c of J and δ but that during stable crack growth the crack tip opening angle (CTOA) remained virtually constant.
Shih et al. (17) found that dJ/da remained constant over a short stretch. The so called nominal crack tip opening angle $d\delta/da$ and the real CTOA remained constant over a large span of a-values.
They concluded that crack re-initiation could be predicted on the basis of J_c or δ_c but that for continued crack growth CTOA or $d\delta/da$ had to have a certain value.
Gudas et al. (18) show results indicating that dJ/da remains fairly constant for $0.5 \leq \frac{a}{w} \leq 0.8$.
They conclude that Paris's tearing modulus $(dJ/da).(E/\sigma_0^2)$ can be a good measure for the onset of instability.

3.6 Net Section Stress

When yielding occurs over the larger part of the reduced section it is expected that crack instability will occur for a critical value of the net section stress σ_{net}.

4. THE GROWTH OF CREEP CRACKS

If a metal specimen, containing a crack due to prior fatigue stressing for instance, is loaded e.g. in tension or in bending at elevated temperature, the crack will continue to grow, perhaps after some incubation period. By measuring and recording the crack length, using the change in electric resistance or in compliance, a crack growth curve as depicted in figure 8 can be determined. In general the crack growth curve will strongly resemble the conventional creep elongation curve with its typical three regions with fast, slow and fast growth rates.
In the case of the creep crack growth curve the primary region may be small or absent, the slope in the secondary region may be shallow or steep, but the basic form will always be there.
We are dealing again with stable crack growth followed by unstable fracture. The phenomenon is determined more strongly by plasticity, however, as can be seen from the following summary:
- Brittle materials, heavy plate: no stable crack growth
- Ductile materials, thin sheet: stable crack growth at monotonically increasing load.
- Creeping materials: stable crack growth at constant load.

It need not be expected that final failure in the third case will require a different analytical treatment than that in the second case. It can be expected however that stable crack growth in the third case will have to be treated differently than that in the second case, as much as stable crack growth in the second case had to be treated differently from unstable crack growth in the first case.
There is a certain resemblance with
- fatigue: stable crack growth at constant cyclic stress
- stress corrosion: stable crack growth at constant static stress.

5. CORRELATION OF THE CREEP CRACK GROWTH RATE WITH THE STRESS INTENSITY FACTOR, THE NET SECTION STRESS AND THE REFERENCE STRESS

As was explained before, the applicability of the K-factor is dependent on some conditions, the most important perhaps that the extent of plasticity should be relatively small.
It is somewhat naive may be to suppose that K will be applicable to a crack in a creep specimen where time dependent plastic deformation occurs over the greater part of the net section and perhaps also of the gross section away from the crack. It will not be very difficult to calculate a K-value in some way and to make a diagram of da/dt versus K. The question is whether this would be meaningful. For that it is necessary that under otherwise identical conditions, for different specimen shapes and sizes, for different crack lengths and gross section stresses, the same da/dt will be found if K is the same. In practice this results in many disappointments.
If a diagram of secondary creep rate versus K is made nevertheless, a curve as shown in figure 9 may result. This is again a sigmoidal curve. One distinguishes a region I where da/dt depends strongly on K, a region II where da/dt depends weakly on K, and a region III where da/dt again rises sharply with K.
In some cases the primary branch may be absent and the secondary branch may be horizontal. In other cases the secondary branch may be nearly as steep as the primary and the tertiary. Some investigators show only one branch and than it is difficult to judge which of the three it is.
Note that the crack velocity diagram for creep has some resemblance to those for stress corrosion and fatigue.
If plasticity is extensive the correlation of da/dt with K can be expected to be bad. One can then attempt to correlate da/dt with net section stress σ_{net}. For a cracked specimen loaded partly in bending, net section stress is not such a meaningful thing and one prefers to use the reference stress σ_{ref}.
It can be defined as

$$\sigma_{ref} = \sigma_{gross} \cdot \frac{P_Y}{P_c} \qquad (5.1)$$

where P_Y is the load at the onset of yielding in the uncracked specimen and P_c is the load at the onset of yielding in the cracked specimen.
Many of the older investigations concentrated on the question whether da/dt would correlate well with K and if so whether it would correlate better with K than with σ_{net} or σ_{ref}.
A typical example is the investigation by Ellison and Walton (19), see figure 10. Single edge notch flat specimens have been loaded axially and in bending at a series of initial stresses. It is seen that for the axially loaded case creep crack growth rates correlate fairly well with the stress intensity factor. For the bending case there is a large spread however, and plotting da/dt versus K does not reduce the data to a single curve.
Another example is the investigation by Neate and Siverns (20), figures 11 and 12. A 0.5 Cr-0.5 Mo-0.25 V steel has been given two different heat treatments, one involving a quench making the steel relatively brittle in order to simulate a weld heat affected zone, the other comprising normalizing and tempering. Correlation of da/dt with K is reasonably good. Somewhat unexpectedly the correlation with σ_{net} is rather bad, especially for the ductile material.
A third example involves AISI 316 type stainless steel (Fig. 13) tested by Nicholson and Formby (21). Here the correlation with σ_{net} is better than with K as one would expect for a ductile stainless steel.
As was shown the results sometimes do live up to expectations and sometimes they don't. Literature in which correlations of da/dt with K, σ_{net} and σ_{ref} were compared have been compiled and classified as to the result in table 1. It is seen that the results are rather erratic and unpredictable. Therefore correlations with either σ_{net} or K should not be trusted.
Note that in some of the investigations reviewed, the material has been quenched to simulate a welded condition or prestrained at high temperature to simulate creep damage. This usually leads to a deterioration of the crack resistance and should be considered when applying crack resistance values to practical cases.

TABLE 1. CORRELATION OF da/dt WITH K, σ_{net} and σ_{ref}

I Good correlation of da/dt with σ_{net}, bad correlation with K

1) Nicholson and Formby (21): type 316 stainless steel, solution heat treated, SENT and CNT specimens, 740°C.
2) Neate (22): 0.5Cr-0.5Mo-0.25V steel, normalized and tempered, SENT specimens, 565 °C (σ_{ref} rather than σ_{net}).
3) Neate (23): 0.5Cr-0.5Mo-0.25V steel, normalized and tempered, SENT and CT specimens, 565 °C (σ_{ref} rather than σ_{net}).

II Bad correlation of da/dt with K, σ_{net} not considered

1) Robson (24): 0.24 % carbon steel, normalized, SEN and CT type specimens, 450 °C.
2) Ellison and Walton (19): 1Cr-1Mo-V steel, SENT specimens, 565 °C, correlation especially bad in bending.
3) Haigh (25): Cr-Mo-V cast steel, normalized and tempered, WOL specimens (≈ CT), 550 °C.
4) Gooch (26): 0.5Cr-0.5Mo-0.25 V steel, several quench rates, SENB specimens, 565 °C.
5) Gooch (27): 0.5Cr-0.5Mo-0.25 V steel, various quench rates and tempers, SENB and SENT specimens.
6) Sadananda and Shahinian (28): Nickel Alloy 718, aged, CT specimens, 650 °C, crack tunneling.

III Good correlation of da/dt with σ_{net}, K not considered

1) Taira and Ohtani (29): 1Cr-1Mo-0.25 V steel, CNRS and DENT specimens, 6000 °C.
2) Nicholson (30): type 316 stainless steel, solution heat treated, DENT specimens, 600-850 °C.

IV Good correlation of da/dt with σ_{net} and with K

1) Neate and Siverns (20): 0.5Cr-0.5Mo-0.25V steel, quenched, SENT specimens, 565 °C.
2) Henshall et al. (31): type 316 stainless steel, solution heat treated, tempered and untempered, DENT specimens, 636 °C; 1Cr-0.5Mo steel, bainite, SENT specimens, 565 °C (σ_{ref} rather than σ_{net}).
3) Lloyd (32): type 316 stainless steel, DENT specimens, 625 °C.
4) Taylor and Batte (33): 1Cr-Mo-V steel, forged, DENT specimens, 550 °C, reinitiation rather than crack growth.

V Good correlation of da/dt with K, σ_{net} not considered

1) James (34): type 316 stainless steel, CT and CNT specimens, 538 °C.
2) Thornton (35): forged and cast CrMoV steel, SENB specimens, 550 °C.
3) Landes and Wei (36): AISI 4340 type steel, CNT and constant K specimens, 20-140 °C.
4) Kenyon et al. (37): RR 58 aluminium alloy, contoured DCB specimens (constant K), 100-200 °C.
5) Pilkington et al. (38): 0.5Cr-0.5Mo-0.25V steel, vacuum melted, SENB specimens, 550 °C.
6) Floreen (39): various nickel alloys, CT specimens, 500-760 °C.
7) Kaufman et al. (40): 2219-T851 aluminium alloy, CT specimens, 100-177 °C.
8) Worswick and Pilkington (41): 0.5Cr-0.5Mo-0.25V steel, ferritic, prestrained at 666 °C, SENB specimens, 550 °C.
9) Sadananda and Shahinian (28): type 718 nickel alloy, aged, CT specimens, 540 °C, Udimet 700, aged, CT specimens, 850 °C.

VI Bad correlation of da/dt with σ_{net}, K not considered

No publications.

VII Bad correlation of da/dt with σ_{net}, good correlation with K

1) Siverns and Price (42): 2.25Cr-1Mo steel, SENT specimens, 565 °C.
2) Neate and Siverns (20): 2.25Cr-1Mo steel, quenched for weld simulation, SENT specimens, 565 °C.
3) Kotesazawa and Iwata (43): type 304 stainless steel, CNRS and DENT specimens, 650 °C.
4) Neate (22): 0.5Cr-0.5Mo-0.25V, quenched for weld simulation, SENT specimens, 565 °C.

6. CORRELATION OF THE CREEP CRACK GROWTH RATE WITH THE CRACK (TIP) OPENING DISPLACEMENT RATE

For a cracked specimen as shown in figure 7, the displacement in the load line v is related to load P and compliance C as follows

$$v = C \cdot P \tag{6.1}$$

Differentiation with respect to time gives

$$\frac{dv}{dt} = C \cdot \frac{dP}{dt} + P \cdot \frac{dC}{da} \cdot \frac{da}{dt} \tag{6.2}$$

For constant load

$$\frac{dv}{dt} = P \cdot \frac{dC}{da} \cdot \frac{da}{dt} \tag{6.3}$$

For a so-called constant K specimen, $\frac{dC}{da}$ is constant. It follows that only for a constant K specimen in the elastic case at constant load there will be a straight proportionality between $\frac{da}{dt}$ and $\frac{dv}{dt}$.
If these three conditions are not fulfilled a more general relationship

$$\frac{da}{dt} = H \cdot \left(\frac{dv}{dt}\right)^m \tag{6.4}$$

may still hold.
It is somewhat surprising therefore that Haigh (1) analysing the results of Robson (24) for a creeping CT specimen finds a straight proportionality nevertheless (Fig. 14). As shown in figures 15 and 16 the time dependence of COD and crack length a can be quite different. A relation as above will have only a limited validity.
For a materiel behaviour as depicted in figure 16 it may be stated that for the onset of crack growth v must first reach a critical value v_c, and that the relationship will than hold for da/dt and

$$\frac{d}{dt}(v - v_c) \tag{6.5}$$

If the relationship does not hold this may show up as a non-eliminated dependence on load P (Fig. 17). Radhakrishnan and McEvily (9, 44) found that in that case the data points could be made to fall on one straight line by plotting $\frac{da}{dt}$ versus the parameter

$$\left(\frac{dv}{dt}\right)\left(\frac{P_0}{P}\right)^\alpha \tag{6.6}$$

They claim a theoretical background for the relationship

$$\frac{da}{dt} (:) \left[\frac{dv}{dt}\left(\frac{P_0}{P}\right)^\alpha\right]^{\frac{1}{\theta}} \tag{6.7}$$

where α and θ are functions of temperature T (45). Sometimes, as for Ti-6Al-2Sn-4Zr-2Mo-0.1Si, α will be very small and even practically zero (46).

While v and dv/dt are directly related to the overall energy dissipation, a more mechanism oriented approach makes use of the crack tip opening displacement δ. The trouble is that δ is much more difficult to determine than v.
Nicholson (30, 47) and Henshall et al. (31) determined δ on metallographic specimens made after the cracking test. They correlated δ with v and then determined $\frac{d\delta}{dt}$ from the time record of v.
The more usual method is to assume that there is a plastic hinge at a certain spot in the unbroken ligament b and that δ will be a certain fraction of v.
Haigh (25) found the relationship

$$\frac{da}{dt} = 2 \cdot \left(\frac{d\delta}{dt}\right)^{0.8} \tag{6.8}$$

Other investigators such as Pilkington et al. (38), Nicholson and Formby (21), Gooch et al. (26, 48) and Henshall et al. (31) have found relations of the type

$$(a - a_0) = \frac{1}{\omega}(\delta - \delta_0) \tag{6.9}$$

where ω is similar to the crack tip opening angle.

The question is, given a relationship between $\frac{da}{dt}$ and $\frac{dv}{dt}$ or $\frac{d\delta}{dt}$, what the practical use of it is. There are two needs:
- for a high temperature installation one would like to determine $\frac{da}{dt}$ from a more easy to measure quantity or
- one would like to predict $\frac{da}{dt}$ from a more easy to calculate quantity.

The conclusion is that the relationship will be of little practical use because for a structure $\frac{dv}{dt}$ and $\frac{d\delta}{dt}$ are neither more easy to measure nor more easy to calculate than $\frac{da}{dt}$ itself.

7. CORRELATION OF THE CREEP CRACK GROWTH RATE WITH THE J-INTEGRAL OR THE RELATED PARAMETER J*

In section 3.3 the J-integral has been defined already and a method was indicated to determine J experimentally (Fig. 7).
With regard to creep cracking Landes and Begley (15) have applied a parameter that strongly resembles the J-integral. They have indicated it as C* whereas other authors use the symbol J. To avoid confusion only the symbol J* will be used in the present paper. The integral in question is defined as (see Fig. 18)

$$J^* = \oint_\Gamma \left\{W^* dy - T_j \frac{\partial \dot{u}_j}{\partial x} ds\right\} \tag{7.1}$$

where

$$W^* = \int_0^{\dot{\varepsilon}_{mn}} \sigma_{jk} d\dot{\varepsilon}_{jk} \tag{7.2}$$

It appears that J* can be obtained from J by substituting strain rates for strains and displacement rates for displacements. It is clear that in general $J^* \neq dJ/dt$ and that hence the indication J is misleading.
Like J, J* can be calculated by finite element analysis or from analytical stress-strain relations.
For J an empirical determination was possible on account of the relation

$$J = -\frac{dU}{da} = -\frac{d}{da}\left\{\int_0^v P dv\right\} \tag{7.3}$$

Likewise J* can be determined from

$$J^* = -\frac{dU^*}{da} = -\frac{d}{da}\left\{\int_0^{\dot{v}} P d\dot{v}\right\}. \tag{7.4}$$

Landes and Begley determined J* from cracking tests at constant displacement rate $\dot{v}$. They processed their test data as shown in figure 19. Diagrams are produced in the following sequence
- Load and crack length as a function of time
- crack growth rate as a function of crack length at constant displacement rate
- load as a function of crack length at constant displacement rate
- load as a function of displacement rate at constant crack length
- energy rate U* as a function of crack length at constant displacement rate
- energy rate derivative J* as a function of displacement rate (at constant crack length)
- crack growth rate (at a certain displacement rate and crack length) as a function of J*.

Sadananda and Shahinian (49) have developed a method to determine both J and J* from the results of creep cracking tests at a series of constant loads P_i.
Their schemes are shown in figure 20 which is self-explanatory.
Many authors have used approximate expressions from which J and J* are more easy to determine. These will be discussed later.
The question posed now is whether there is an unambiguous relation between da/dt and J or J*, i.e. a relation that will hold even for different geometries and sizes of specimens, different load levels and initial crack lengths etc. Only in that case will one be able in principle to accurately predict da/dt from J or J*.
Landes and Begley (15) testing CCP (=CNT) specimens of the FeNiCrMo alloy Discalloy at 647 °C found a single relation between da/dt and J* if the same specimen was tested either at a single or at a series of displacement rates $\dot{v}$. If, however, they tested CT specimens rather than CCP they found the curve to be offset relative to the former (Fig. 21). The correlation was better, however, than with K or nominal stress (= reference stress).
Nikbin, Webster and Furner (50) tested the aluminium alloy RR58 at 150 °C and steel type 0.5Cr-0.5Mo-0.25V at 565 °C. They used contoured DCB specimens which give a constant K at constant load P. They found that da/dt was not constant. If, however, they adjusted P repeatedly to arrive at a constant J* they found that da/dt was constant for a large interval of crack lengths, i.e. excluding small primary and a tertiary regions.
Harper and Ellison (51) tested 1CrMoV steel at 565 °C. They used SENB and CT specimens. The correlation of da/dt with J* was quite good at high values of these quantities. Curves for constant bending moment were fanning out however at low values, giving lower da/dt values at higher applied moments. The authors ascribed it to the effect of primary creep.
Sadananda and Shahinian (49) tested nickel alloy 718 at 538, 649 and 760 °C using CT specimens. They found that for a series of applied loads P, the crack growth rate correlated rather well with both J and J* and rather badly with both stress intensity factor K and nominal or reference stress σ_n.
Pilkington and Worswick (52) continuing work reported in (41) tested 0.5Cr-0.5Mo-0.25V at 649 °C using SENB specimens. The material had been prestrained plastically 0.26 resp. 0.58 % at 666 °C to introduce cavitation damage. For different applied loads they found that da/dt correlated rather well with $d\delta/dt$, and with quantities $J^*(\dot{v})$ and $J^*(\dot{\delta})$ defined as

$$J^*(\dot{v}) = \frac{P}{Ba} \cdot \frac{dv}{dt} \text{ and } J^*(\dot{\delta}) = \frac{P}{Ba} \cdot \frac{d\delta}{dt} \tag{7.5, 7.6}$$

Earlier they had reported good correlation with log K but had found distinct effects of primary creep and prestraining. This no longer showed up in their newer plots. This will be because cavitation not only increases $\frac{da}{dt}$ but also $\frac{dv}{dt}$ and $\frac{d\delta}{dt}$, and the same may be true for primary creep.
Branco and Radon (53) have continued the work of Kenyon et al. (37) trying to correlate da/dt not with K but with J. They did find a correlation but did not report whether this was any better than with K, σ_{net} or J*. They introduce the relation

$$\frac{da}{dt} = C \cdot J^{\gamma} \tag{7.7}$$

where C and J are strongly dependent on temperature T. Since the relations with T involved are not monotonic the validity of the equation is doubtful.

Saxena (54) tested annealed 304 type stainless steel at temperatures between 538 and 705 °C. He applied CCT and CT specimens using constant displacement rates $\dot{v}$ that were sometimes varied in a stepwise manner. The correlation of da/dt with J* was rather good but deviations occurred for very long cracks in the CCT specimens.

In Japan very comprehensive investigations have been made to determine the validity of J* as a governing parameter for creep crack growth.
Koterazawa and Mori (55, 56 and Fig. 22) tested type 304 stainless steel at 650 °C in air. They used three different double edge notch specimens and one central notch specimen.
The material came from three heats (A, B and C) which was accounted for in the specimen designation, e.g. DEN 2C. They approximated J* as

$$J^* = \sigma_{net} \cdot \frac{dv}{dt} \tag{7.8}$$

The crack growth rate appeared to correlate rather well with J* (Fig. 22). The correlation with K was quite bad, the one with σ_{net} was much better, and better still if a was divided by w to eliminate a size effect (Fig. 23).
Ohji (4) and Ohji et al. (57) tested type 304 stainless steel at 650 °C using a large number of specimens

of various sizes and shapes. Figures 24 and 25 show that the correlation of da/dt with J* was superior to those with K and σ_{net}. This is quite obvious also for some added results for CT specimens.
In (57) results are presented also for circumferentially notched round specimens at three diameters. Results have been added of tests on single and double edge notch specimens as well as central notch specimens.
In a diagram of da/dt versus J* all results fall in a relatively narrow scatter band.
Taira, Ohtani and Kitamura (58) have done comprehensive tests on 0.16 % carbon steel at 400 and 500 °C in air, at 400 °C in vacuum, on type 304 stainless steel at 650 °C in air and in vacuum, on type 316 stainless steel at 600 and 650 °C in air.
They used three types of specimens, each in three different sizes (Large, Medium and Small) i.e.
- hollow cylindrical specimens with a local through crack: CNC-L, CNC-M, CNC-S.
- solid cylindrical specimens with a circumferential notch: RNB-L, RNB-M, RNB-S.
- flat plate specimens with a central notch: CNP-L, CNP-M, CNP-S.

J* was again approximated as $\sigma_{net} \cdot \frac{dv}{dt}$.
As figure 26 shows, the J* integral approach can cope quite well and much better than the σ_{net} approach with differences in stress level and specimen size and shape.

An investigation similar to those conducted in Japan was carried out in Great Britain by Christian et al. (59). These authors tested 0.5CrMoV steel and 1CrMoV steel at 565 °C using CT, SENB and DCB type specimens. For these different geometries they tried to correlate the crack growth rate with K, σ_{ref} and J*. Correlations with J* were more satisfactory throughout. The diagrams they have produced closely resemble those by the Japanese authors shown in figures 24 and 25, meaning that in the diagram of da/dt versus J* there was still quite a bit of spread although it was less than with the other parameters.
Seemingly alarming results in this context have been presented by Donath et al. (60). These authors tested the nickel-base superalloy IN 100 at 732 °C using two different specimen types. The first one was the common CT specimen but the second a closed ring tested in tension and cracked from the inner side at locations 90° away from the points of load application. A range of thicknesses was used for both specimen types. They evaluated the stress intensity factor K, net section stress σ_{net} and the contour-integral J* as correlating parameters describing crack growth. A special feature of their investigation was that cracking occurred at increasing K in the case of the CT specimens and at practically constant K in the case of the ring specimens. They applied a scheme like that in figure 20 to determine J* from the test results. They encountered a problem already encountered by other authors (e.g. Worswick and Pilkington, 41) in that, due to primary creep effects, crack rates were high initially, gradually decreased to a minimum and then increased again at increasing crack length or remained constant. This means that in the da/dt versus K diagram a V-shaped or root-sign-shaped curve (Fig. 28 top) is obtained rather than the sigmoidal one sketched in figure 9.
Barring the initial downward branches Donath et al. found good correlations in spite of thickness variations of da/dt with all three parameters K, σ_{net} and J* (Fig. 27). The situation was different for the ring-shaped specimen, however.
In the da/dt versus K plot they obtained a series of parallel vertical lines corresponding to the various initial K-values (Fig. 28). The thickness effect was negligible. Since during each test K was practically constant, each line depicted nothing but the decreasing crack growth rates due to primary creep. This situation really is not alarming since the bottom ends of the lines lay fairly close to the da/dt versus K curve derived for CT specimens. They considered the σ_{net} approach useless for the ring specimen, but then it ought to be possible to define a reference stress σ_{ref} even for this geometry. They claim the J* approach to be useless too for the ring specimen because of the decreasing crack growth rate at increasing crack length. Apparently they have not realized that the J* approach should be restricted to secondary creep and crack growth rates and excludes the primary ones.
All in all the impression is gained that the J* integral holds better promise as a governing parameter than K or σ_{net} or σ_{ref}, although the situation is still not ideal.
One deterrent to working with J* is the laborious way in which it has to be determined if one strives for greater accuracy than with the approximations used e.g. by the Japanese authors. Fortunately several alternative methods are available for the quantitative determination of both J and J*. These will be discussed in the next sections.

8. ALTERNATIVE EMPIRICAL DETERMINATION OF J AND J*

In figures 7 and 20 methods have been shown to determine J from a series of load-displacement diagrams. Rice and other authors have developed methods to determine J from one single load-displacement diagram, i.e. from one test.
In principle the same methods can be used for J* working with a diagram of load versus displacement rate, but it would require more than one test to obtain a load-displacement rate diagram.
J has been related to the energy dissipation as

$$J = -\frac{1}{B}\frac{\partial U}{\partial a} \tag{8.1}$$

where B is specimen thickness and U is the area below the load displacement curve (Fig. 29, A and B).
Now

$$U = \int_0^v P dv = Pv - \int_0^P v dP = Pv - \bar{U} \tag{8.2}$$

It follows that:

$$J = \frac{1}{B}\int_0^v \left(-\frac{\partial P}{\partial a}\right)_v dv \tag{8.3}$$

and

$$J = \frac{1}{B}\int_0^P \left(\frac{\partial v}{\partial a}\right)_P dP \tag{8.4}$$

It can be shown that the latter two integrals can be build up from elementary areas of the P-v diagram

such as shown in figure 29C.
According to Rice (61) it has advantages to split up v in two components.
Either

$$v_{tot} = v_{nocr} + v_{cr} \tag{8.5}$$

or

$$v_{tot} = v_{el} + v_{pl} \tag{8.6}$$

In the first case v has been split up in a part that would occur in the absence of a crack and in a part that is contributed by the crack.
In the second case v has been split up in elastic and plastic contributions.
For a flat double edge crack specimen, where the unbroken ligament measures b, loaded by a force per unit thickness P, it can be shown that v_{pl} should have the form

$$v_{pl} = b\, H\left(\frac{P}{b}\right) \tag{8.7}$$

where H is an unknown function of (P/b).
It can be derived, however, that

$$J = J_{el} + \int_0^P \left(-\frac{\partial v_{pl}}{\partial b}\right) dP \tag{8.8}$$

It follows that

$$-\frac{\partial v_{pl}}{\partial b} = \frac{P}{b} H'\left(\frac{P}{b}\right) - H\left(\frac{P}{b}\right) = \frac{1}{b}\left\{P\left(\frac{\partial v_{pl}}{\partial P}\right)_b - v_{pl}\right\} \tag{8.9}$$

Moreover, J_{el} is equal to the elastic strain energy release rate $G = K^2/E$. Partial integration leads to

$$J = G + \frac{1}{b}\left\{2\int_0^{v_{pl}} P dv_{pl} - P v_{pl}\right\}. \tag{8.10}$$

Now the quantities between parentheses can be identified as elementary areas in figure 29C.
$v_{pl,nocr}$ is usually neglected.
It is seen that

$$P v_{pl} \approx P v_{pl,cr} = U_{pl,cr} + \bar{U}_{pl,cr} \tag{8.11}$$

and that

$$\int_0^{v_{pl}} P dv_{pl} = U_{pl,cr} = P v_{pl,cr} - \bar{U}_{pl,cr} \tag{8.12}$$

Hence

$$J = G + \frac{1}{b}\left\{U_{pl,cr} - \bar{U}_{pl,cr}\right\} \tag{8.13}$$

The same results holds for a plate with a central crack.
Rice et al have made similar analyses, leading to similar but different expressions for a circumferentially notched round specimen, for a cracked three-point bend specimen and for a compact tension specimen.
In the last case there is found

$$J = \frac{2}{b}\int_0^{v_{cr}} P dv_{cr} = \frac{2}{b}\left\{U_{tot} - U_{nocr}\right\} \approx \frac{2}{b} U_{tot}. \tag{8.14}$$

These and other analyses have been reviewed by Keller and Munz (62).
Kanazawa et al. have attempted to derive more accurate expressions for the three-point bend specimen and the compact tension specimen.
Merkle and Corten have derived a more complicated and supposedly more accurate expression again for the compact tension specimen.
In a more recent publication Clarke and Landes (63) have simplified the Merkle and Corten analysis for the compact tension specimen.
They arrived at the expression

$$J = \frac{1 + \alpha}{1 + \alpha^2} \cdot \frac{2U_{tot}}{Bb} \tag{8.15}$$

Here α is a rather complex expression in crack length a and ligament b. However, the authors present an approximation obtained by curve fitting

$$\frac{1 + \alpha}{1 + \alpha^2} = 1 + 0.261\left(1 - \frac{a}{w}\right) \tag{8.16}$$

Rice et al. (61) have derived also equations with which J can be calculated from one single point on the P-v curve. The accuracy is doubtful however, and the result may serve only as a quick estimate.

9. ANALYTICAL DETERMINATION OF J AND J* USING NON-LINEAR STRESS-STRAIN RELATIONS

Rice and Hutchinson and several of their co-workers have calculated stresses and strains around the

tip of a stationary crack on the basis of a quasi-plastic, non-linear elastic relation between stress and strain

$$\frac{\sigma}{\sigma_0} = \left(\frac{\varepsilon}{\varepsilon_0}\right)^N \text{ or } \frac{\varepsilon}{\varepsilon_0} = \alpha \left(\frac{\sigma}{\sigma_0}\right)^m \tag{9.1}$$

and accounting for tri-axiality by means of the Von Mises effective stress

$$\sigma_e^{\,2} = \frac{3}{2} S_{ij} S_{ij} \tag{9.2}$$

where S_{ij} are the deviatoric stresses.

By working with polar coordinates around the crack tip, the J-integral can be calculated in a straightforward manner by integrating along a circular path.
It should be noted that in these analyses so-called deformation theory of plasticity has been used, which makes the results valid only for monotonically increasing stresses.
By replacing the above stress-strain relationship by the so-called Norton law

$$\frac{\dot{\varepsilon}}{\dot{\varepsilon}_0} = \beta \left(\frac{\sigma}{\sigma_0}\right)^n \tag{9.3}$$

the J*-integral can be calculated in an identical way by making use of the elastic analogue, although the equations have been derived for a non-growing crack.
The publications with which it all started are Rice and Rosengren (64) and Hutchinson (65, 66).
Hilton and Hutchinson (67) present the results by introducing plastic stress and strain intensity factors

$$\sigma_{ij} = K_\sigma \cdot r^{-\frac{1}{1+m}} \cdot \sigma^\infty{}_{ij}(\theta) \tag{9.4}$$

$$\varepsilon_{ij} = K_\varepsilon \cdot r^{-\frac{m}{1+m}} \cdot \varepsilon^\infty{}_{ij}(\theta) \tag{9.5}$$

where K_σ and K_ε are directly related to the elastic stress intensity factor

$$K_\sigma = c_m (K_{el}/\sqrt{\pi})^{\frac{2}{1+m}} \tag{9.6}$$

$$K_\varepsilon = (K_\sigma)^m \tag{9.7}$$

and $$c_m = \left(\frac{\pi}{I_m}\right)^{\frac{1}{1+m}} \tag{9.8}$$

I_m is a rather complicated integral tabulated by Hutchinson (66).
The authors have applied the analysis to a variety of specimen shapes and for the cases of plane strain as well as plane stress..

Goldman and Hutchinson (68) write

$$J = \alpha \sigma_0 \varepsilon_0 K_\sigma K_\varepsilon I_m \tag{9.9}$$

The analysis is applied to a flat strip of width 2w and a central crack 2a, loaded in plane strain by a stress σ^∞ at infinity. They also calculate the COD Δ in the axis of symmetry. The results are presented as functions of $\frac{a}{w}$ and m and they are normalized with respect to the parameters from the stress-strain relation, crack length and applied stress σ^∞ or strain ε^∞.
The equations are as follows

$$J = J_N\left(\frac{a}{w},m\right)\left\{\alpha^{-1/m}\sigma_0\varepsilon_0 a\left(\frac{\varepsilon^\infty}{\varepsilon_0}\right)^{1+m/m}\right\} = J_n\left(\frac{a}{w},m\right)\left\{\alpha\sigma_0\varepsilon_0 a\left(\frac{\sqrt{3}}{2}\right)^{1+m/m}\left(\frac{\sqrt{3}}{2}\frac{\sigma^\infty}{\sigma_0}\right)^{1+m}\right\} \tag{9.10}$$

$$\Delta = \Delta_N\left(\frac{a}{w},m\right)\left\{2\varepsilon_0 a \frac{\varepsilon^\infty}{\varepsilon_0}\right\} = \Delta_N\left(\frac{a}{w},m\right)\left\{2\varepsilon_0 a\alpha \frac{\sqrt{3}}{2}\left(\frac{\sqrt{3}}{2}\frac{\sigma^\infty}{\sigma_0}\right)^m\right\} \tag{9.11}$$

J is normalized also with respect to Δ

$$J = J_{N\Delta}\left(\frac{a}{w},m\right)\left\{\alpha^{-1/m}\sigma_0\varepsilon_0 a\left(\frac{w}{w-a}\right)^{1/m}\left(\frac{\Delta}{2\varepsilon_{0a}}\right)^{1+m/m}\right\} \tag{9.12}$$

Goldman and Hutchinson have calculated also the load line displacement v, and have split it up as $v = v_{cr} + v_{nocr}$ where $v_{nocr} = 2h\varepsilon^\infty$ and 2h is the strip length.
The results are presented as

$$v_{cr} = v_{crN} \cdot \Delta \tag{9.13}$$

The quantities J_N and Δ_N appear to depend strongly on $\frac{a}{w}$. Therefore they are normalized further with respect

to a and w.
The following forms have been chosen

$$J = J_{Naw}\left(\frac{a}{w},m\right)\left\{\alpha^{-1/m}\sigma_0\varepsilon_0 a\left(\frac{w}{w-a}\right)^m\left(\frac{\varepsilon^\infty}{\varepsilon_0}\right)^{1+m/m}\right\} = J_{Naw}\left(\frac{a}{w},m\right)\left\{\alpha\sigma_0\varepsilon_0 a\left(\frac{w}{w-a}\right)^m\left(\frac{\sqrt{3}}{2}\right)^{1+m/m}\left(\frac{\sqrt{3}}{2}\frac{\sigma^\infty}{\sigma_0}\right)^{1+m}\right\} \tag{9.14}$$

$$\Delta = \Delta_{Naw}\left(\frac{a}{w},m\right)\left\{2\varepsilon_0 a\left(\frac{w}{w-a}\right)^m \cdot \frac{\varepsilon^\infty}{\varepsilon_0}\right\} = \Delta_{Naw}\left(\frac{a}{w},m\right)\left\{2\varepsilon_0 a\alpha\left(\frac{w}{w-a}\right)^m \frac{\sqrt{3}}{2}\left(\frac{\sqrt{3}}{2}\frac{\sigma^\infty}{\sigma_0}\right)^m\right\} \tag{9.15}$$

The numerical results are presented in table 2.
Shih and Hutchinson (69) have continued the work. They consider a flat strip with central crack in plane stress. They normalize their results with respect to load P per unit thickness and a reference value P_0

$$J = g_1\left(\frac{a}{w},m\right)\left\{\alpha\sigma_0\varepsilon_0 a\left(1-\frac{a}{w}\right)\left(\frac{P}{P_0}\right)^{m+1}\right\} \tag{9.16}$$

$$\Delta = g_2\left(\frac{a}{w},m\right)\left\{\alpha\varepsilon_0 a\left(\frac{P}{P_0}\right)^m\right\} \tag{9.17}$$

$$v_{cr} = g_3\left(\frac{a}{w},m\right)\left\{\alpha\varepsilon_0 a\left(\frac{P}{P_0}\right)^m\right\} \tag{9.18}$$

Note that $P = 2w\sigma^\infty$ and that $\frac{P}{P_0} = \frac{\sigma^\infty w}{\sigma_0(w-a)}$ (9.19, 9.20)

Numerical values are given in table 3.
The results in their present form do not allow interpolation for $m > 10$ and to the limit values $\frac{a}{w} = 0$ and $\frac{a}{w} = 1$. An adapted way of normalizing is suggested by Amazigo's exact solution for the anti-plane shear case. This leads to the equation

$$G\left(\frac{a}{w},m\right) = g_1\left(\frac{a}{w},m\right)\left[\frac{1+\xi(m-1)\frac{a}{w}}{c\sqrt{m}\left(1-\frac{1}{m}\right)+g_1\left(\frac{a}{b},1\right)\frac{1}{m}}\right] \tag{9.21}$$

The result is that $G(\frac{a}{w},m)$ varies far less strongly with $\frac{a}{w}$ and m than $g_1(\frac{a}{w},m)$ and thereby allows extrapolation.
Shih and Hutchinson state that the calculations presented so far are good approximations for the case of "large scale yielding" where the contributions from elasticity can be be neglected.
For the elastic-plastic case they propose to add the linear elastic to the non-linear elastic solution.
The linear elastic solution is of course a special case of the non-linear elastic one.
Symbolically

$$J = J(a = a_e, m = 1) + J(a,m) \tag{9.22}$$

Note that they apply the Irwin correction in the elastic case, i.e. $a_e = a + r_Y$.
In the present notation

$$\frac{r_Y}{a} = \frac{1}{2\pi}\cdot\frac{m-1}{m+1}\cdot\frac{w-a}{a}\cdot g_1\left(\frac{a}{w},1\right)\left(\frac{P}{P_0}\right)^2 \tag{9.23}$$

This leads to the following equations

$$\frac{J}{\sigma_0\varepsilon_0 a\left(1-\frac{a}{w}\right)} = \psi\cdot g_1\left(\frac{a_e}{w},1\right)\left(\frac{P}{P_0}\right)^2 + \alpha g_1\left(\frac{a}{w},m\right)\left(\frac{P}{P_0}\right)^{m+1} \tag{9.24}$$

$$\frac{\Delta}{\varepsilon_0 a} = \psi\cdot g_2\left(\frac{a_e}{w},1\right)\frac{P}{P_0} + \alpha g_2\left(\frac{a}{w},m\right)\left(\frac{P}{P_0}\right)^m \tag{9.25}$$

$$\frac{v_{cr}}{\varepsilon_0 a} = \psi\cdot g_3\left(\frac{a_e}{w},1\right)\frac{P}{P_0} + \alpha g_3\left(\frac{a}{w},m\right)\left(\frac{P}{P_0}\right)^m \tag{9.26}$$

Here:

$$a_e = a + r_Y \text{ for } P \le P_0 \tag{9.27}$$

$$a_e = \left(a_e\right)_{P=P_0} \text{ for } P > P_0 \tag{9.28}$$

$$r_Y = \frac{1}{2\pi}\frac{m-1}{m+1}\left(\frac{K_I}{\sigma_0}\right)^2 \tag{9.29}$$

$$\psi = \frac{a_e}{a}\cdot\frac{w-a}{w-a_e} \tag{9.30}$$

Results of calculations using these equations are reported to agree well with results of FEM calculations.
Shih and Hutchinson (69) have considered also the single edge crack strip loaded in bending in the plane

strain condition. The width of the uncracked ligament is b = w - a.
For reasons of brevity only the equations for the elastic-plastic case are presented here.

$$\frac{J}{\sigma_0 \varepsilon_0 b} = \psi^3 h_1\left(\frac{a}{w}, 1\right)\left(\frac{M}{M_0}\right)^2 + \alpha h_1\left(\frac{a}{w}, m\right)\left(\frac{M}{M_0}\right)^{m+1} \tag{9.31}$$

$$\frac{\Delta}{\varepsilon_0 a} = \psi^2 \frac{a}{a} h_2\left(\frac{a}{w}, 1\right) \frac{M}{M_0} + \alpha h_2\left(\frac{a}{w}, m\right)\left(\frac{M}{M_0}\right)^m \tag{9.32}$$

$$\frac{\theta_{cr}}{\alpha \varepsilon_0} = \psi^2 h_3\left(\frac{a}{w}, 1\right) \frac{M}{M_0} + \alpha h_3\left(\frac{a}{w}, m\right)\left(\frac{M}{M_0}\right)^m \tag{9.33}$$

Note that θ_{cr} is the contribution of the crack to the relative rotation of the ends of the strip.
Some results of a FEM analysis for $\frac{a}{w} = 0.5$ are presented below.

	m = 1	m = 2	m = 3	m = 5	m = 7	m = 10
h_1	1,104	0,957	0,851	0,717	0,653	0,551
h_2	5,129	3,640	2,947	2,255	1,953	1,606
h_3	2,749	2,359	2,032	1,590	1,373	1,121

Also in this case there was good agreement between results of analytical and of FEM calculations.

Kumar and Shih (70) have applied the Shih and Hutchinson analysis to the creeping CT specimen in plane stress and in plane strain.
They present the equations

$$J^* = h_1\left(\frac{a}{w}, n\right)\left\{\beta \sigma_0 \dot{\varepsilon}_0 b \left(\frac{P}{P_0}\right)^{n+1}\right\} \tag{9.34}$$

$$\dot{\Delta} = h_2\left(\frac{a}{w}, n\right)\left\{\beta \dot{\varepsilon}_0 a \left(\frac{P}{P_0}\right)^n\right\} \tag{9.35}$$

$$\dot{v}_{cr} = h_3\left(\frac{a}{w}, n\right)\left\{\beta \dot{\varepsilon}_0 a \left(\frac{P}{P_0}\right)^n\right\} \tag{9.36}$$

Here:

$$P_0 = 1{,}455\ \eta b \sigma_0 \quad \text{(plane strain)} \tag{9.37}$$

$$P_0 = 1{,}072\ \eta b \sigma_0 \quad \text{(plane stress)} \tag{9.38}$$

$$\eta = \left\{\left(\frac{2a}{b}\right)^2 + 2\left(\frac{2a}{b}\right) + 2\right\}^{\frac{1}{2}} - \left\{\frac{2a}{b} + 1\right\} \tag{9.39}$$

Results of their calculations are presented in tables 4 and 5. In another publication (71) the authors give the same tables but then relating to time independent plastic deformation. In the latter publication they also treat the elastic-plastic case in the way discussed before.

An interesting question is whether values for J and J* calculated from the above analyses agree with values determined from P-v diagrams or P-$\dot{v}$ diagrams.
Saxena (54) has compared the results from both techniques using creep law parameters reported in the literature. He found discrepancies between the derived J* values to range from 8 to 40 %, which is not bad at all, considering the many possible sources of error.

10. VARIOUS OTHER WAYS TO CALCULATE J AND J*

Nikbin, Webster and Turner (50) have calculated J and J* for a Contoured Double Cantilever Beam specimen.
They assume the non-linear stress-strain relation

$$\frac{\varepsilon}{\varepsilon_0} = \alpha\left(\frac{\sigma}{\sigma_0}\right)^m \tag{10.1}$$

Webster has shown that for a material that obeys this law J can be calculated as

$$J = \frac{P}{B_n(m+1)} \cdot \frac{dv}{da} \tag{10.2}$$

The quantity $\frac{dv}{da}$ is calculated for a cantilever beam of length a and the final result is

$$J = \frac{2(\alpha \varepsilon_0 \sigma_0^{-m})}{B_n(m+1)} \cdot \left\{\frac{2m+1}{2mB}\right\}^m \cdot \frac{(aP)^{m+1}}{(h/2)^{2m+1}} \tag{10.3}$$

Here B and B_n are the nominal thickness and the local thickness in the side groove and h is the local beam height.
For a material that obeys Norton's law

$$\frac{\dot{\varepsilon}}{\dot{\varepsilon}_0} = \beta\left(\frac{\sigma}{\sigma_0}\right)^n \tag{10.4}$$

there is found similarly

$$J^* = \frac{2(\beta\dot{\varepsilon}_0\sigma_0^{-n})}{B_n(n+1)}\left\{\frac{(2n+1)}{2nB}\right\}^n \frac{(aP)^{n+1}}{(h/2)^{2n+1}} \tag{10.5}$$

These equations will not be very accurate. Similar calculations have been made for stress corrosion specimens strained elastically and important errors were found to result from ignoring the deformation by shear and the lack of rigidity at the "clamped" cross section at the crack tip.
Branco and Radon (53) have refined the above analysis by considering elastic and creep deformation in both bending and shear. They also account for the crack tip influence by adding an extra elastic deformation in bending calculated by assuming that the beam is clamped at a distance ½ b from the crack tip inside the ligament b.
Nikbin et al. (72) give an approximate solution for J* starting with the equation

$$J^* = \frac{P}{B_n(n+1)}\frac{d\dot{v}}{da} \tag{10.6}$$

They assume that

$$\dot{v} = \frac{1}{B} \cdot a^{\eta} \cdot g(P) \tag{10.7}$$

so that

$$\frac{d\dot{v}}{da} = \eta\frac{\dot{v}}{a} \tag{10.8}$$

and thus

$$J^* = \frac{\eta \cdot P \cdot \dot{v}}{a \cdot B_n(n+1)} \tag{10.9}$$

Harper and Ellison (51) calculate J* using a method based on the reference stress concept. They assume that during creep the stress distribution is the same as at limit load. This enables then to calculate the quantity U* (see section 7), which after differentation with respect to a gives

$$J^* = \frac{-n}{n+1} \cdot \frac{P\dot{v}}{Bw} \cdot \left[\frac{1}{\mu} \cdot \frac{d\mu}{d(a/w)}\right] \tag{10.10}$$

For the usual large values of n this approximates to

$$J^* = -\frac{P\dot{v}}{Bw}\left[\frac{1}{\mu} \cdot \frac{d\mu}{d(a/w)}\right] \tag{10.11}$$

For bend specimens there is found similarly

$$J^* = \frac{M\dot{\theta}}{Bw}\left[\frac{1}{\mu} \cdot \frac{d\mu}{d(a/w)}\right] \tag{10.12}$$

Here μ is the ratio of the yield load for a cracked specimen to that for an uncracked specimen. Values of μ as a function of (a/w) have been compiled for a variety of specimens by CEGB in the U.K.

Koterazawa and Mori (55) start with an equation for J* analgous to one for J used by Rice (section 8)

$$J^* = \frac{1}{B}\int_0^P \frac{\partial\dot{v}}{\partial a}\,dP \tag{10.13}$$

In further analogy they write for a double edge crack specimen

$$\dot{v} = bf(P/Bb) \tag{10.14}$$

and on the basis of Norton's law:

$$\dot{v} = Cb(P/Bb)^n \tag{10.15}$$

where C is a constant.

From the first equation they find

$$J^* = \frac{1}{n+1}\frac{P}{B}\left(\frac{\partial \dot{v}}{\partial a}\right)_{P=\text{const.}} \tag{10.16}$$

and finally

$$J^* = \frac{n-1}{n+1}\frac{P\dot{v}}{Bb} \tag{10.17}$$

For large n this reduces to

$$J^* = \frac{P\dot{v}}{Bb} \tag{10.18}$$

This equation holds also for a centre crack flat specimen.
Similar equations have been derived, for a circumferentially notched round specimen

$$J^* = Pv/\pi r^2 \tag{10.19}$$

(where 2r is the diameter of the ligament) and for a compact tension specimen

$$J^* = \frac{2P\dot{v}}{Bb} \tag{10.20}$$

Taria et al (58) use similar equations developed by Ohji.
For the centre crack flat specimen they write

$$J^* = \frac{n-1}{n+1}\sigma_{net}\dot{\Delta} \tag{10.21}$$

and for the circumferentially notched round one

$$J^* = \frac{2n-1}{2n+1}\sigma_{net}\dot{\Delta} \tag{10.22}$$

Here $\dot{\Delta}$ is the COD rate at the axis of symmetry in the first case, and the COD rate at the outer surface in the second case.

Musicco et al. (73) have compared various different methods to determine J*. These include the Hutchinson approach leading to an equation of the form

$$J^* = A_n \cdot a \cdot \left(\frac{\sigma^\infty}{\sigma_0}\right)^{n+1} \cdot \hat{J}\left(\frac{a}{w}, n\right) \tag{10.23}$$

The Landes and Begley graphical method based on

$$J^* = -\frac{dU^*}{da} \tag{10.24}$$

the Ohji et al. simplified equation (see also eq. 10.17)

$$J^* = g(n)\frac{P}{B(w-a)}\dot{v} \tag{10.25}$$

the Harper and Ellison formula (see also eq. 10.10)

$$J^* = h(n,\mu)\frac{P}{Bw}\dot{v} \tag{10.26}$$

and an equation derived by Musicco and Bernasconi

$$J^* = g(n) \cdot \sigma_0 \cdot \dot{\delta} \tag{10.27}$$

They applied these to CT specimens of 304 type stainless steel tested at 550 °C in argon. They observed a fair agreement for the various formulae and with test results reported by Saxena.

11. THEORETICAL PREDICTIONS OF THE CRACK PROPAGATION RATE

Various authors have derived equations relating the crack propagation rate to a parameter such as K,

G, σ_{net} or J*.
These analyses do not give proof that the parameter in question really determines the crack propagation rate. Often assumptions are made that lead to the result envisaged.
For the sake of completeness the formulae will be presented. For their derivation the reader is referred to the original publications.
Landes and Wei (36) start with Krafft's ligament model and apply equations derived by Rice, Rosengren and Hutchinson (section 9). They arrive at the formula

$$\frac{da}{dt} = \dot{\varepsilon}_{min}\left\{\frac{K_c}{\sigma_Y\sqrt{\pi}}\right\}^2 \cdot (0{,}75\ N\varepsilon_Y)^{\frac{N+1}{N}} (N+1) \cdot \left[1 - \left(\frac{K}{K_c}\right)^{\frac{2N}{N+1}}\right]^{-1} \tag{11.1}$$

Here K_c is the critical stress intensity factor and $\dot{\varepsilon}_{min}$ is the secondary creep rate in a point at a distance $\bar{d}_T$ from the crack tip.

$$\bar{d}_T = \left\{\frac{K_c}{\sigma_Y\sqrt{\pi}}\right\}^2 (0{,}75\ N\varepsilon_Y)^{\frac{N+1}{N}} \tag{11.2}$$

Taira and Ohtani (29) have made a phenomenological analysis involving grain boundary creep rate, crack nucleation rate and fracture strain, and a typical length ρ^* measured from the crack tip.
The result is

$$\frac{da}{dt} = b_{gb}c_1c_2(\rho^*)^{-1}\int_0^{\rho^*} \sigma^{*\alpha_{gb}} dx \tag{11.3}$$

Here b_{gb}, c_1, c_2 and α_{gb} are constants.

Barnby (74, 75) applies Hoff's elastic analogue and Norton's law to calculate stresses near the crack tip. He assumes the crack propagation rate to be proportional with the creep rate at a characteristic distance from the crack tip. He arrives at the formulae

$$\frac{da}{dt} = \varepsilon_0'\left(\frac{\sigma_{net}}{\sigma_0}\right)^m \tag{11.4}$$

$$\frac{da}{dt} = \varepsilon_0'\left(\frac{2m-1}{2m} \cdot \frac{2K''}{\sigma_0(2\pi)^{0,5}}\right\} (w-a)^{\frac{1-m}{2}} \tag{11.5}$$

Here ε_0' is an empirical constant and K" is a stress intensity factor under creep conditions.

Barnby and Nicholson (76) use Neuber's rule in addition to Hoff's elastic analogue and Norton's law to calculate stresses. They take the crack propagation rate to be proportional to the deformation rate of an element of length L orthogonal to the crack and at a distance d_c from the critical tip. This leads to the result

$$\frac{da}{dt} = LB\left[\frac{(K')}{(EB2\pi d_c)^{0,5}}\right]^{\frac{2n}{n+1}} \tag{11.6}$$

Ohji (4) and Kubo et al. (77) consider a creep crack loaded in mode III (anti-plane shear). They calculate shear stresses using equations by Hutchinson et al. and Norton's law, and they introduce Kachanov's damage parameter concept by writing the damage accumulation rate as

$$\dot{\eta} = A \cdot \tau^b \tag{11.7}$$

The crack is assumed to grow in a stepwise manner over a length ρ each time the accumulated damage at the crack tip reaches a critical value.
The final result depends strongly on the relative values of the exponent b and n the exponent in Norton's law.

b/(n + 1) > 1

$$\frac{da}{dt} = A\left\{\frac{2n}{\pi(n+1)} \cdot \frac{\tau_0}{\dot{\gamma}_0}\right\}^{n\frac{b}{n+1}} \cdot \zeta\left(\frac{b}{n+1}\right) \cdot \rho^{1-\frac{b}{n+1}} \cdot (J^*)^{\frac{b}{n+1}} \tag{11.8}$$

Here ζ is Riemann's zeta function.

b/(n + 1) = 1

$$\frac{da}{dt} = A \cdot \frac{2n}{\pi(n+1)} \cdot \frac{\tau_0^n}{\dot{\gamma}_0} \cdot \ln\left[\frac{(a-a_0)}{\rho}\right] \cdot J^* \tag{11.9}$$

$$a - a_0 >> \rho$$

b/(n + 1) < 1

$$\frac{da}{dt} = A \cdot \Gamma\left(\frac{b}{n+1}\right) \cdot \Gamma\left(1 - \frac{b}{n+1}\right) \cdot \left\{\frac{2n}{\pi(n+1)} \frac{\tau_0^n}{\dot{\gamma}_0}\right\}^{\frac{b}{n+1}} * (a-a_0)^{1-\frac{b}{n+1}} \cdot (J^*)^{\frac{b}{n+1}} \tag{11.10}$$

$$a - a_0 >> \rho$$

Here Γ is the gamma function.
Freeman (78) calculates the crack propagation rate as a function of the reference stress defined as

$$\sigma_{ref} = \frac{P}{\mu B_s w} \tag{11.11}$$

where μ is the usual ratio of yield loads and where B_s and w are specimen thickness and width.
For the single edge crack tension specimen (SENT)

$$\mu = \left(1 - \frac{a}{w}\right)^2 \tag{11.12}$$

Experimentally it was found that σ_{ref} varies with time according to the equation

$$\sigma_{ref}{}^{p}(t_{RO} - t) = Z \tag{11.13}$$

Here t_{RO} is the rupture time associated with the initial value of σ_{ref} and is related to rupture stress σ_R according to the empirical formula:

$$\sigma_R{}^{p} \cdot t_R = Z \tag{11.14}$$

The result is

$$\frac{da}{dt} = \frac{1}{2p} \cdot \frac{w^{0.5} \cdot P^{0.5}}{B_s{}^{0.5} Z} \cdot \sigma_{ref}{}^{(2p-1)/2} \tag{11.15}$$

For the compact tension specimen there is found similarly:

$$\frac{da}{dt} = \frac{1}{1.15p} \cdot \frac{w^{0.5} \cdot P^{0.5}}{B_s{}^{0.5} Z} \cdot \sigma_{ref}{}^{(2p-1)/2} \tag{11.16}$$

Using concepts from the reference stress method, Freeman relates creep and elastic CODs of the SENT specimen to creep and elastic strains of a creep specimen.
Using the elastic analogue and Norton's law he then calculates the creep COD rate as a function of reference stress

$$\dot{v}_c = P \cdot C(a/w) \cdot \frac{B_N}{B_s} \cdot \sigma_{ref}{}^{n-1} \tag{11.17}$$

Here C(a/w) is the non-dimensional compliance and B_N is the Norton law constant

$$C(a/w) = CEB_s = \frac{v}{P} \cdot EB_s \tag{11.18}$$

Crack propagation rate can now be related to creep COD rate for the SENT specimen as

$$\frac{da}{dt} = \frac{1}{2p} \frac{w^{0.5} P^{0.5}}{B_s{}^{0.5} Z} \left[\frac{B_s \dot{v}c}{B_N \cdot P \cdot C(a/w)}\right]^{\frac{2p-1}{2n-2}} \tag{11.19}$$

and for the CT specimen as:

$$\frac{da}{dt} = \frac{1}{1.15p} \cdot \frac{w^{0.5} P^{0.5}}{B_s{}^{0.5} Z} \cdot \left[\frac{B_s \dot{v}_c}{B_N \cdot P \cdot C(a/w)}\right]^{\frac{2p-1}{2n-2}} \tag{11.20}$$

Radhakrishnan et al. (46) treat the single edge crack bend specimen and relate the incremental COD to the increment of the non-dimensional crack length λ = (a/w) as

$$d\delta = Ak \cdot \sigma_{tip}{}^{m} \cdot d\lambda \tag{11.21}$$

where A and k are constants.
They than calculate stresses near the crack tip by taking four terms instead of the usual first one of the LEFM series expansion of stress as a function of distance to the crack tip and the distance from the crack tip to the neutral axis. Bending moment and load P are introduced through the equilibrium equation. This leads to the equation

$$d\delta = \bar{A}\left\{\frac{P}{4B}(1 + \lambda)\left(\frac{1 - \lambda}{2}\right)^{-2 + \frac{1}{2n}} (GF)\right\}^{m} (d\lambda)^{1 - \frac{m}{2n}} \tag{11.22}$$

Here n is the exponent from Norton's law and (GF) is an expression containing gamma functions of arguments

containing n.
The authors state that consequently the following equation must also hold

$$\frac{d\delta}{dt} = A^{*}\left(\frac{P}{P_0}\right)^{m}\left(\frac{d\lambda}{dt}\right)^{1-\frac{m}{2n}} \tag{11.23}$$

and that finally

$$\frac{d\lambda}{dt}(:)\left\{\frac{d\delta}{dt}\left(\frac{\sigma_0}{\sigma_g}\right)^{m}\right\}^{\frac{2n}{2n-m}} \tag{11.24}$$

Here σ_g is the initial value of the nominal bending stress due to P. These equations are the basis of the correlating parameter used in figure 17.

Rice et al (79) have analysed stresses and strains at the tip of a growing crack on the basis of Prandtl's slip line field theory. They present the formula

$$\frac{d}{dt}\delta_r = \frac{\alpha}{\sigma_0}\frac{d}{dt}J + \beta\frac{\sigma_0}{E}\frac{da}{dt}\ln\frac{R}{r} \tag{11.25}$$

Here δ_r is the COD at a distance r behind the crack tip. The constants α, β and R were determined by comparison to results of a FEM analysis. It was found that

$\alpha = 0{,}65$, $\beta = 5{,}08$ and

$$R = 0{,}2\frac{EJ}{\sigma_0^2} \tag{11.26}$$

Purushothaman and Tien (80) assume an Orowan-Irwin elastic stress distribution at the crack tip. They take it that for any line element dx in front of the crack tip there will be a rupture time $t_R(x)$ determined by the local stress and that the crack propagation rate can be calculated as

$$\frac{da}{dt} = \frac{dx}{dt_R}\Big/_{\text{at the crack tip}} \tag{11.27}$$

Rupture time is calculated from the empirical equation

$$t_R = B_R(\dot{\varepsilon}_{min})^{-\alpha} \tag{11.28}$$

and minimum creep rate from the phenomenological equation

$$\dot{\varepsilon}_{min} = B_N\left\{\frac{\sigma(x)}{E(T)}\right\}^{n}\exp\frac{-Q_c}{RT} \tag{11.29}$$

The result is

$$\frac{da}{dt} = \frac{2B_N^{\alpha}}{\alpha n B_R}\cdot\rho^{1-\frac{\alpha n}{2}}\left\{\frac{K}{YE\pi^{0.5}}\right\}^{\alpha n}\exp\frac{-\alpha Q_c}{RT} \tag{11.30}$$

Here ρ is the crack tip radius and Y is the function Y(a/w) from the relation

$$K = Y\cdot\sigma(\pi a)^{0.5} \tag{11.31}$$

It should be noted that the use of the debatable relation between rupture time and minimum creep rate is not necessary since one can use a phenomenological equation directly relating rupture time to stress and temperature.

Van Leeuwen (2, 3) has considered the diffusion of vacancies towards the crack tip and related the chemical potential of a vacancy at the crack tip to the rate of energy dissipation G.
The result is

$$\frac{da}{dt} = \frac{D\Omega}{R}(C_t - C_w)\frac{\lambda_{11}J_1\left(\lambda_{11}\frac{a}{R}\right)}{1 - J_0\left(\lambda_{11}\frac{a}{R}\right)} \tag{11.32}$$

Here $(C_t - C_w)$ is the difference between the vacancy concentrations at the crack tip and the crack wall

$$\frac{C_t - C_w}{C_0} = \exp\frac{p\Omega - \gamma\Omega\left(\frac{1}{\rho_t} + \frac{1}{a}\right) + G(a)\Omega^{2/3}}{kT} - \exp\frac{p\Omega}{kT} \tag{11.33}$$

C_0 is the vacancy concentration at infinity
p is numerically equal to the nominal tensile stress normal to a circular embedded crack with diameter 2a.
γ is the surface tension
ρ_t is the crack tip radius

Ω is the atomic volume
D is the diffusion constant
R is the average distance between crack nuclei
k is Boltzmann's constant
T is the absolute temperature
J_0 and J_1 are Bessel functions of the first kind
λ_{11} is the first root of the equation $J_1(\lambda) = 0$

Henshall et al. (31) consider creep crack growth by vacancy diffusion using equations derived by Vitek and by Speight and Beere respectively.
In the first case there is found

$$\frac{da}{dt} = \frac{0.516\ \lambda}{d_c^4} \left(\frac{K}{\mu}\right)^4 \tag{11.34}$$

Here

$$\lambda = \frac{D_B \delta_B \Omega \mu}{kT} \tag{11.35}$$

D_B is the coefficient of self diffusion for the grain boundary
δ_B is the width of the grain boundary
Ω^B is the atomic volume
μ is the shear modulus
k is Boltzmann's constant
T is the absolute temperature
d_c is the width of the crack

In the second case there is found

$$\frac{da}{dt} = \frac{0.63\ \lambda}{\mu} \cdot \sigma^{\frac{n+2}{2}} \cdot \left\{\frac{BkT}{D_B \gamma \Omega^{4/3}}\right\}^{\frac{1}{2}} \tag{11.36}$$

Here n and B are constants from Norton's law and γ is the surface tension.

12. DISCUSSION, CONCLUSIONS AND RECOMMENDATIONS

It has been found that linear elastic fracture mechanics can be applied sucessfully to the residual strength of brittle materials, crack growth due to stress corrosion and crack growth due to fatigue. Even then the stress intensity factor K is not the sole parameter determining residual strength or crack propagation rate. The relationships are influenced by some additional geometric and environmental parameters. Therefore it is not realistic to expect that the growth rate of creep cracks will be determined by one single fracture mechanics parameter.
With the methods to account for plasticity in residual strength problems a return is discernible from the stress-oriented K-based approached to the energy-oriented approach based on G, R or J. Therefore it may be expected that the crack growth rate under creep conditions will correlate well with a parameter directly related to the dissipation of energy.

In the case that a stress-oriented approach is selected nevertheless, the redistribution of stresses due to creep and stress relaxation has to be accounted for. The K factor then loses the greater part of its relevance.
Notable is the erratic success of K, σ_{net} and σ_{ref} as a correlating parameter for crack growth rate.
The expectation is not borne out that in the cases of nominally brittle materials or narrow intercrystalline cracks the K-factor will do better than σ_{net} or σ_{ref}. The specimen geometry plays an important role. If it is such that lateral contraction at the crack tip is highly constrained, then the energy dissipated will be spent much more on crack propagation than on plastic deformation and the crack propagation rate will correlate fairly well with K. If correlation is bad, this means that the relation of da/dt with K or σ_{net} is influenced heavily by specimen shape or dimensions and the initial values of crack length or load. Sometimes a better correlation is obtained by working with the relative crack length a/w or by incorporating rupture time or load in the correlation parameter. These seem to be tricks that will work only under limited conditions.
Because COD and COD rate are closely related to energy dissipation it can be expected that they will correlate well with the crack propagation rate, it being understood the re-initiation of a crack will probably occur at a critical value of δ and that afterwards da/dt will correlate with $d\delta/dt$. In practice this will be of little use because of the lack of fast methods to calculate δ and $d\delta/dt$ for a crack in a structural element, with the aim to predict da/dt. Some use can be made nevertheless of the approximate expressions for G, J and J* applicable to certain specimens and containing δ and $d\delta/dt$.
A static quantity like K, σ_{ref}, G or J seems to be better suited for predictive purposes than a dynamic quantity such as $d\delta/dt$ or J*.
Coleman et al. (81) have been fairly successful in correlating the growth rate of creep cracks in pressure vessels with K and σ_{net}.
It is remarkable that relatively few attempts have been made to correlate da/dt with J, and that much more is expected from the dynamic parameter J*. It should be considered that in order to calculate J* one needs values of creep rates and deformation rates and that these in their turn will be determined by static quantities like σ_{ref} or J. Then, nobody challenges the fact that creep rate will be determined by a static quantity like stress σ.
It is recommended therefore to put more effort in attempts to correlate da/dt with J.
An interesting development is that attempts are already made to correlate the crack growth rate in high temperature fatigue with J. (Saxena and Shahinian, 82). It is a fortunate fact that so many alternative

and fast methods are available to calculate J and J*. The extent of agreement in their results is encouraging.
In addition it is felt that parameters like dJ/da, dδ/da and even dJ*/da merit more attention.
The literature has shown that da/dt correlates rather well with J* although the specemen geometry still seems to have some influence.
Riedel (83) and Riedel and Rice (84) define a creep zone in analogy with the plastic zone. Its boundary is the locus of points where creep strain equals elastic strain. The creep zone grows with time.
Riedel and Rice state that at the start of the creep cracking process the creep zone will be small and that then K will be determining. Lateron the creep zone will be relatively large and then J* will be determining.
The present author is rather opposed to a discontinuous approach like that. It is the demonstration of a desire to keep on using the K-factor whenever possible and pushing it to or even beyond its limits of applicability. It should be remembered that the K-factor strictly speaking is relevant only under the conditions that
- the deformations are elastic
- the crack is not too small relative to typical dimensions of the cracked body
- the problem is two-dimensional.

If these conditions are not fulfilled it is better to depart from the stress-oriented K-based approach and to return to an energy-oriented approach based on parameters like J or J*.
If the conditions are fulfilled one can nevertheless take the energy-oriented approach since then K is so closely related to G and J.

A very important complication in the application of fracture mechanics to creep cracks is that the materials properties of the structures considered are influenced so heavily by processing (welding and heat treatment) and by accumulated creep and high-temperature exposure (cavitation and ageing). Therefore, if creep growth parameters are determined experimentally, this will have to be done on material that has undergone a representative pre-treatment. Examples can be found in Siverns and Price (42, 85), Neate and Siverns (20), Neate (22), Gooch (26, 27, 48), Gooch and King (86), Ritter and Formby (87), Worswick and Pilkington (41, 52, 88), Christian et al. (59).

Finally it has to be noted that in the present review of the literature it has been assumed tacitly that failure of a high-temperature structure is initiated by formation and growth of a single or dominant crack. This will not always be the truth. Another failure mode consists of creep cavitation, i.e. the formation of micro-pores at critical locations. These voids will grow by plastic deformation and/or vacancy diffusion until the cross section has been weakened to such an extent that rupture occurs by overload. A critical review of the literature concerning void growth by vacancy diffusion has been given by Van Leeuwen among others (2). A model to predict the residual strength of a material weakened by voids has been developed by Scott et al. (89).
Relevant to this problem is the analysis by Van Elst (90) who considered an array of defects or cracks rather than a single or dominant one. He has based his approach on an analysis by Koiter concerning a linear periodic array of through cracks of size a and distance d leading to a representatitve stress intensity factor

$$K = \sigma(2d \cdot \tan \frac{\pi}{2} \lambda)^{0.5} \qquad (12.1)$$

where $\lambda = (a/d)$. A finite element analysis of a two dimensional array of parallel through crack, length a, at mutual distances $d_1 \approx d_2 \approx d$ has shown a similar tangent-like dependence of the effective K factor on $\lambda = (a/d)$. This analysis is now being extended to three-dimensional arrays.

13. REFERENCES

1. Haigh, J.R. — The mechanisms of macroscopic high temperature crack growth. Part II: Review and re-analysis of previous work. Materials Science and Engineering, Vol. 20, 1975, pp. 225-235.

2. Van Leeuwen, H.P. — The application of fracture mechanics to creep crack growth. Engineering Fracture Mechanics, Vol. 9, 1977, pp. 951-974.

3. Van Leeuwen, H.P. — Fracture mechanics applied to creep cracking. NLR MP 77020 U, 1977.

4. Ohji, K. — Nonlinear fracture mechanics approach to creep crack growth problems. Theoretical and Applied Mechanics, Vol. 27, 1977, pp. 3-20.

5. Ellison, E.G. and Harper, M.P. — Creep behaviour of components containing cracks - A critical review. Journal of Strain Analysis, Vol. 13, No. 1, 1978, pp. 35-51.

6. Ashby, M.F. and Tomkins, B. — Micromechanisms of fracture and elevated temperature fracture mechanics. Mechanical Behaviour of Materials, ICM-3, Cambridge, England, 1979, Vol. 1, pp. 47-89.

7. Pilkington, R. — Creep crack growth in low-alloy steels. Metal Science, Vol. 13, 1979, pp. 555-564.

8. Fu, L.S. — Creep crack growth in technical alloys at elevated temperature - A review. Engineering Fracture Mechanics, Vol. 13, 1980, pp. 307-330.

9. Radhakrishnan, V.M. and McEvily, A.J. — A critical analysis of crack growth in creep. Transactions of the ASME, Journal of Engineering Materials and Technology, Vol. 102, 1980, pp. 200-206.

10. Sahananda, K. and Shahinian, P. — Review of the fracture mechanics approach to creep crack growth in structural alloys. Engineering Fracutre Mechanics, Vol. 15, No. 3-4, 1981, pp. 327-342.

11. Eftis, J. and Liebowithz, H. — On fracture toughness evaluation for semi-brittle fracture. Engineering Fracture Mechanics, Vol. 7, 1975, pp. 101-135.

12. Sullivan, A.M. and Freed, C.N. — A review of the plane-stress fracture mechanics parameter K_c determined using the center-cracked tension specimen. Naval Research Laboratory Report 7460, 1972.

13. Speidel, M.O. — Current understanding of stress corrosion crack growth in aluminium alloys. The Theory of Stress Corrosion Cracking in Alloys. NATO Scientific Affairs Division, Brussels, 1971, pp. 289-344.

14. Speidel, M.O. — Corrosion-fatigue crack growth in high-strength aluminium alloys with and without susceptibility to stress-corrosion. Fifth International Congress on Metallic Corrosion, Tokyo, Japan, 1972.

15. Landes, J.D. and Begley, J.A. — A fracture mechanics approach to creep crack growth. ASTM STP 590, 1976, pp. 128-148.

16. De Koning, A.U. — A contribution to the analysis of slow stable crack growth. Euromech Colloquium 64, Stockholm, 1975, NLR MP 75035 U.

17. Shih, C.F., Andrews, W.R. and Wilkinson, J.P.D. — Characterization of crack initiation and growth with applications to pressure vessel steels. Mechanical Behaviour of Materials, ICM-3, Cambridge, England, 1979, Vol. 3, pp. 589-601.

18. Gudas, J.P., Joyce, J.A. and Vanderveldt, H.H. — J-integral elastic-plastic fracture mechanics technology in the U.S. Navy. Mechanical Behaviour of Materials, ICM-3, Cambridge, England, 1979, Vol. 3, pp. 579-587.

19. Ellison, E.G. and Walton, D. — Fatigue, creep and cyclic creep crack propagation in a 1 Cr-Mo-V steel. International Conference on Creep and Fatigue in Elevated Temperature Applications, Philadelphia, 1973, Sheffield UK, 1974, Paper C173/73.

20. Neate, G.J. and Siverns, M.J. — The application of fracture mechanics to creep crack growth. International Conference on Creep and Fatigue in Elevated Temperature Applications, Philadelphia 1973, Sheffield UK 1974, Paper C234/73.

21. Nicholson, R.D. and Formby, C.L. — The validity of various fracture mechanics methods at creep temperatures. International Journal of Fracture, Vol. 11, No. 4, 1975, pp. 595-604.

22. Neate, G.J. — Creep crack growth in ½ % Cr--½ % Mo-¼ % V steel at 565 °C. Engineering Fracture Mechanics, Vol. 9, 1977, pp. 297-306.

23. Neate, G.J. — The effect of size and geometry on the creep cracking behaviour of normalized and tempered 0.5 Cr-Mo-V steel at 565 °C. Materials Science and Engineering, Vol. 33, 1978, pp. 165-173.

24. Robson, K. — Creep crack growth in two carbon steels at 450 °C. International Conference on Properties of Creep Resistant Steels, Düsseldorf, 1972, Paper 4.5.

25. Haigh, J.R. — The mechanisms of macroscopic high temperature crack growth. Part I: Experiments on tempered Cr-Mo-V steels. Materials Science and Engineering, Vol. 20, 1975, pp. 213-223.

26. Gooch, D.J. — The effect of microstructure on creep crack growth in notched bend tests on 0.5 Cr-0.5 Mo-0.25 V steel. Materials Science and Engineering, Vol. 27, 1977, pp. 57-68.

27. Gooch, D.J. — Creep crack growth in variously tempered bainitic and martensitic 0.5 Cr-0.5 Mo- 0.25 V steel. Materials Science and Engineering, Vol. 29, 1977, pp. 227-240.

28. Sadananda, K. and Shahinian, P. — The effect of environment on the creep crack growth behaviour of several structural alloys. Materials Science and Engineering, Vol. 43, 1980, pp. 159-168.

29. Taira, S. and Ohtani, R. — Creep crack propagation and creep rupture of notched specimens. International Conference on Creep and Fatigue in Elevated Temperature Applications, Philadelphia 1973, Sheffield UK 1974, Paper C213/73.

30. Nicholson, R.D. — The effect of temperature on creep crack propagation in AISI 316 stainless steel. Materials Science and Engineering, Vol. 22, 1976, pp. 1-6.

31. Henshall, J.L., Gee, M.G., Singh, G. and Boyd, G.A.C. — Creep crack growth in AISI 316 stainless steel and a quenched 1 Cr - 1/2 Mo steel. Mechanical Behaviour of Materials, ICM-3, Cambridge, England, 1979, Vol. 2, pp. 309-319.

32. Lloyd, G.J. — The relationship between creep crack growth rates and creep-fatigue crack growth rates in austenitic type 316 steel. International Conference on Engineering Aspects of Creep, Sheffield UK, 1980, Paper C213/80.

33. Taylor, E. and Batte, A.D. — Creep crack formation in a 1 % CrMoV rotor forging steel. International Conference on Engineering Aspects of Creep, Sheffield UK, 1980, Paper C216/80.

34. James, L.A. — Some preliminary observations on the extension of cracks under static loadings at elevated temperatures. International Journal of Fracture Mechanics, Vol. 8, 1972, pp. 347-349.

35. Thornton, D.V. — Creep crack growth characteristics of feritic steels. International Conference on Properties of Creep Resistant Steels, Düsseldorf, 1972, Paper 6.5.

36. Landes, J.D. and Wei, R.P. — Kinetics of subcritical crack growth and deformation in a high strength steel. Transactions of the ASME, Journal of Engineering Materials and Technology, Vol. 95, 1973, pp. 2-9.

37. Kenyon, J.L., Webster, G.A., Radon, J.C. and Turner, C.E. — An investigation of the application of fracture mechancis to creep cracking. International Conference on Creep and Fatigue in Elevated Temperature Applications, Philadelphia 1973, Sheffield UK 1974, Paper C156/73.

38. Pilkington, R., Hutchinson, D. and Jones, C.L. — High-temperature crack-opening displacement measurements in a ferritic steel. Metal Science, Vol. 8, 1974, pp. 237-241.

39. Floreen, S. — The creep fracture of wrought nickel-base alloys by a fracture mechanics approach. Metallurgical Transactions A, Vol. 6A, 1975, pp. 1741-1749.

40. Kaufman, J.G., Bogardus, K.O., Mauney, D.A. and Malcolm, R.C. — Creep cracking in 2219-T851 plate at elevated temperatures. ASTM STP 590, 1976, pp. 149-168.

41. Worswick, D. and Pilkington, R. — The effect of prior damage on creep-crack propagation in ferritic steels. Strength of Metals and Alloys, Fifth International Conference, Aachen, 1979, pp. 409-416.

42. Siverns, M. and Price, A.T. — Crack growth under creep conditions. Nature, Vol. 228, 1970, pp. 760-761.

43. Koterazawa, R. and Iwata, Y. — Fracture mechanics and fractography of creep and fatigue crack propagation at elevated temperature. Transactions of the ASME, Journal of Engineering Materials and Technology, Vol. 98, 1976, pp. 296-304.

44. Radhakrishnan, V.M. and McEvily, A.J. — Effect of temperature on creep crack growth. Transactions of the ASME, Journal of Engineering Materials and Technology, Vol. 102, 1980, pp. 350-355.

45. Krishnan, V.M.R., Mutoh, Y. and McEvily, A.J. — An analysis of crack extension in creeping solids. Engineering Fracture Mechanics, Vol. 13, 1980, pp. 819-828.

46. Radhakrisknan, V.M. and McEvily, A.J. — Time dependent crack growth in a titatinium alloy. Scripta Metallurgica, Vol. 15, 1981, pp. 51-54.

47. Nicholson, R.D. — The measurement of creep crack growth rates by a notch region extension method, Journal of Physics E: Scientific Instruments, Vol. 7, 1974, pp. 741-743.

48. Gooch, D.J., King, B.L. and Briers, H.D. — High-temperature crack growth in a 2.25 Cr - 1 Mo weld metal - Effects of tempering, pre-strain and grain refinement. Materials Science and Engineering, Vol. 32, 1977, pp. 81-91.

49. Sadananda, K. and Shahinian, P. — Creep crack growth in Alloy 718. Metallurgical Transactions A, Vol. 8A, 1977, pp. 439-449.

50. Nikbin, K.M., Webster, G.A. and Turner, C.E. — Relevance of nonlinear fracture mechanics to creep cracking. ASTM STP 601, 1976, pp. 47-62.

51. Harper, M.P. and Ellison, E.G. — The use of the C* parameter in predicting creep crack propagation rates. Journal of Strain Analysis, Vol. 12, No. 3, 1977, pp. 167-179.

52. Pilkington, R. and Worswick, D. — Crack propagation in creep damaged components. International Conference on Engineering Aspects of Creep, Sheffield UK, 1980, Paper C206/80.

53. Branco, C.M. and Radon, J.C. — Analysis of creep cracking by the J integral concept. International Conference on Engineering Aspects of Creep, Sheffield UK, 1980, Paper C210/80.

54. Saxena, A. — Evaluation of C* for the characterization of creep crack growth behaviour in 304 stainless steel. ASTM STP 700, 1980, pp. 131-151.

55. Koterazawa, R. and Mori, T. — Applicability of fracture mechanics parameters to crack propagation under creep condition. Transactions of the ASME, Journal of Engineering Materials and Technology, Vol. 99, 1977, pp. 298-305.

56. Koterazawa, R. and Mori, T. — Fracture mechanics and fractography of creep and fatigue crack propagation at elevated temperatures. International Conference on Engineering Aspects of Creep, Sheffield UK, 1980, Paper C238/80.

57. Ohji, K., Ogura, K., Kubo, S. and Katada, Y. — The application of modified J-integral to creep crack growth in austenitic stainless steel and Cr-Mo-V steel. International Conference on Engineering Aspects of Creep, Sheffield UK, 1980, Paper C240/80.

58. Taira, S., Ohtani, R. and Kitamura, T. — Application of J-integral to high-temperature crack propagation. Transactions of the ASME, Journal of Engineering Materials and Technology, Vol. 101, 1979, pp. 154-161.

59. Christian, E.M., Smith, D.J., Webster, G.A. and Ellison, E.G. — Critical examination of parameters for predicting creep crack growth. Advances in Fracture Research, ICF-5, Cannes 1981, Vol. 3, pp. 1295-1302.

60. Donath, R.C., Nicholas, T. and Fu, L.S. — An experimental investigation of creep crack growth in IN 100. ASTM STP 743, 1981, pp. 186-206.

61. Rice, J.R., Paris, P.C. and Merkle, J.G. — Some further results of J-integral analysis and estimates. ASTM STP 536, 1973, pp. 231-245.

62. Keller, H.P. Munz, D. — Comparison of different equations for calculation of J-integral from one load-displacement curve. DFVLR FB 76-56, 1976.

63. Clarke, G.A. and Landes, J.D. — Evaluation of the J-integral for the compact specimen. ASTM Journal of Testing and Evaluation, Vol. 7, No. 5, 1979, pp. 264-269.

64. Rice, J.R. and Rosengren, G.F. — Plane strain deformation near a crack tip in a power-law hardening material. Journal of the Mechanics and Physics of Solids, Vol. 16, 1968, pp. 1-12.

65. Hutchinson, J.W. — Singular behaviour at the end of a tensile crack in a hardening material. Journal of the Mechanics and Physics of Solids, Vol. 16, 1968, pp. 13-31.

66. Hutchinson, J.W. — Plastic stress and strain fields at a crack tip. Journal of the Mechanics and Physics of Solids, Vol. 16, 1968, pp. 337-347.

67. Hilton, P.D. and Hutchinson, J.W. — Plastic intensity factors for cracked plates. Engineering Fracture Mechanics, Vol. 3, 1971, pp. 435-451.

68. Goldman, N.L. and Hutchinson, J.W. — Fully plastic crack problems: The center-cracked strip under plane strain. International Journal of Solids and Structures, Vol. 11, 1975, pp. 575-591.

69. Shih, C.F. and Hutchinson, J.W. — Fully plastic solutions and large scale yielding estimates for plane stress crack problems. Transactions of the ASME, Journal of Engineering Materials and Technology, Vol. 98, Series H, 1976, pp. 289-295.

70. Kumar, V. and Shih, C.F. — Fully plastic crack solutions with applications to creep crack growth. International Conference on Engineering Aspects of Creep, Sheffield UK, 1980, Paper C228/80.

71. Kumar, V. and Shih, C.F. — Fully plastic crack solutions, estimation scheme, and stability analyses for the compact specimen. ASTM STP 700, 1980, pp. 406-438.

72. Nikbin, K.M., Webster, G.A. and Turner, C.E. — A comparison of methods of correlating creep crack growth in a 1/2 % Cr 1/2 % Mo 1/4 % V steel. Fracture 1977, ICF-4, Waterloo, 1977, Vol. 2, pp. 627-634.

73. Musicco, G.G., Boerman, D.J. and Piatti, G. — Creep crack growth characterization of austenitic stainless steel. Advances in Fracture Research, ICF-5, Cannes 1981, Vol. 3, pp. 1323-1331.

74. Barnby, J.T. — Crack tip stresses under creep conditions. Engineering Fracture Mechanics, Vol. 6, 1974, pp. 627-630.

75. Barnby, J.T. — Crack propagation during steady state creep. Engineering Fracture Mechanics, Vol. 7, 1975, pp. 299-304.

76. Barnby, J.T. and Nicholson, R.D. — Local stress and strain during crack growth by steady state creep. Journal of Materials Science, Vol. 12, 1977, pp. 2099-2108.

77. Kubo, S., Ohji, K. and Ogura, K. — An analysis of creep crack propagation on the basis of the plastic singular stress field. Engineering Fracture Mechanics, Vol. 11, 1979, pp. 315-329.

78. Freeman, B.L. — The estimation of creep crack growth rates by reference stress methods. International Journal of Fracture, Vol. 15, No. 2, 1979, pp. 179-190.

79. Rice, J.R., Drugan, W.J. and Sham, T.L. — Elastic-plastic analysis of growing cracks. ASTM STP 700, 1980, pp. 189-221.

80. Purushothaman, S. and Tien, J.K. — A theory for creep crack growth. Scripta Metallurgica, Vol. 10, 1976, pp. 663-666.

81. Coleman, M.C., Price, A.T. and Williams, J.A. — Crack growth in pressure vessels under creep conditions. Fracture 1977, ICF-4, Waterloo 1977, Vol. 2, pp. 649-662.

82. Sadananda, K. and Shahinian, P. — Elastic-plastic fracture mechanics for high-temperature fatigue crack growth. ASTM STP 700, 1980, pp. 152-163.

83. Riedel, H. — A contribution to the theory of fracture mechanics under creep conditions. International Conference on Engineering Aspects of Creep, Sheffield UK, 1980, Paper C188/80.

84. Riedel, H. and Rice, J.R. — Tensile cracks in creeping solids. ASTM STP 700, 1980, pp. 112-130.

85. Siverns, M.J. and Price. A.T. — Crack propagation under creep conditions in a quenched 2 1/4 chromium 1 molydenum steel. International Journal of Fracture, Vol. 9, No. 2, 1973, pp. 199-207.

86. Gooch, D.J. and King, B.L. — Creep crack growth in CrMoV weld heat affected zone microstructures under stress relaxation conditions. International Conference on Engineering Aspects of Creep. Sheffield UK, 1980, Paper C200/80.

87. Ritter, J.C. and Formby, C.L. — The effect of residual stress on creep crack propagation in type 316 stainless steel weld metal. International Conference on Engineering Aspects of Creep, Sheffield UK, 1980, Paper C219/80.

88. Worswick, D. and Pilkington, R. — The interrelation between prior creep damage and creep crack propagation in steels. Advances in Fracture Research, ICF-5, Cannes 1981, Vol. 3, pp. 1303-1311.

89. Scott, V.D., Stott, F.G. and Wilcock, A.D. — Model for loss of static strength caused by the presence of microcracks. Journal of the Institute of Metals, Vol. 101, 1973, pp. 315-319.

90. Van Elst, H.C. — A fracture mechanics description of material damage in absence of a macrodefect as a collective of macrodefects. Metal Research Institute TNO. Rep.No. 80M/35/08383/ELS/MSL. Presented at International Conference on Analytical and Experimental Fracture Mechanics, Rome, June 1980.

TABLE 2
Results of the calculations by Goldman and Hutchinson

		m = 1	m = 1,5	m = 2	m = 3	m = 5	m = 7
$\frac{a}{w} \to 0$	J_N	$= 4\pi/3$*	$J_N = 1,25$§	1,37§	1,50§	1,64§	1,76§
	Δ_N	= 2,0*					
	$J_{N\Delta}$	$= \pi/3$*					
	v_{crN}	= -					
	J_{Naw}	$= 4\pi/3$*					
	Δ_{Naw}	= 2,0*					
$\frac{a}{w} = 1/8$	J_N	= 4,23	4,97	5,46	6,02	7,08	8,15
	Δ_N	= 1,92	2,22	2,45	2,77	3,30	3,74
	$J_{N\Delta}$	= 1,00	1,20	1,33	1,48	1,65	1,77
	v_{crN}	= 0,100	0,129	0,154	0,211	0,314	0,408
	J_{Naw}	= 3,70	4,07	4,18	4,04	3,63	3,20
	Δ_{Naw}	= 1,68	1,82	1,87	1,8[illegible]	1,69	1,47
$\frac{a}{w} = 1/4$	J_N	= 4,59	5,90	7,07	9,30	14,58	22,06
	Δ_N	= 2,01	2,44	2,87	3,73	5,76	8,60
	$J_{N\Delta}$	= 0,855	1,10	1,26	1,46	1,69	1,81
	v_{crN}	= 0,197	0,253	0,307	0,405	0,572	0,681
	J_{Naw}	= 3,44	3,83	3,98	3,92	3,46	2,94
	Δ_{Naw}	= 1,51	1,58	1,61	1,57	1,37	1,15
$\frac{a}{w} = 1/2$	J_N	= 6,24	9,28	13,03	24,26	80,08	264,3
	Δ_N	= 2,31	3,11	4,12	6,97	20,41	62,80
	$J_{N\Delta}$	= 0,586	0,882	1,10	1,45	1,87	2,11
	v_{crN}	= 0,396	0,493	0,580	0,719	0,887	0,959
	J_{Naw}	= 3,12	3,28	3,26	3,03	2,50	2,06
	Δ_{Naw}	= 1,15	1,10	1,03	0,872	0,638	0,491
$\frac{a}{w} = 3/4$	J_N	=10,92	20,73	37,28	119,2	1273,0	14040,0
	Δ_N	= 2,92	4,61	7,26	19,34	170,1	1749,0
	$J_{N\Delta}$	= 0,321	0,645	0,952	1,45	2,03	2,27
	v_{crN}	= 0,597	0,726	0,821	0,932	0,992	0,999
	J_{Naw}	= 2,73	2,59	2,33	1,86	1,24	0,857
	Δ_{Naw}	= 0,729	0,576	0,454	0,302	0,116	0,107

* Exact value
§ Extrapolated value
Limit values for $\left(m = 1, \frac{a}{b} \to 1\right)$ are: $J_{N\Delta} = 0$, $J_{\Delta aw} = \frac{16\pi}{3(\pi^2-4)}$.
Limit values for $m \to \infty$ are $J_{N\Delta} = \frac{4}{\sqrt{3}}$, $v_{crN} = 1.0$, for all values of $\frac{a}{w}$.

TABLE 3
Results of the analysis by Shih and Hutchinson

		m = 1	m = 1,5	m = 2	m = 3	m = 5	m = 7	m = 10
$\frac{a}{w}$ = 0	G	1,0	1,03	1,02	1,01	1,005	1,00	1,00
$\frac{a}{w}$ = 1/8	g_1	1,800	3,231	3,543	4,00	4,518	4,761	4,861
	g_2	3,532	3,867	4,107	4,464	4,827	4,945	4,894
	g_3	0,347	0,491	0,640	0,949	1,537	2,048	2,630
	G	1,0	1,022	1,010	1,004	1,031	1,069	1,114
$\frac{a}{w}$ = 1/4	g_1	2,544	2,820	2,972	3,140	3,195	3,106	2,896
	g_2	3,116	3,235	3,286	3,304	3,151	2,926	2,595
	g_3	0,611	0,820	1,010	1,352	1,830	2,083	2,191
	G	1,0	1,014	1,004	1,008	1,037	1,059	1,072
$\frac{a}{w}$ = 1/2	g_1	2,211	2,242	2,195	2,056	1,811	1,643	1,465
	g_2	2,382	2,182	2,003	1,703	1,307	1,084	0,892
	g_3	0,924	1,085	1,180	1,254	1,183	1,051	0,888
	G	1,0	0,994	0,975	0,952	0,939	0,944	0,957
$\frac{a}{w}$ = 3/4	g_1	2,073	1,893	1,708	1,458	1,208	1,082	0,956
	g_2	1,611	1,215	0,970	0,685	0,452	0,361	0,292
	g_3	0,933	0,886	0,802	0,642	0,450	0,361	0,292
	G	1,0	0,977	0,931	0,880	0,860	0,875	0,895
$\frac{a}{w}$ = 1	G	1,0	0,966	0,880	0,805	0,80	0,83	0,88

$$J = g_1\left(\frac{a}{w},m\right).\left\{\alpha\sigma_0\varepsilon_0 a\left(1-\frac{a}{w}\right)\left(\frac{P}{P_0}\right)^{m+1}\right\}$$

$$\Delta = g_2\left(\frac{a}{w},m\right).\left\{\alpha\varepsilon_0 a\left(\frac{P}{P_0}\right)^{m}\right\}$$

$$v_{cr} = g_3\left(\frac{a}{w},m\right).\left\{\alpha\varepsilon_0 a\left(\frac{P}{P_0}\right)^{m}\right\}$$

$$G\left(\frac{a}{w},m\right) = g_1\left(\frac{a}{w},m\right)\left[\frac{1+\zeta(n-1)\,\frac{a}{w}}{c\sqrt{m}\left(1-\frac{1}{m}\right)+g_1\left(\frac{a}{w},1\right)\cdot\frac{1}{m}}\right]$$

ζ = 1,40 and c = 3,85.

TABLE 4
Results of calculations by Kumar and Shih. The CT specimen in plane stress

	n = 1	n = 2	n = 3	n = 5	n = 7	n = 10	n = 13	n = 16	n = 20
$\frac{a}{w}$ = 1/4 h_1	1,609	1,464	1,284	1,060	0,903	0,729	0,601	0,511	0,395
h_2	17,552	12,042	10,706	8,736	7,316	5,744	4,629	3,746	2,916
h_3	9,670	7,996	7,205	5,944	5,000	3,945	3,191	2,591	2,023
$\frac{a}{w}$ = 3/8 h_1	1,552	1,249	1,047	0,801	0,647	0,484	0,377	0,284	0,220
h_2	12,410	8,203	6,538	4,563	3,447	2,442	1,830	1,360	1,019
h_3	7,800	5,734	4,615	3,253	2,475	1,765	1,330	0,990	0,746
$\frac{a}{w}$ = 1/2 h_1	1,398	1,084	0,901	0,686	0,558	0,436	0,356	0,298	0,238
h_2	9,155	5,673	4,212	2,801	2,123	1,571	1,245	1,026	0,814
h_3	6,288	4,149	3,107	2,087	1,590	1,181	0,938	0,774	0,614
$\frac{a}{w}$ = 5/8 h_1	1,274	1,031	0,875	0,695	0,593	0,494	0,423	0,370	0,310
h_2	7,471	4,483	3,347	2,367	1,923	1,539	1,292	1,116	0,928
h_3	5,419	3,375	2,536	1,804	1,468	1,176	0,988	0,853	0,710
$\frac{a}{w}$ = 3/4 h_1	1,234	0,977	0,833	0,683	0,598	0,506	0,431	0,373	0,314
h_2	6,252	3,780	2,893	2,135	1,775	1,437	1,204	1,030	0,857
h_3	4,767	2,992	2,242	1,657	1,379	1,116	0,936	0,800	0,666
$\frac{a}{w} \rightarrow 1$ h_1	1,133	1,010	0,775	0,680	0,650	0,620	0,490	0,470	0,420
h_2	5,288	3,536	2,412	1,905	1,734	1,592	1,232	1,166	1,029
h_3	4,231	2,829	1,930	1,524	1,387	1,274	0,985	0,933	0,824

$h = 0,6w$
$h_1 = 0,275w$
$D = 0,25w$
$d = 0,25w$
$B = 0,5b$
B: Thickness

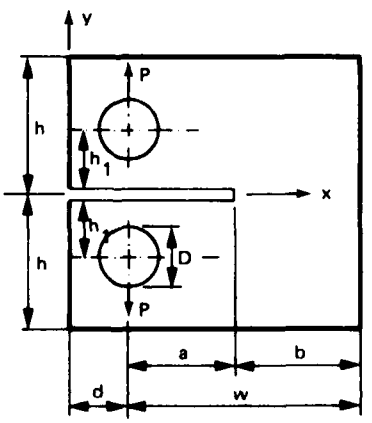

TABLE 5
Results of calculations by Kumar and Shih. The CT specimen in plane strain

		n = 1	n = 2	n = 3	n = 5	n = 7	n = 10	n = 13	n = 16	n = 20
$\frac{a}{w} = 1/4$	h_1	2,227	2,048	1,783	1,475	1,334	1,248	1,258	1,325	1,566
	h_2	17,883	12,481	11,675	10,788	10,538	10,745	11,460	12,570	14,563
	h_3	9,852	8,506	8,170	7,774	7,706	7,942	8,517	9,371	10,887
$\frac{a}{w} = 3/8$	h_1	2,148	1,716	1,392	0,970	0,693	0,443	0,276	0,176	0,098
	h_2	12,644	8,176	6,521	4,319	2,970	1,794	1,102	0,686	0,370
	h_3	7,944	5,760	4,643	3,103	2,139	1,292	0,793	0,494	0,266
$\frac{a}{w} = 1/2$	h_1	1,935	1,509	1,242	0,919	0,685	0,461	0,314	0,216	0,132
	h_2	9,327	5,846	4,304	2,747	1,912	1,199	0,788	0,530	0,317
	h_3	6,406	4,268	3,157	2,024	1,413	0,888	0,585	0,393	0,236
$\frac{a}{w} = 5/8$	h_1	1,763	1,449	1,237	0,974	0,752	0,602	0,459	0,347	0,248
	h_2	7,612	4,572	3,423	2,359	1,810	1,319	0,983	0,749	0,485
	h_3	5,521	3,431	2,583	1,787	1,373	1,000	0,746	0,568	0,368
$\frac{a}{w} = 3/4$	h_1	1,709	1,424	1,263	1,033	0,864	0,717	0,575	0,448	0,345
	h_2	6,370	3,948	3,179	2,337	1,876	1,441	1,124	0,887	0,665
	h_3	4,857	3,048	2,456	1,807	1,450	1,114	0,869	0,686	0,514
$\frac{a}{w} \to 1$	h_1	1,568	1,450	1,350	1,180	1,080	0,950	0,850	0,730	0,630
	h_2	5,388	3,738	3,093	2,433	2,121	1,795	1,573	1,333	1,136
	h_3	4,310	2,990	2,474	1,946	1,697	1,436	1,258	1,066	0,909

$$J^* = h_1\left(\frac{a}{w}, n\right)\left\{\beta\sigma_0\dot{\varepsilon}_0 b\left(\frac{P}{P_0}\right)^{n+1}\right\}$$

$$\dot{\Delta} = h_2\left(\frac{a}{w}, n\right)\left\{\beta\dot{\varepsilon}_0 a\left(\frac{P}{P_0}\right)^{n}\right\}$$

$$v_{cr} = h_3\left(\frac{a}{w}, n\right)\left\{\beta\dot{\varepsilon}_0 a\left(\frac{P}{P_0}\right)^{n}\right\}$$

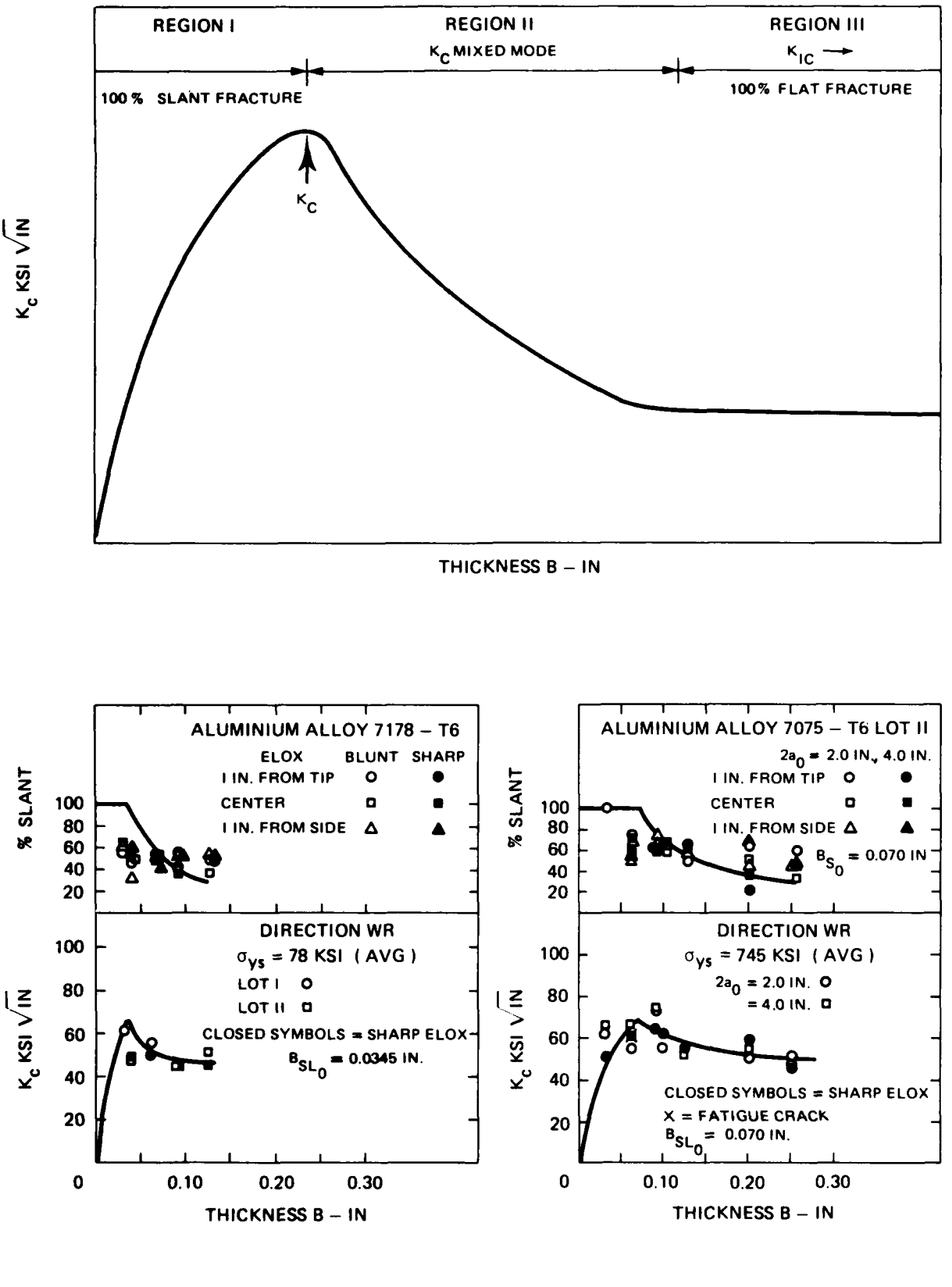

Fig. 1 Effect of sheet thickness on the critical value of the stress intensity factor. (Sullivan and Freed, 12)

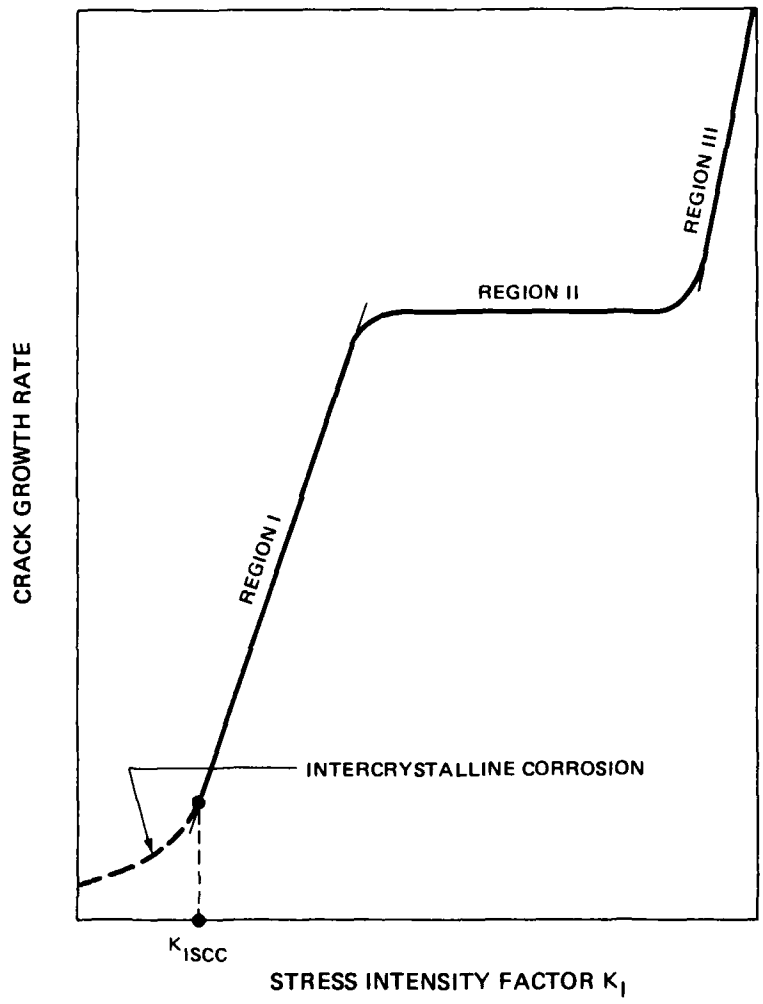

Fig. 2 The K-dependence of crack growth rate in stress corrosion. (Speidel, 13)

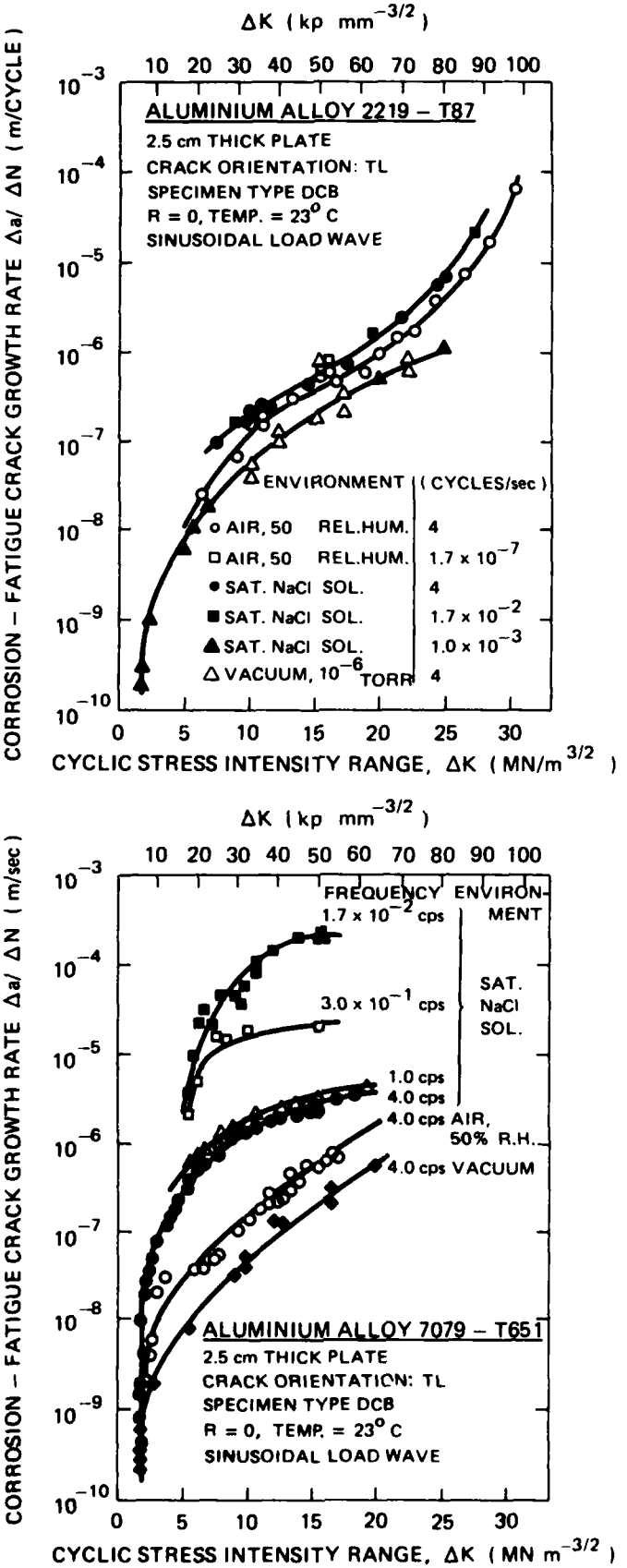

Fig. 3 Crack growth rate in corrosion-fatigue of two aluminium alloys. (Speidel, 14)

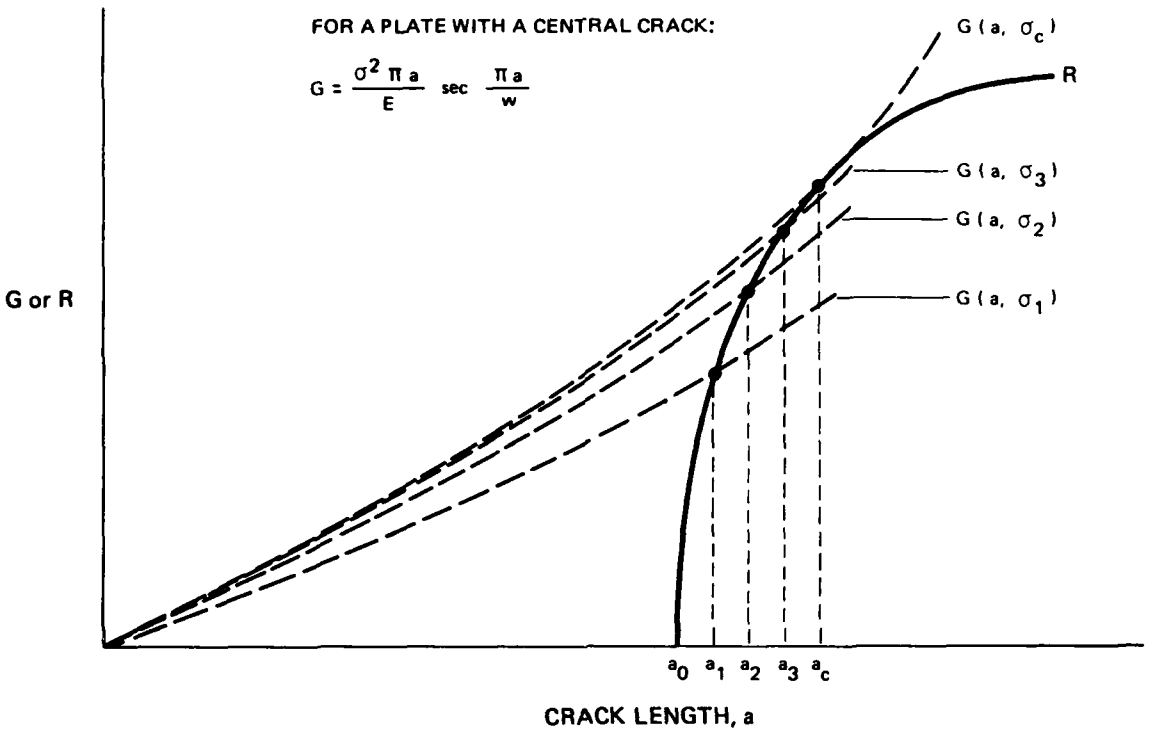

Fig. 4 The R-curve or crack resistance curve

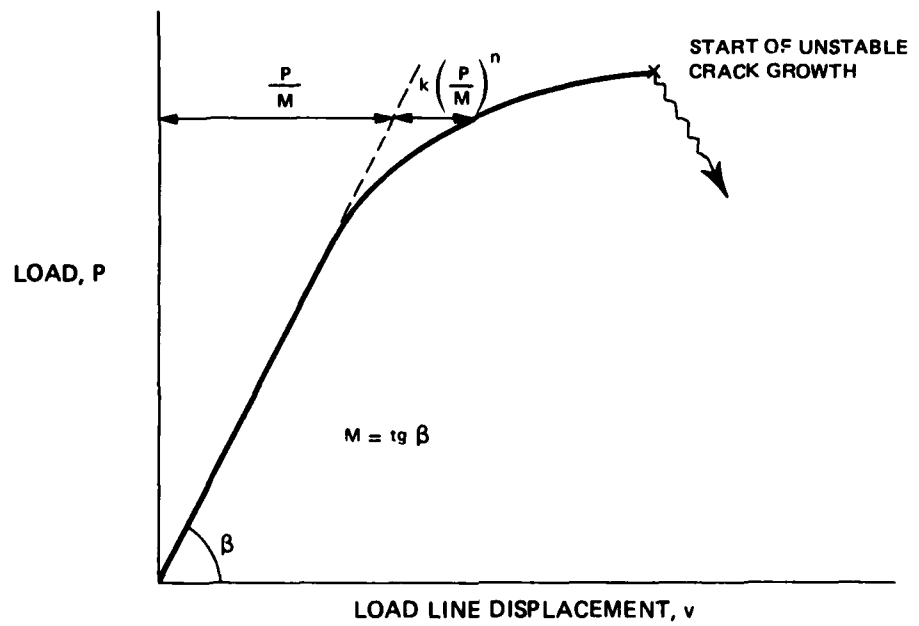

Fig. 5 Load-displacement diagram for appreciable plasticity

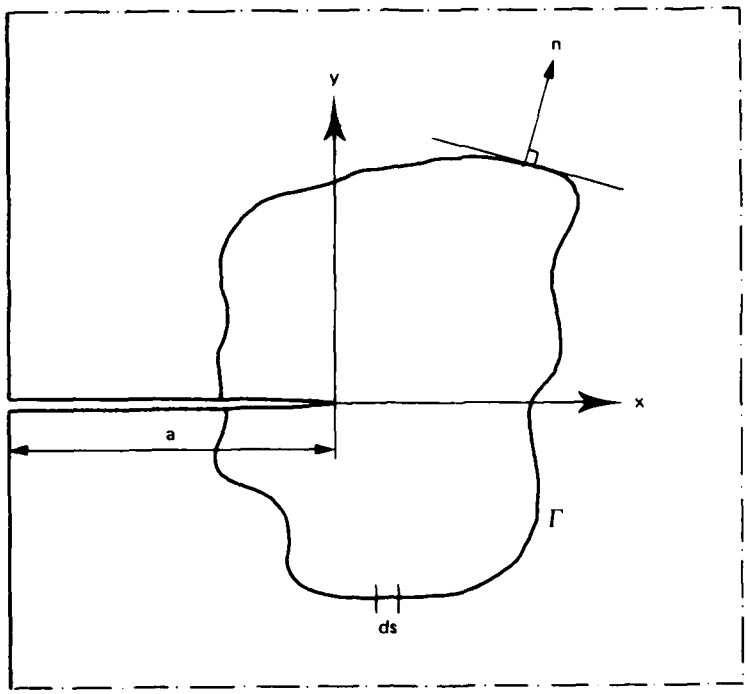

Fig. 6 The contour-integral $J=\oint_\Gamma\{W\,dy-T_j\frac{\partial u_j}{\partial x}\,ds\}$

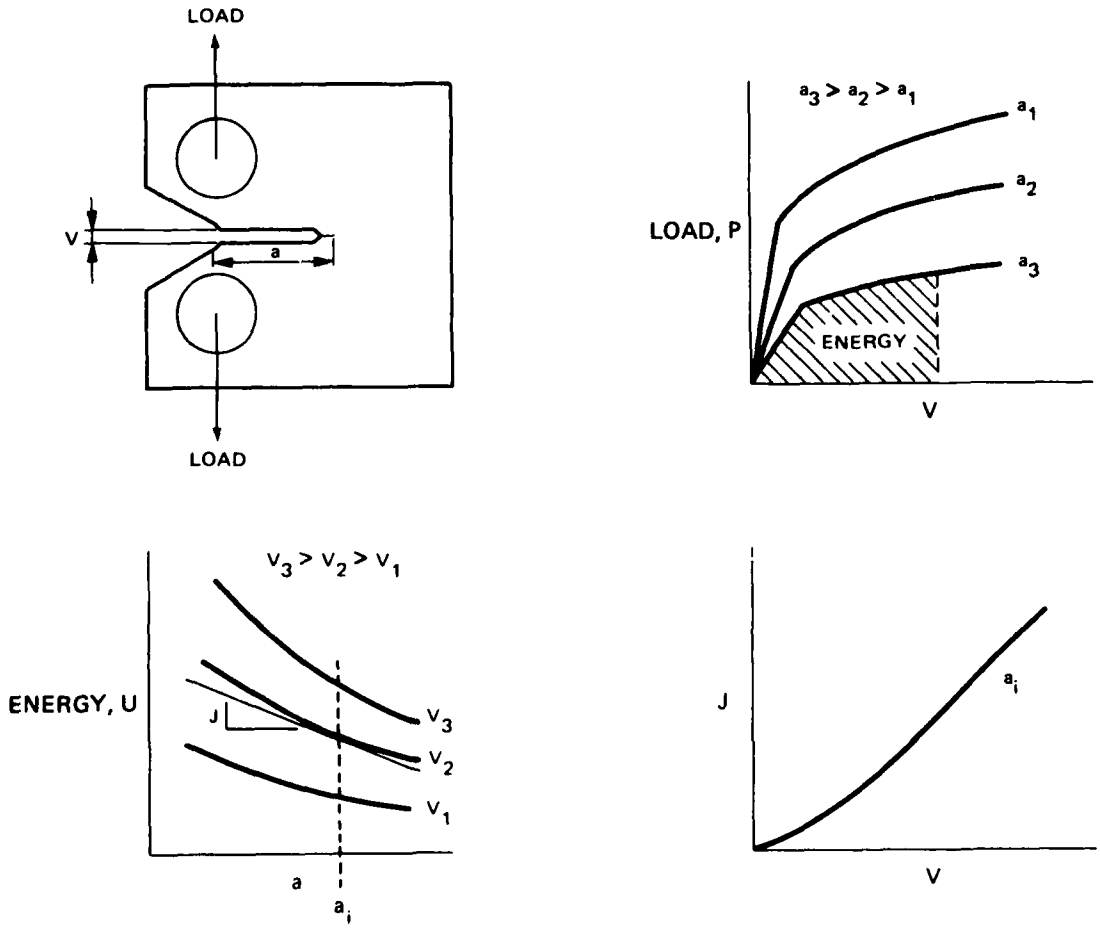

Fig. 7 Empirical determination of the J-integral. (Landes and Begley, 15)

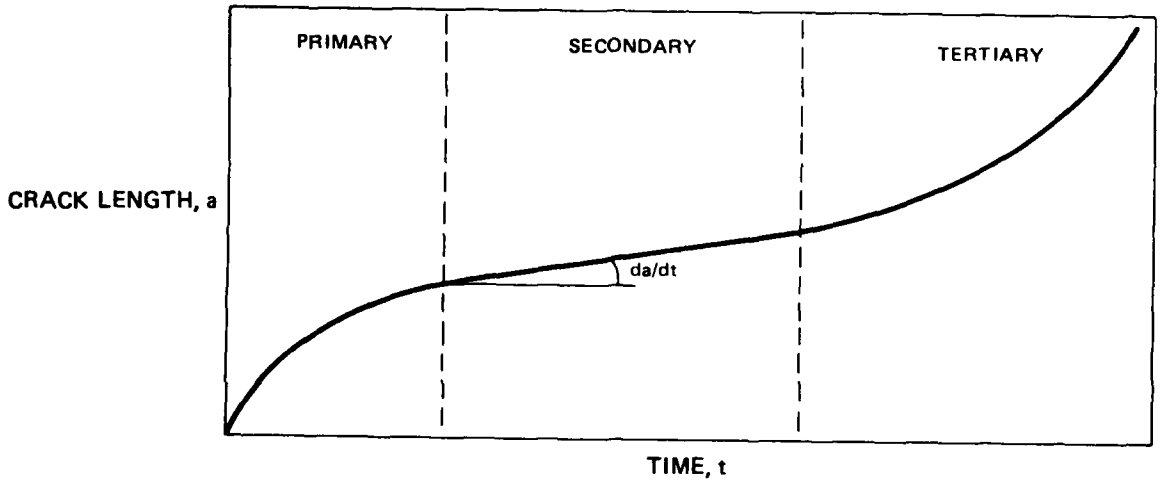

Fig. 8 The creep crack growth curve

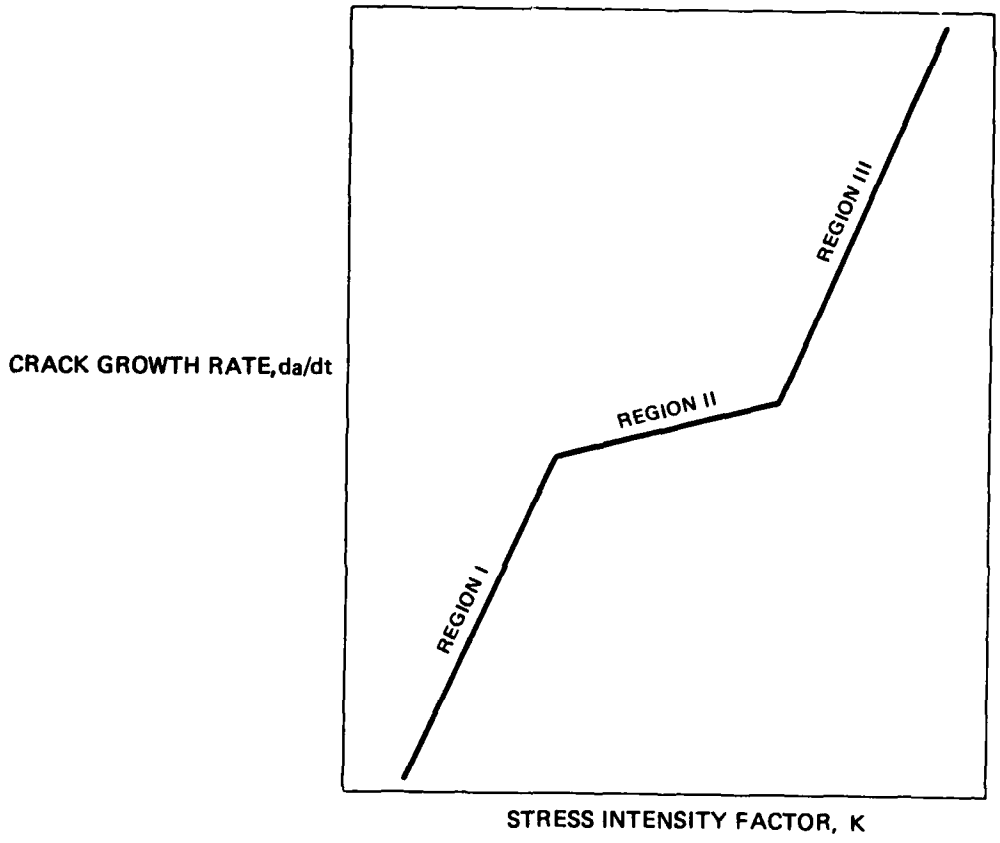

Fig. 9 The stationary crack growth rate as a function of K

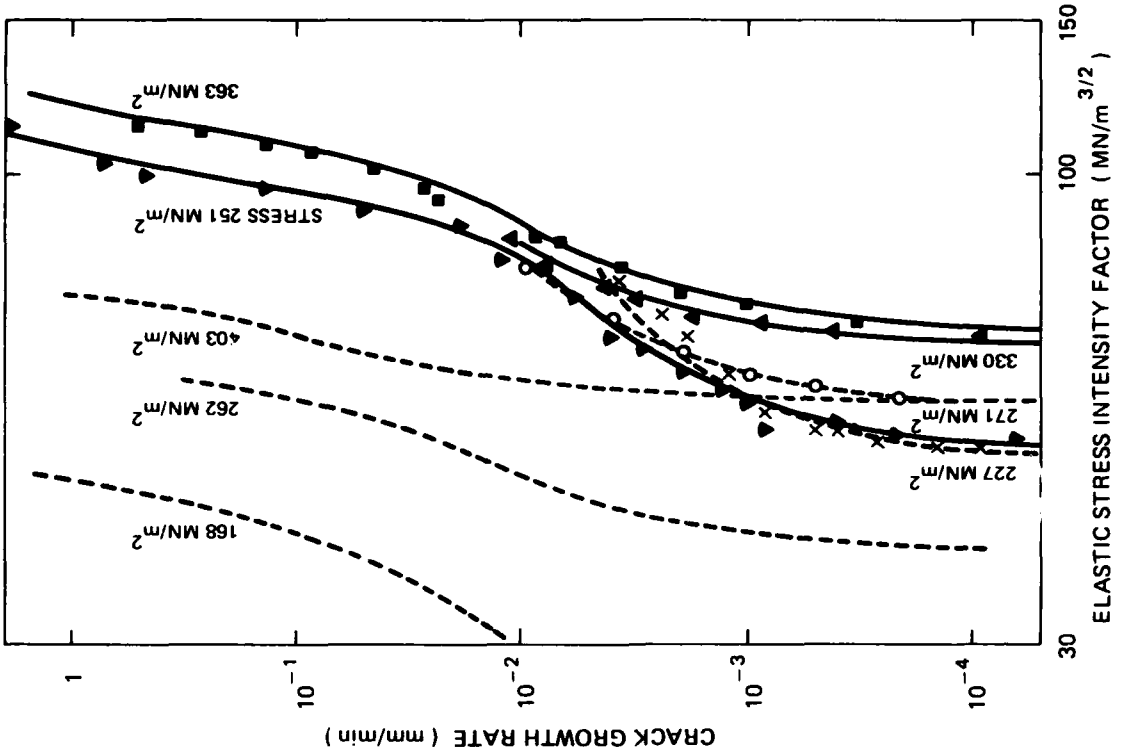

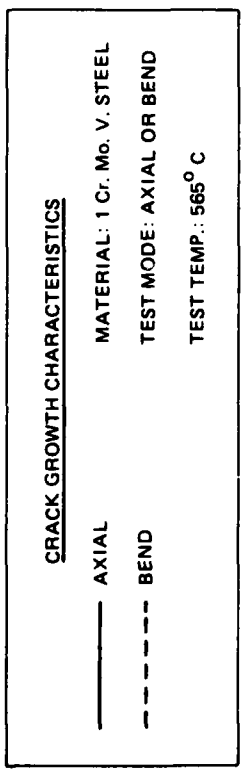

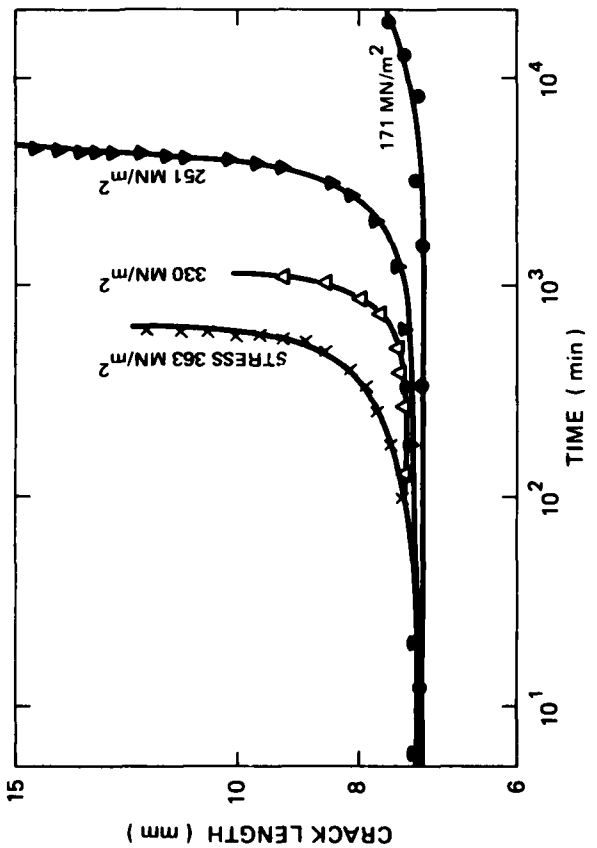

Fig. 10 Test results by Ellison and Walton (19) for single edge notch flat specimens

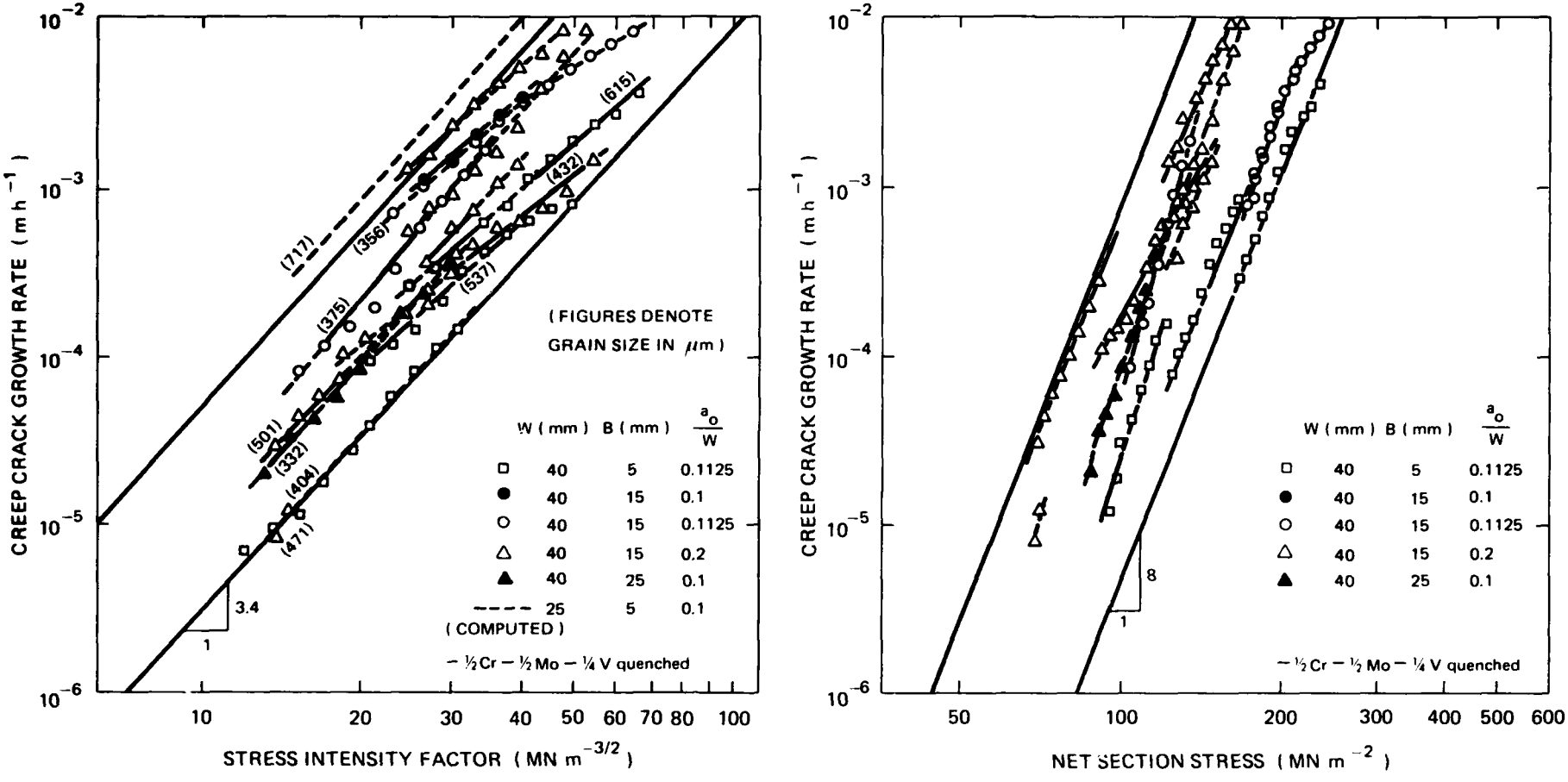

Fig. 11 Results of tests on flat specimens with a single edge notch at 565 °C. Steel 0.5 Cr-0.5 Mo-0.25 V quenched. (Neate and Siverns, 20)

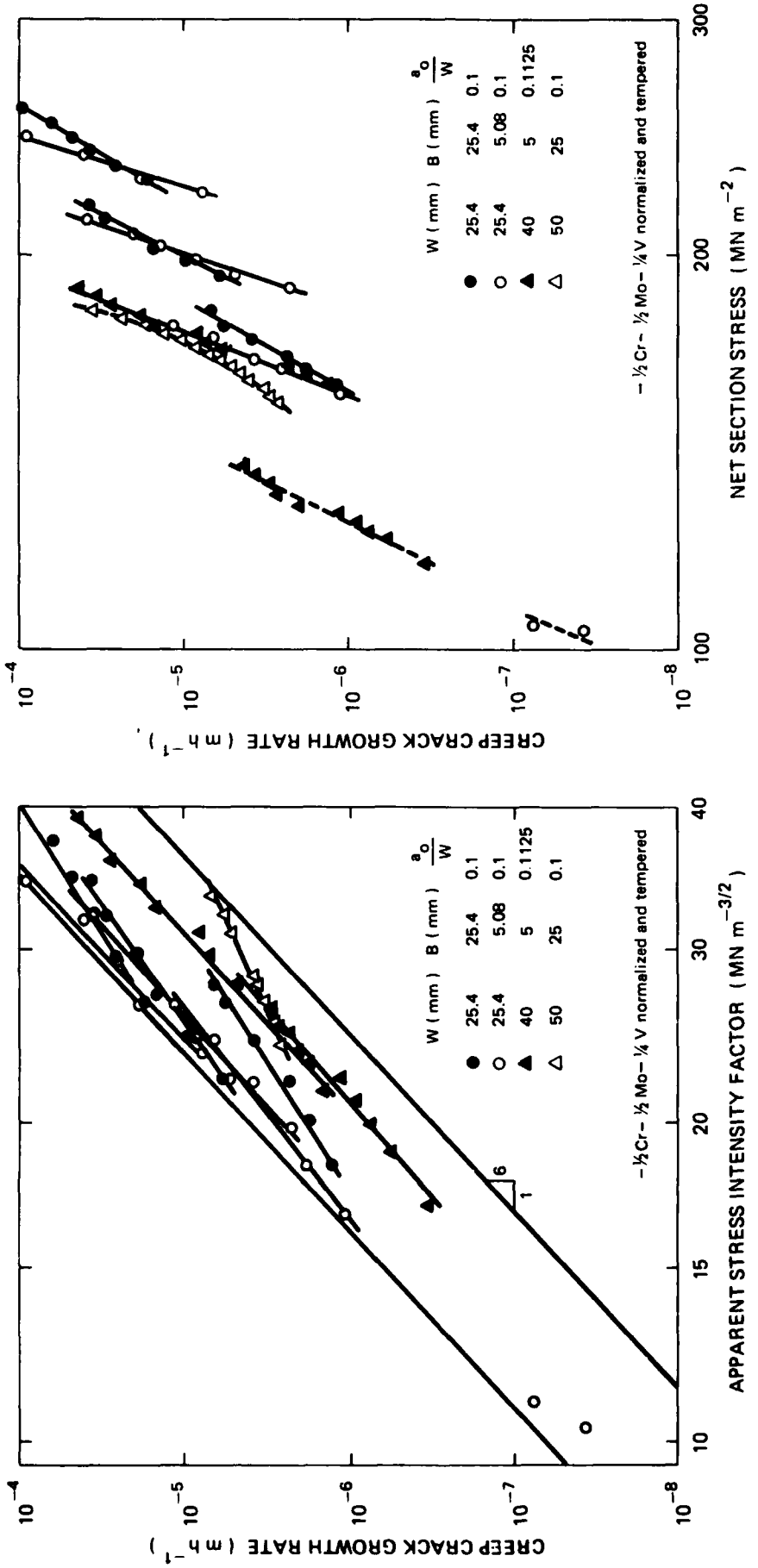

Fig. 12 Results of tests on flat specimens with a single edge notch at 565 °C.
Steel 0.5 Cr-0.5 Mo-0.25 V normalized and tempered. (Neate, and Siverns, 20)

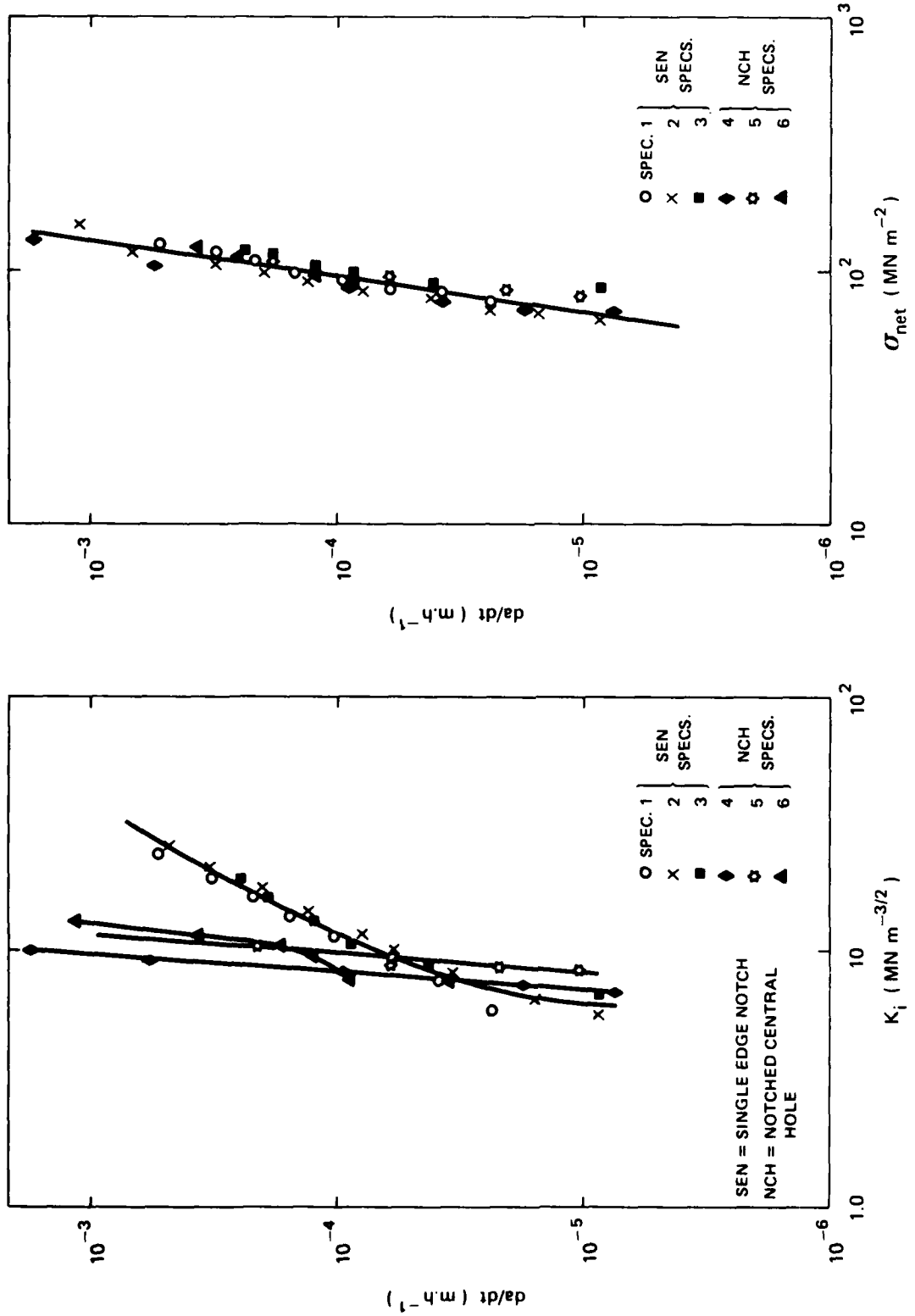

Fig. 13 Results by Nicholson and Formby (21) for 316 type stainless steel at 740 °C

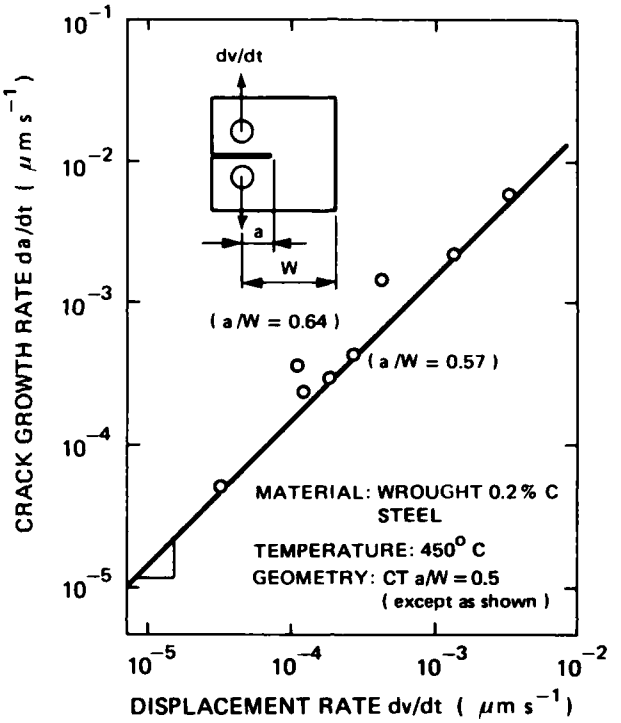

Fig. 14 The relation between crack growth rate and COD rate according to Robson (24) and Haigh (1)

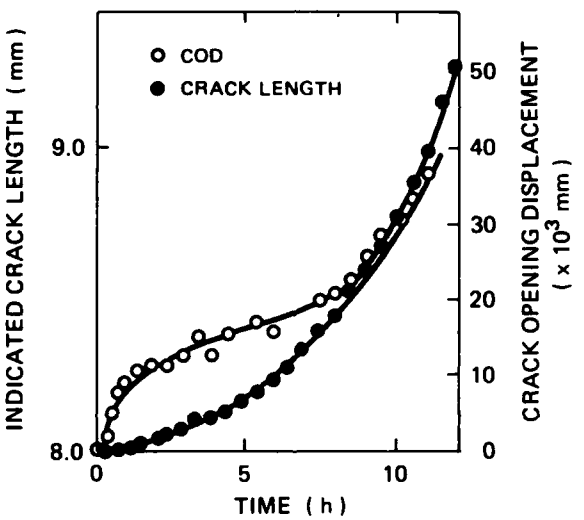

Fig. 15 Crack growth and COD curves for 0.5 Cr-0.5 Mo-0.25 V steel according to Neate and Siverns (20)

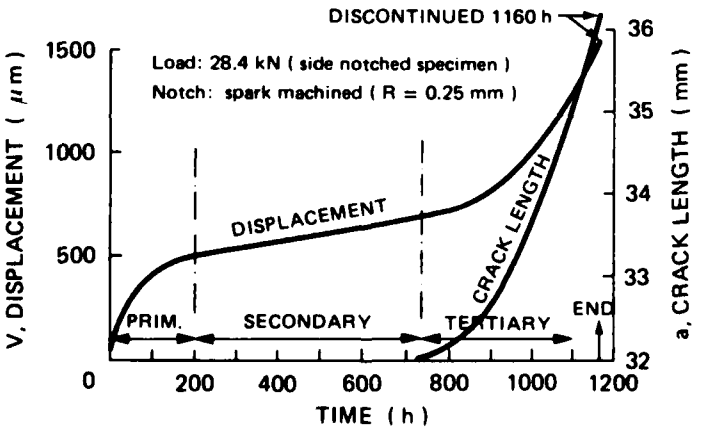

Fig. 16 Crack growth and COD curves for 1% Cr-Mo-V steel according to Haigh (25)

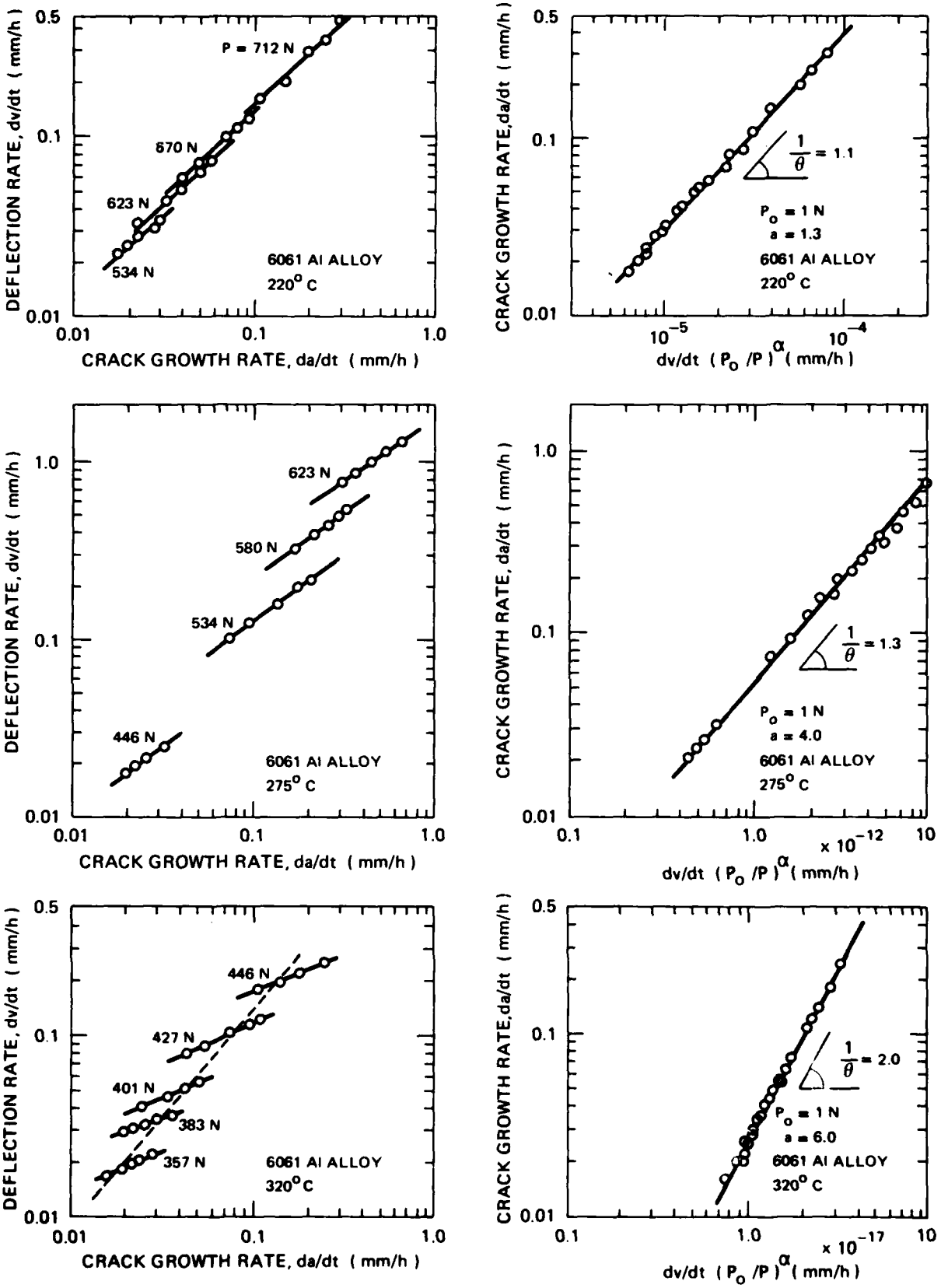

Fig. 17 Crack growth in the aluminium alloy 6061.
Correlation of da/dt with dv/dt and with the parameter dv/dt $(P_o/P)^{\alpha}$, Radhakrishnan and McEvily (4.)

$$J^{*} = \oint \{ W^{*} \, dy - T_j \, (\partial \dot{u}_j / \partial x) \, ds \} \qquad (1)$$

WHERE

$$W^{*} = \int_0^{\dot{\varepsilon}_{mn}} \sigma_{jk} \, d\dot{\varepsilon}_{jk} \qquad (2)$$

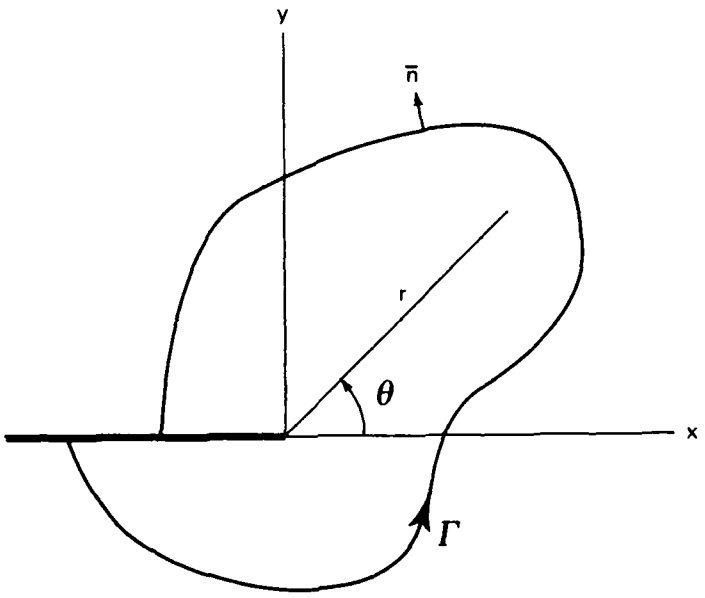

Fig. 18 Definition of the J^{*}-integral, Landes and Begley (15)

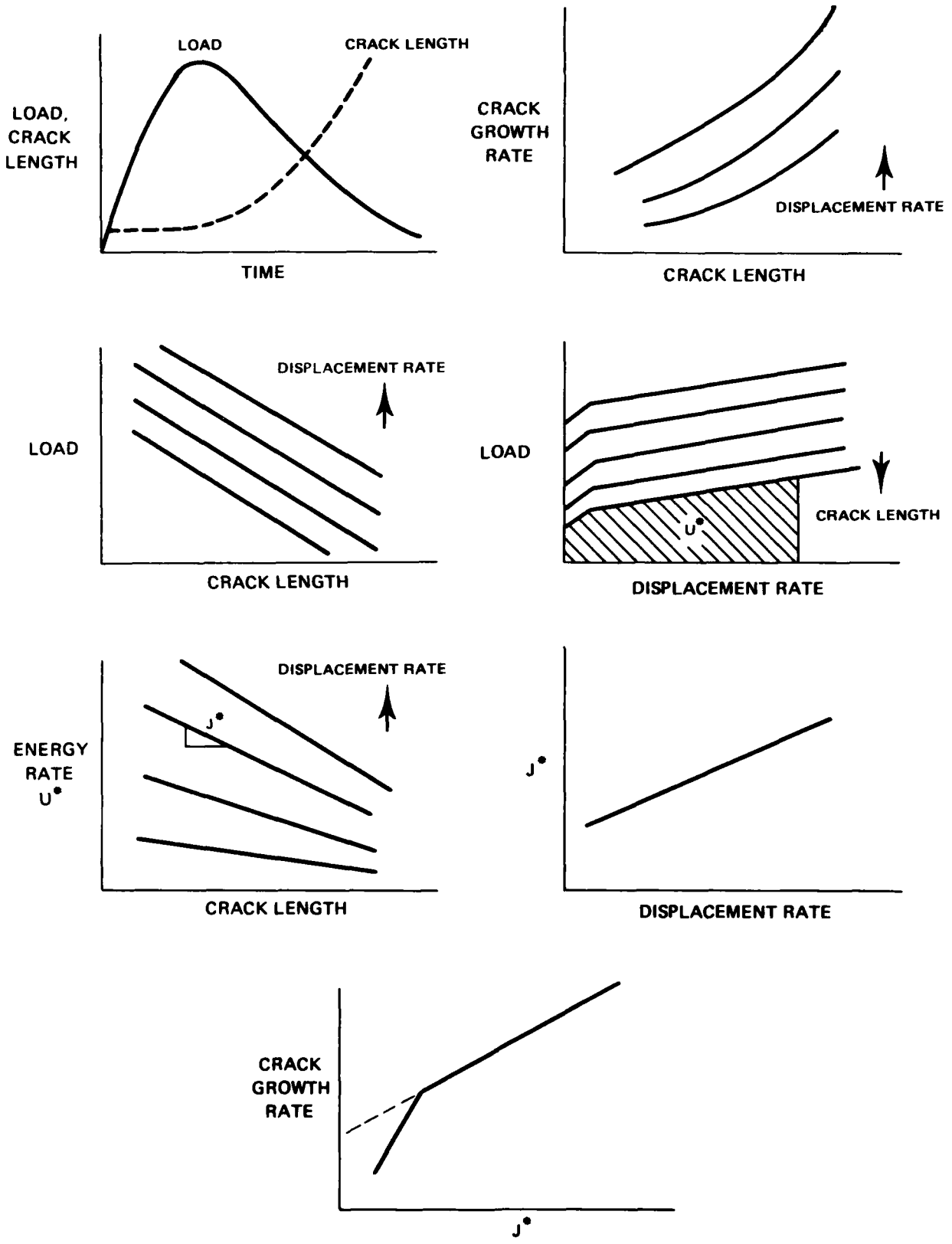

Fig. 19 Determination of the relation between da/dt and J^*, Landes and Begley (15)

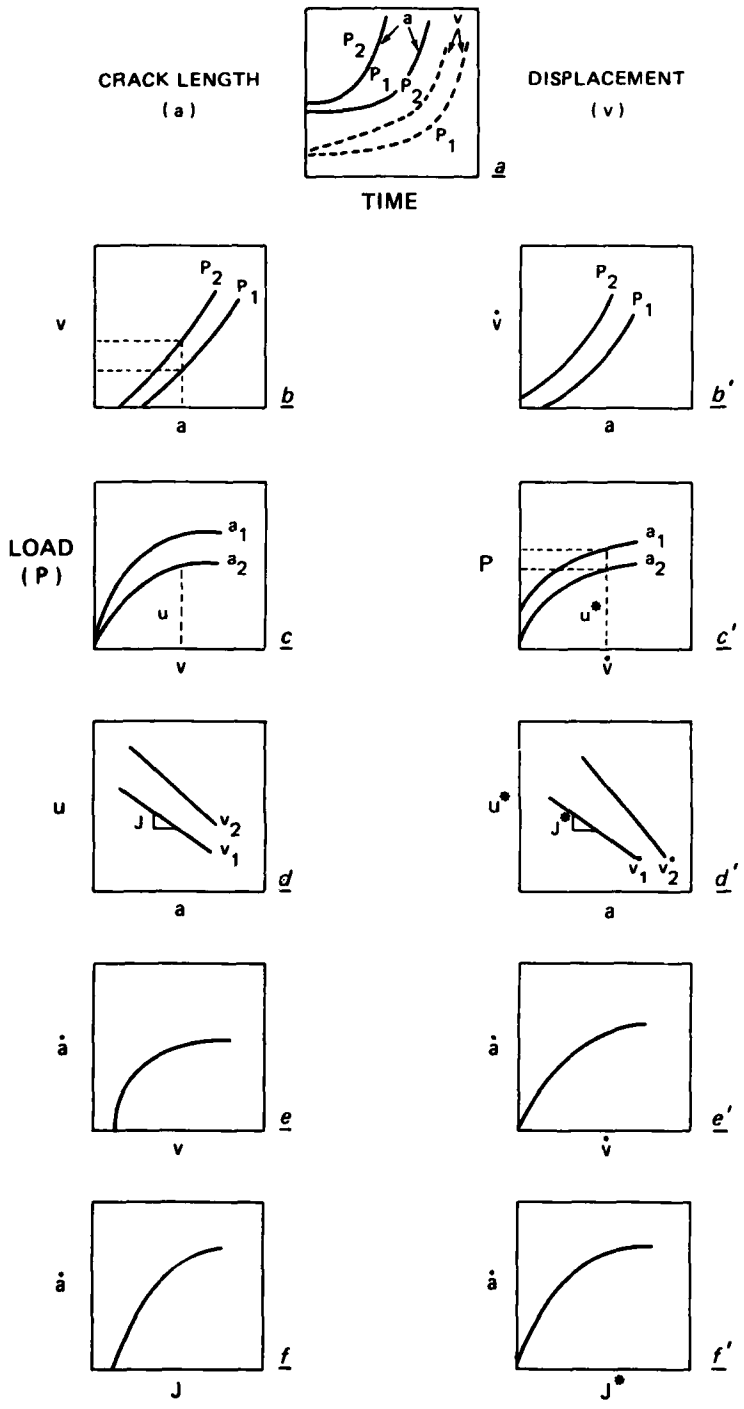

Fig. 20 Processing of test data for the determination of J and J* according to Sadananda and Shahinian (49)

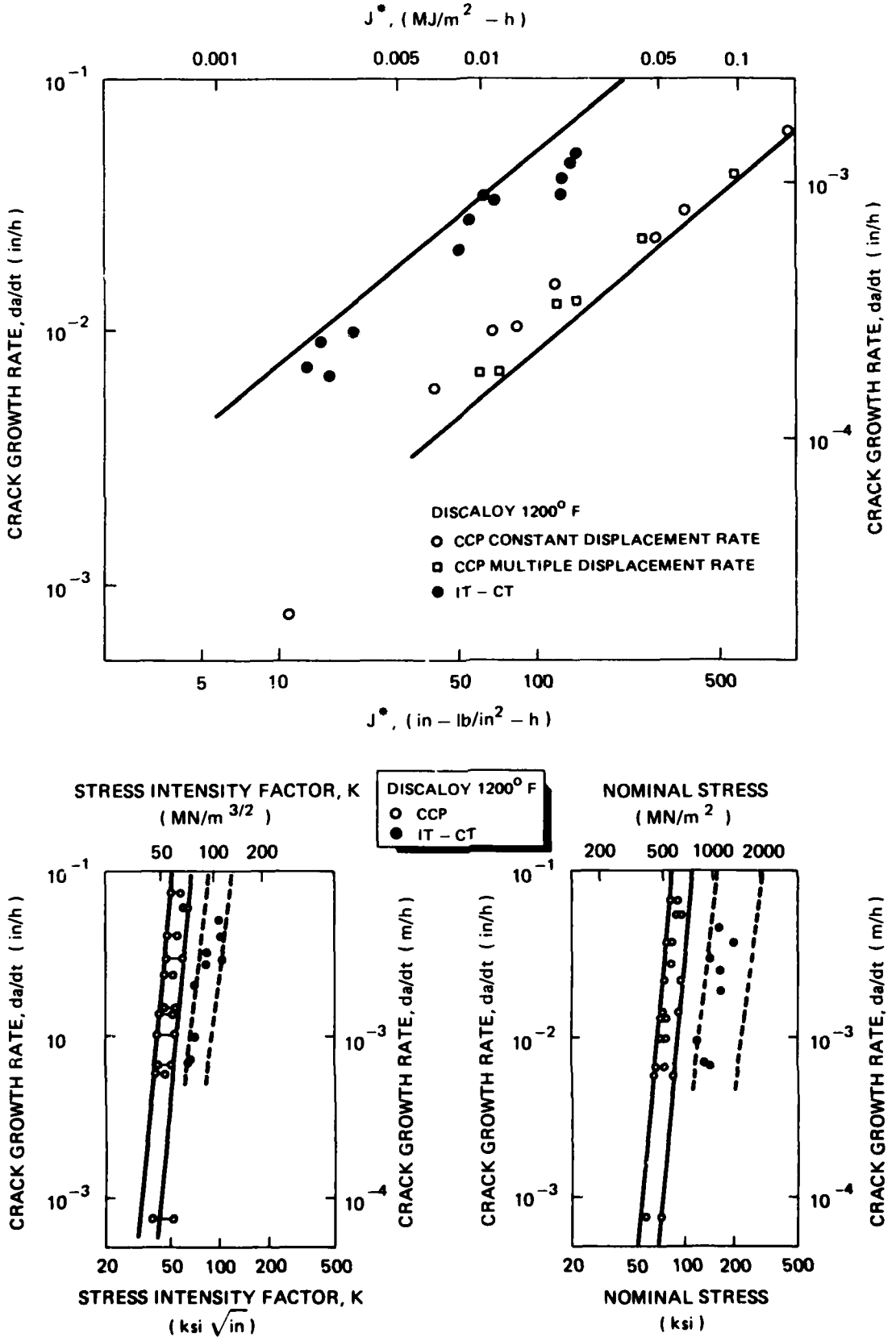

Fig. 21 Correlation of da/dt with J*, the stress intensity factor K and the nominal stress for center cracked and compact tension specimens. (Landes and Begley, 15)

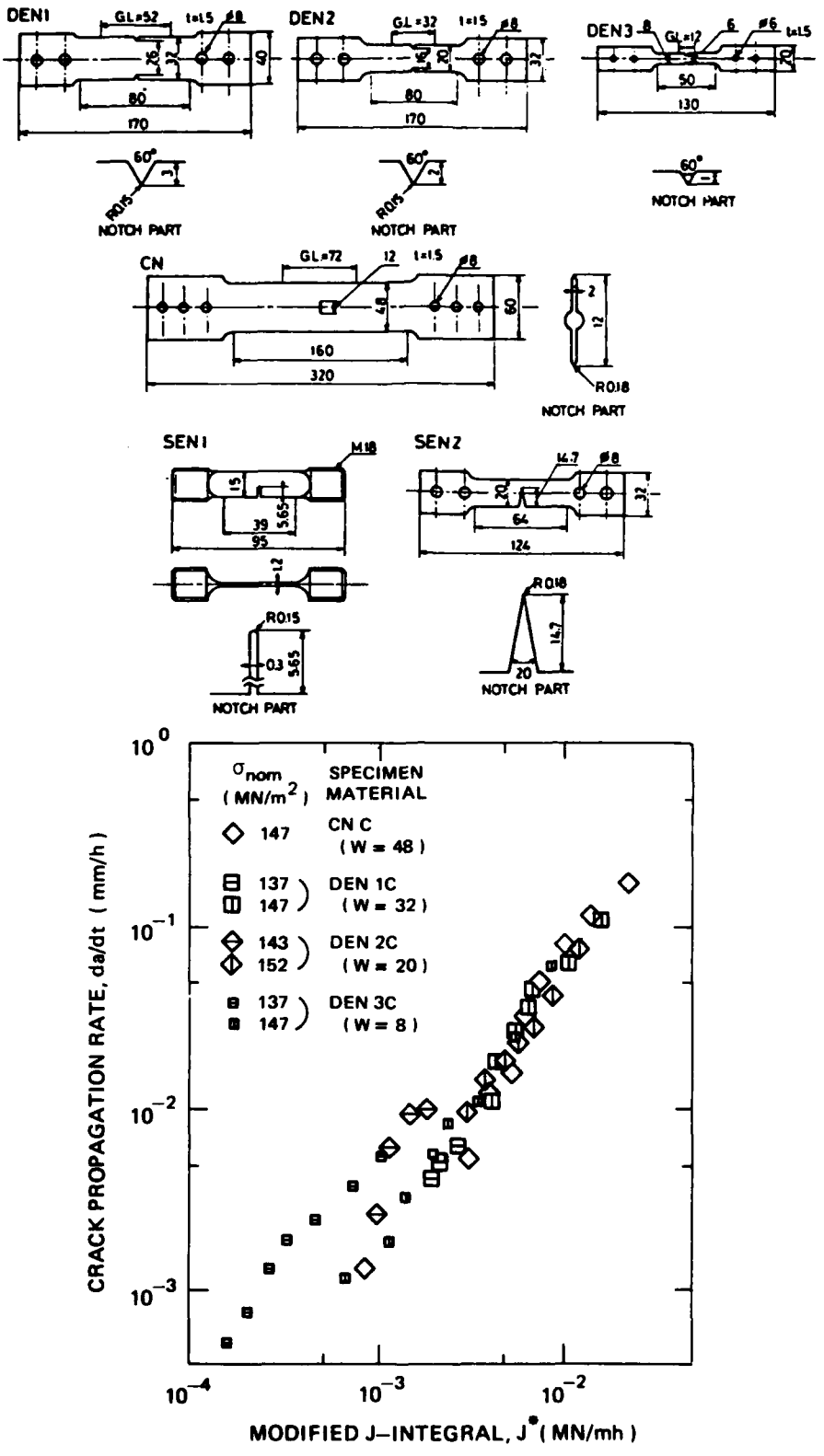

Fig. 22 Test results by Koterazawa and Mori for type 316 stainless steel at 650 °C in air. Good correlation of da/dt with J* for various specimen geometries. (55, 56)

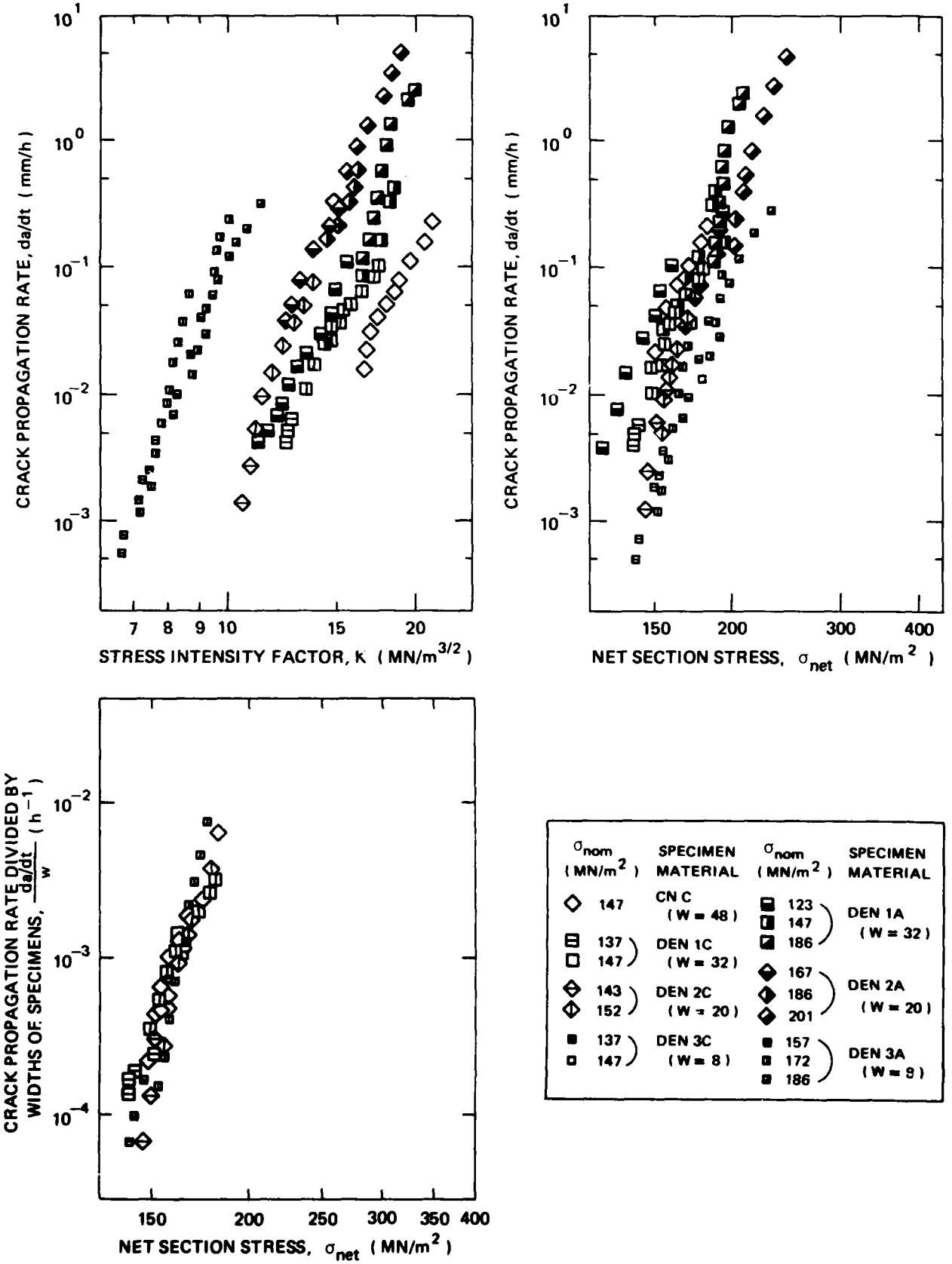

Fig. 23 Test results by Koterazawa and Mori (56). Bad correlation of da/dt with K, better correlation with σ_{net}, especially if a is divided by w

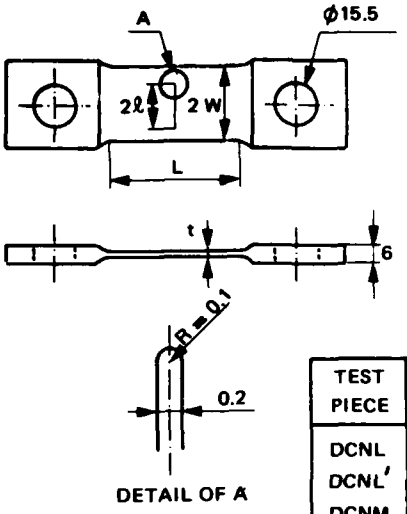

TEST PIECE	2 W	2ℓ	L	t
DCNL	52	32	88	1.5
DCNL′	56	36	50	
DCNM	26	16	44	
DCNS	13	8	22	
SCNL	52	1.5	88	
SCNM	26	0.75	44	

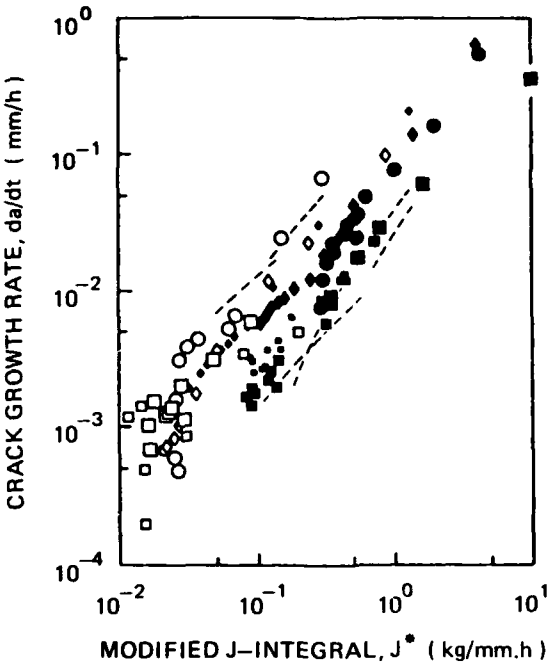

	σ_{nom} (kg/mm^2)		σ_{nom} (kg/mm^2)
● DCNL 1	14.5	■ DCNL 1	14.5
○ DCNL 2	11.0	□ DCNL 2	12.0
◆ SCNL 1	14.5	▪ DCNM 1	14.5
◇ SCNL 2	12.0	▫ DCNM 2	12.0
• SCNM 1	14.5	• DCNS 1	14.5
--- C T			

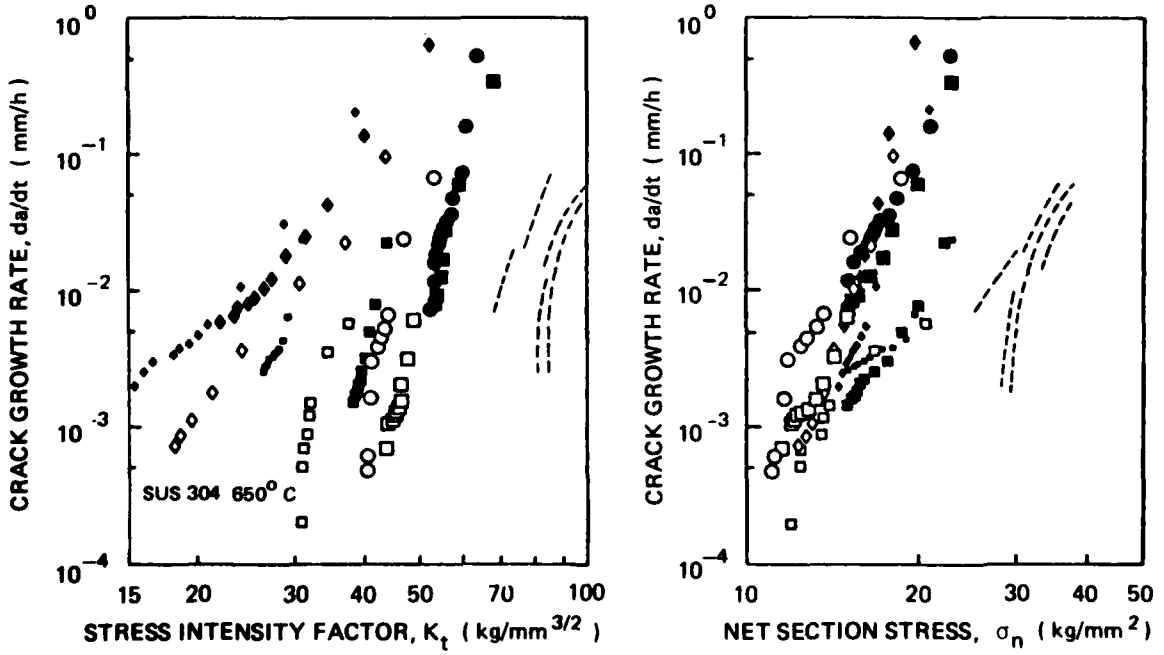

Fig. 24 Test results by Ohji for type 304 stainless steel at 650 °C (4).
N.B. dashed curves pertain to CT specimens

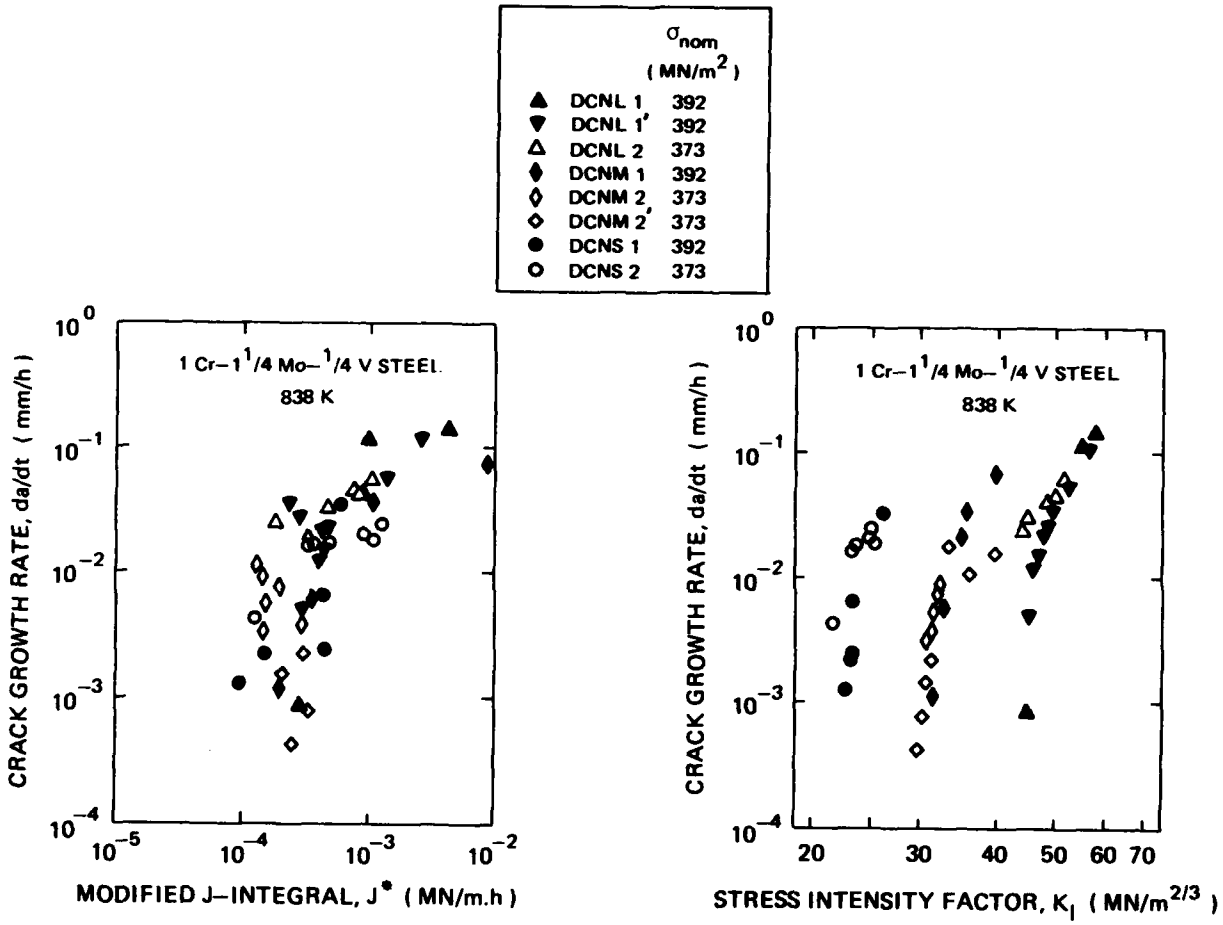

Fig. 25 Test results by Ohji, Ogura, Kubo and Katada (57)

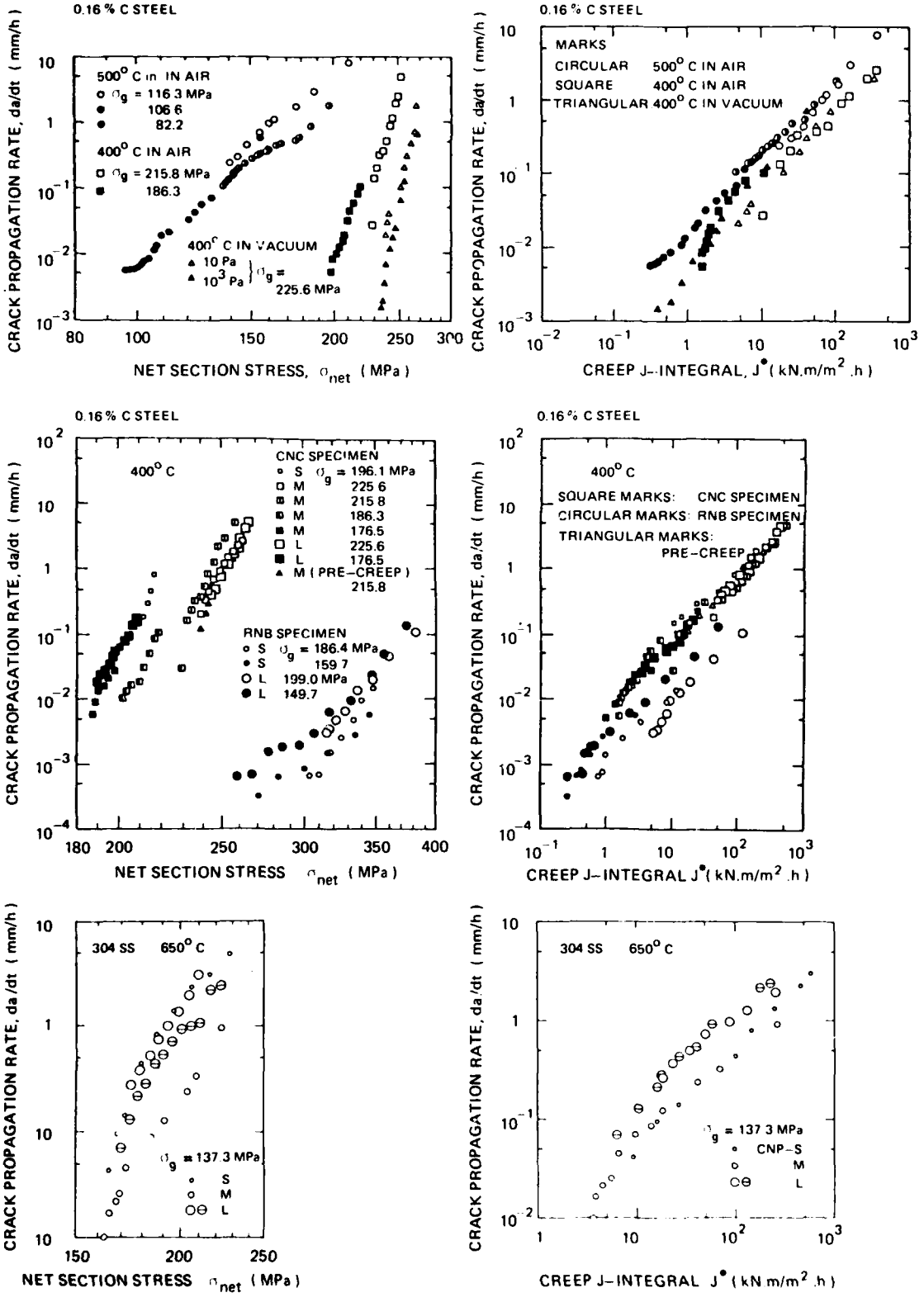

Fig. 26 Correlation of da/dt with σ_{net} and J^* for tests on CNC-M specimens at various stress levels (upper plots), on CNC and RNB specimens of different sizes at various stress levels (middle plots), on CNP specimens of several sizes at one stress level (lower plots). Taira et al. (58)

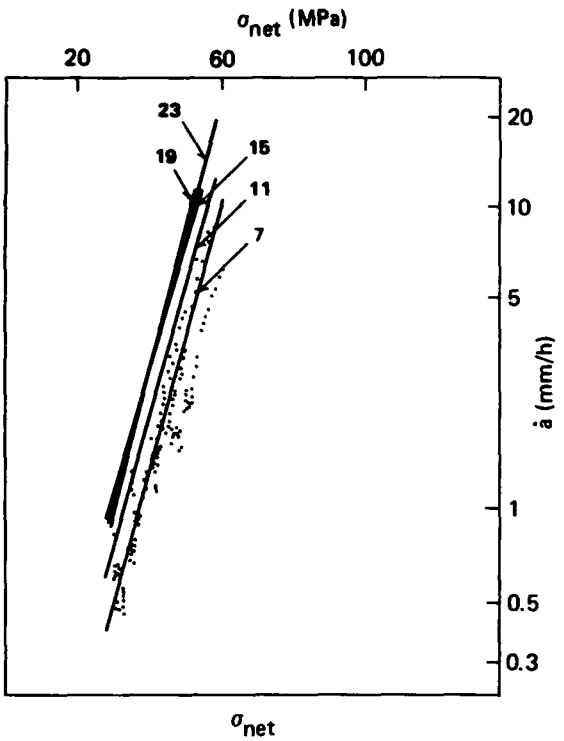

$-\dot{a}$-σ_{net} for all-thickness CT specimens
(data points are shown only for 5.6 mm thick specimens).

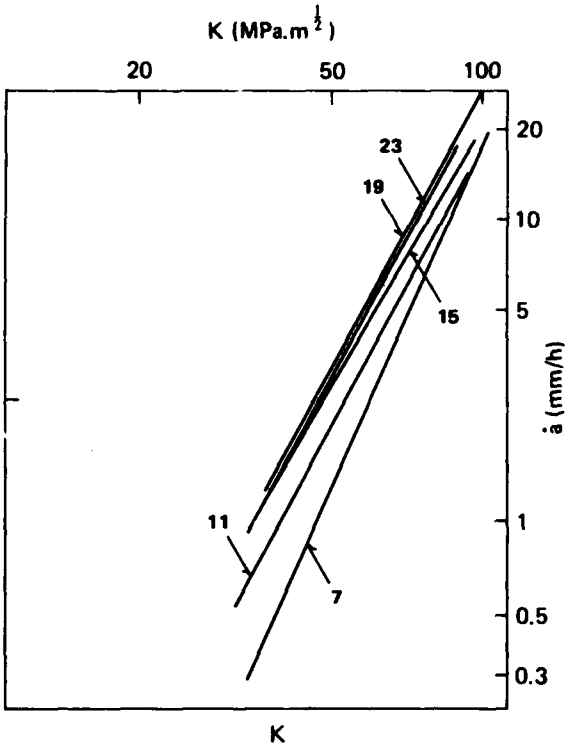

$-\dot{a}$-K for all-thickness CT specimens.

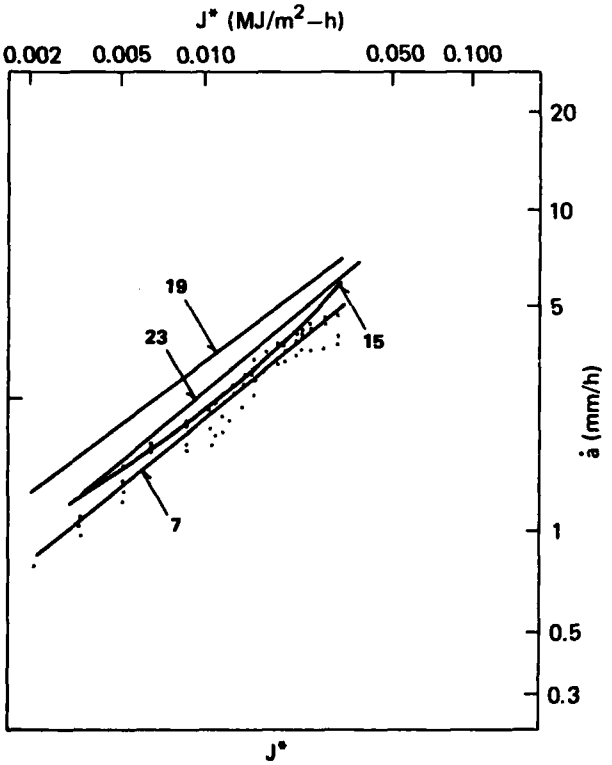

$-\dot{a}$-J* for all-thickness CT specimens
(data points are shown only for 5.6 mm thick specimens).

NUMBERS REFER TO SPECIMEN THICKNESS IN 32nds INCH.

7/32" = 6 mm
11/32" = 9 mm
15/32" = 12 mm
19/32" = 15 mm
23/32" = 18 mm

Fig. 27 Test results by Donath, Nicholas and Fu (60) showing good correlation of da/dt with σ_{net}, K and J*

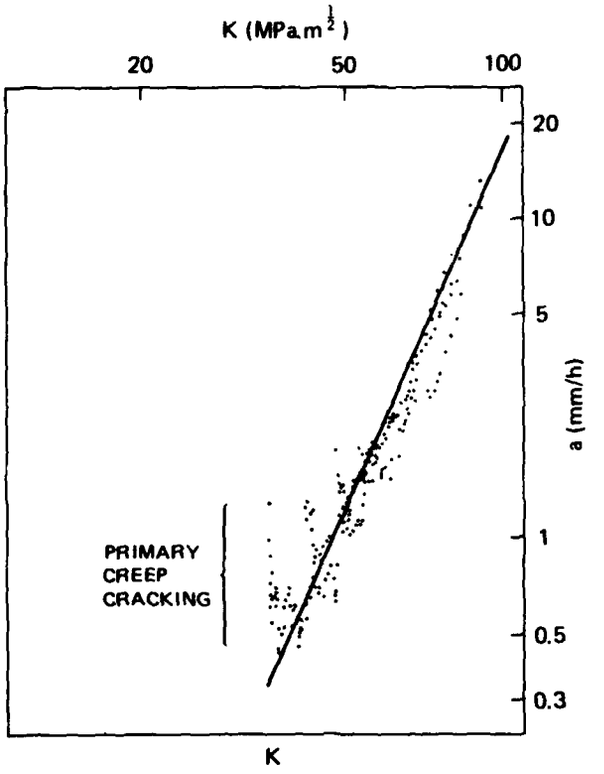

–ȧ-K for 5.6 mm thick CT specimens.

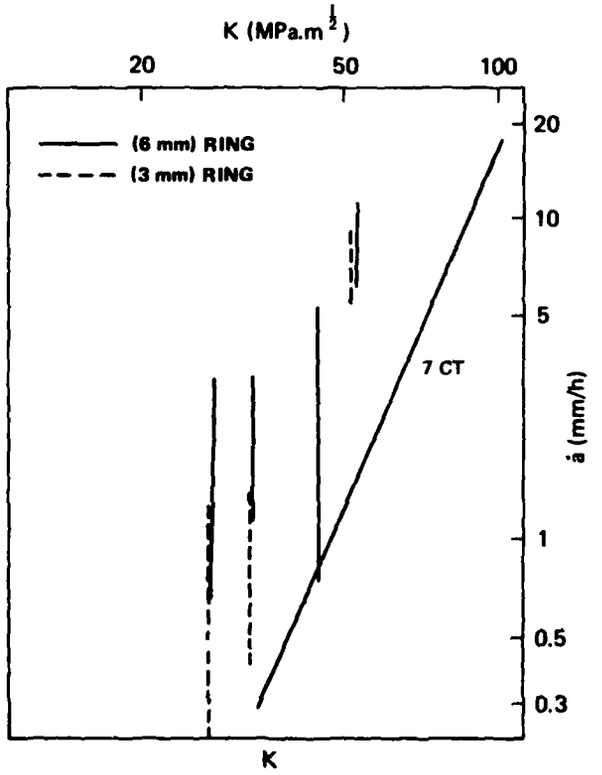

–ȧ-K for all ring tests
(6 mm CT data are shown for comparison).

Fig. 28 Test results by Donath, Nicholas and Fu (60) showing effects of primary creep

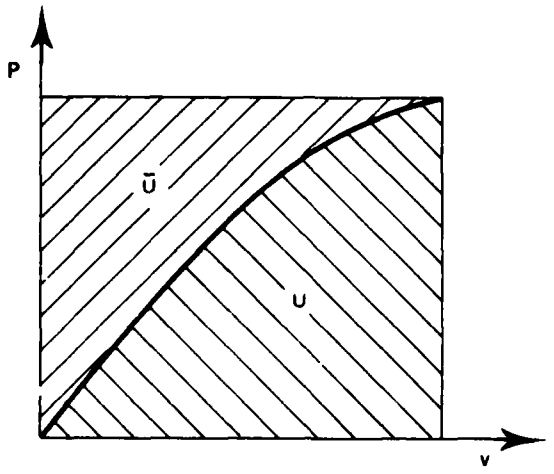

A) The load–displacement diagram

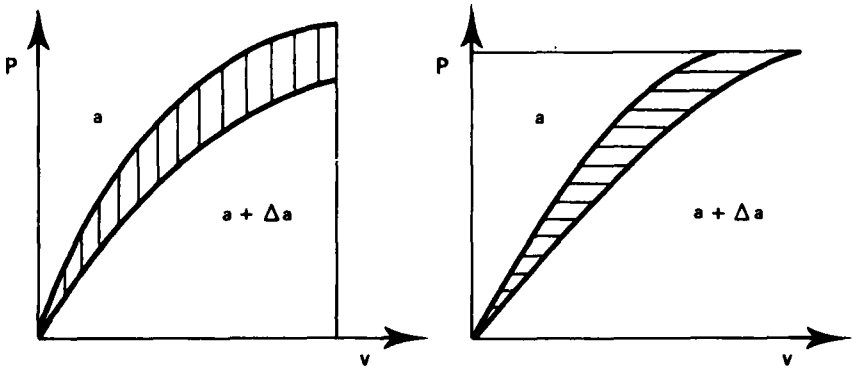

B) Variation of the energy $U = \int P dv$ with crack length a

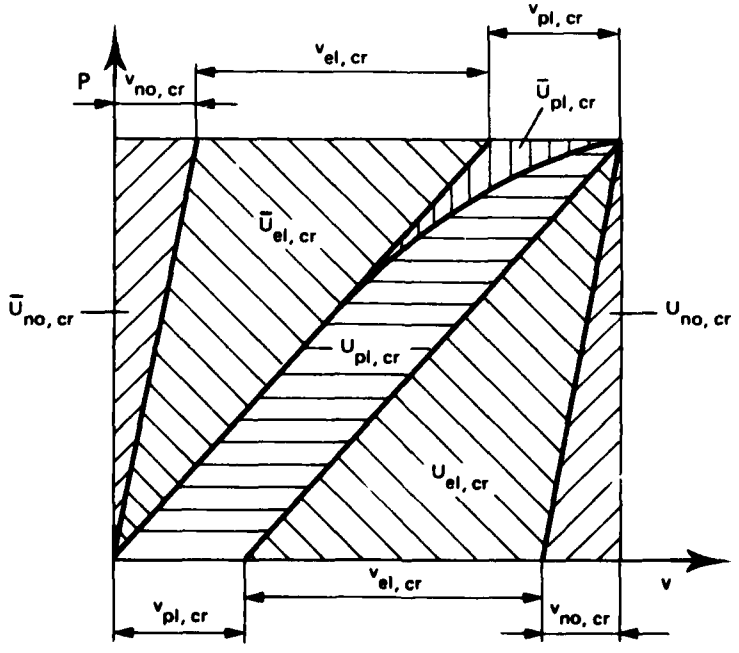

C) Elementary areas in the P–v diagram

Fig. 29 Features of the load-displacement diagram

REPORT DOCUMENTATION PAGE

1. Recipient's Reference	2. Originator's Reference	3. Further Reference	4. Security Classification of Document
	AGARD-R-705	ISBN 92-835-1453-X	UNCLASSIFIED

5. Originator Advisory Group for Aerospace Research and Development
North Atlantic Treaty Organization
7 rue Ancelle, 92200 Neuilly sur Seine, France

6. Title THE APPLICATION OF FRACTURE MECHANICS TO THE GROWTH OF CREEP CRACKS

7. Presented at the 56th Meeting of the Structures and Materials Panel in London, UK, April 1983.

8. Author(s)/Editor(s) H.P. van Leeuwen

9. Date June 1983

10. Author's/Editor's Address
National Aerospace Laboratory NLR
P.O. Box 90502
1006 BM Amsterdam, The Netherlands

11. Pages 58

12. Distribution Statement This document is distributed in accordance with AGARD policies and regulations, which are outlined on the Outside Back Covers of all AGARD publications.

13. Keywords/Descriptors

Fracture properties
Fractures (materials)
Cracking (fracturing)
Crack propagation
Creep properties
Engines

14. Abstract

The behaviour of materials at elevated temperatures is of crucial interest to both engine designers and operators, and there is a need for a base on which to build an approach to damage tolerant design. This paper discusses the literature relating the application of fracture mechanics to the growth of creep cracks, and shows that the linear elastic approach has been applied successfully to topics such as the residual strength of brittle materials, and crack growth due to stress corrosion and to fatigue; the difficulties in accounting for plastic behaviour are considered. A survey is made of attempts to correlate crack growth rate under creep conditions with various parameters; alternative methods of calculating the contour integrals J and J* are reviewed. A survey of theoretical crack growth rates, as functions of parameters which are considered to be determining, is also included. The paper ends with a discussion and some conclusions.

AGARD Report No. 705 Advisory Group for Aerospace Research and Development, NATO THE APPLICATION OF FRACTURE MECHANICS TO THE GROWTH OF CREEP CRACKS by H.P. van Leeuwen Published June 1983 58 pages The behaviour of materials at elevated temperatures is of crucial interest to both engine designers and operators, and there is a need for a base on which to build an approach to damage tolerant design. This paper discusses the literature relating the application of fracture mechanics to the growth of creep cracks, and shows that the linear elastic approach has been applied successfully P.T.O.	AGARD-R-705 Fracture properties Fractures (materials) Cracking (fracturing) Crack propagation Creep properties Engines	AGARD Report No. 705 Advisory Group for Aerospace Research and Development, NATO THE APPLICATION OF FRACTURE MECHANICS TO THE GROWTH OF CREEP CRACKS by H.P. van Leeuwen Published June 1983 58 pages The behaviour of materials at elevated temperatures is of crucial interest to both engine designers and operators, and there is a need for a base on which to build an approach to damage tolerant design. This paper discusses the literature relating the application of fracture mechanics to the growth of creep cracks, and shows that the linear elastic approach has been applied successfully P.T.O.	AGARD-R-705 Fracture properties Fractures (materials) Cracking (fracturing) Crack propagation Creep properties Engines
AGARD Report No. 705 Advisory Group for Aerospace Research and Development, NATO THE APPLICATION OF FRACTURE MECHANICS TO THE GROWTH OF CREEP CRACKS by H.P. van Leeuwen Published June 1983 58 pages The behaviour of materials at elevated temperatures is of crucial interest to both engine designers and operators, and there is a need for a base on which to build an approach to damage tolerant design. This paper discusses the literature relating the application of fracture mechanics to the growth of creep cracks, and shows that the linear elastic approach has been applied successfully P.T.O.	AGARD-R-705 Fracture properties Fractures (materials) Cracking (fracturing) Crack propagation Creep properties Engines	AGARD Report No. 705 Advisory Group for Aerospace Research and Development, NATO THE APPLICATION OF FRACTURE MECHANICS TO THE GROWTH OF CREEP CRACKS by H.P. van Leeuwen Published June 1983 58 pages The behaviour of materials at elevated temperatures is of crucial interest to both engine designers and operators, and there is a need for a base on which to build an approach to damage tolerant design. This paper discusses the literature relating the application of fracture mechanics to the growth of creep cracks, and shows that the linear elastic approach has been applied successfully P.T.O.	AGARD-R-705 Fracture properties Fractures (materials) Cracking (fracturing) Crack propagation Creep properties Engines

to topics such as the residual strength of brittle materials, and crack growth due to stress corrosion and to fatigue; the difficulties in accounting for plastic behaviour are considered. A survey is made of attempts to correlate crack growth rate under creep conditions with various parameters; alternative methods of calculating the contour integrals J and J* are reviewed. A survey of theoretical crack growth rates, as functions of parameters which are considered to be determining, is also included. The paper ends with a discussion and some conclusions.

This Report was presented at the 56th Meeting of the Structures and Materials Panel in London, UK, April 1983.

ISBN 92-835-1453-X

to topics such as the residual strength of brittle materials, and crack growth due to stress corrosion and to fatigue; the difficulties in accounting for plastic behaviour are considered. A survey is made of attempts to correlate crack growth rate under creep conditions with various parameters; alternative methods of calculating the contour integrals J and J* are reviewed. A survey of theoretical crack growth rates, as functions of parameters which are considered to be determining, is also included. The paper ends with a discussion and some conclusions.

This Report was presented at the 56th Meeting of the Structures and Materials Panel in London, UK, April 1983.

ISBN 92-835-1453-X

to topics such as the residual strength of brittle materials, and crack growth due to stress corrosion and to fatigue; the difficulties in accounting for plastic behaviour are considered. A survey is made of attempts to correlate crack growth rate under creep conditions with various parameters; alternative methods of calculating the contour integrals J and J* are reviewed. A survey of theoretical crack growth rates, as functions of parameters which are considered to be determining, is also included. The paper ends with a discussion and some conclusions.

This Report was presented at the 56th Meeting of the Structures and Materials Panel in London, UK, April 1983.

ISBN 92-835-1453-X

to topics such as the residual strength of brittle materials, and crack growth due to stress corrosion and to fatigue; the difficulties in accounting for plastic behaviour are considered. A survey is made of attempts to correlate crack growth rate under creep conditions with various parameters; alternative methods of calculating the contour integrals J and J* are reviewed. A survey of theoretical crack growth rates, as functions of parameters which are considered to be determining, is also included. The paper ends with a discussion and some conclusions.

This Report was presented at the 56th Meeting of the Structures and Materials Panel in London, UK, April 1983.

ISBN 92-835-1453-X

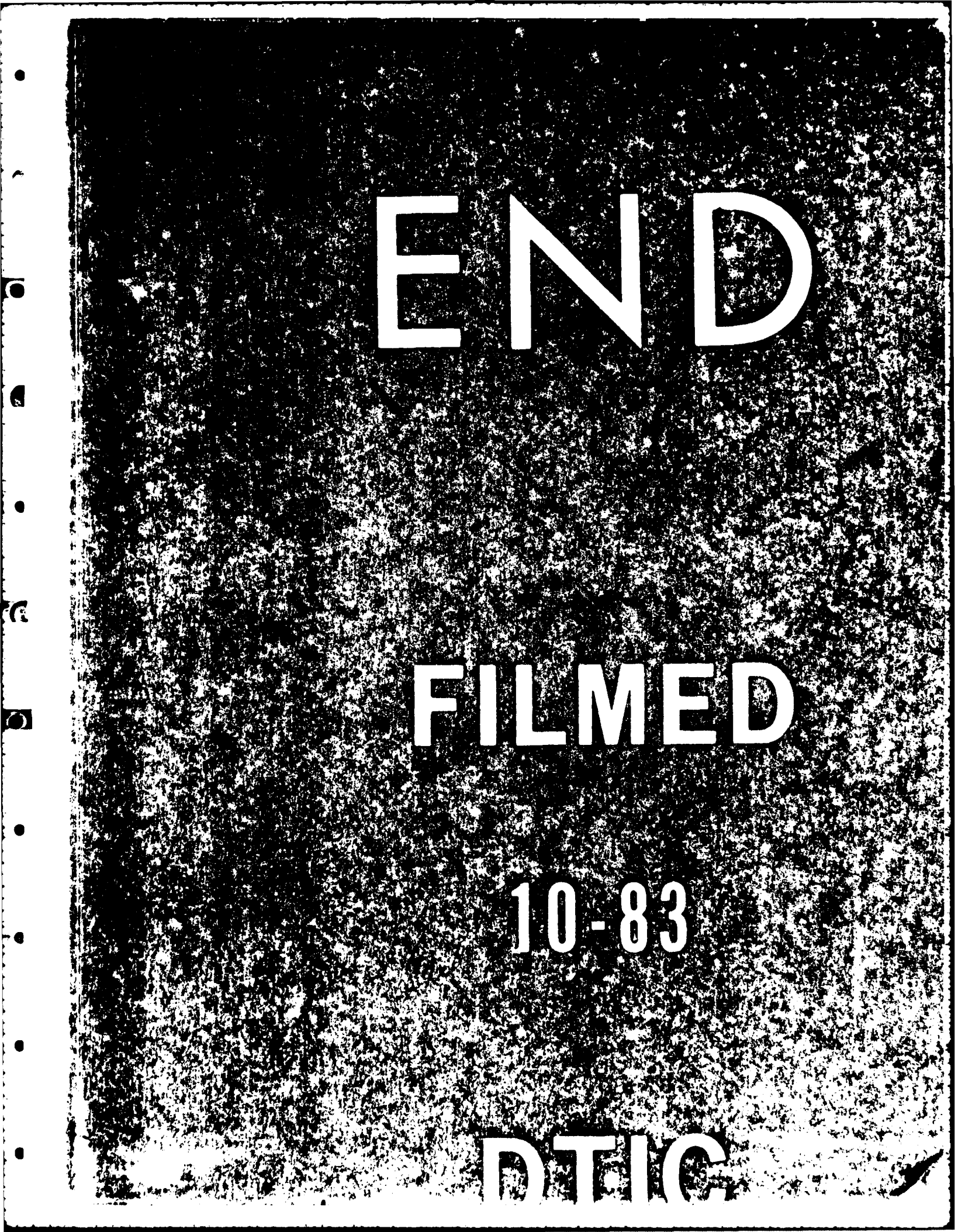
END
FILMED
10-83
DTIC